University of Stavanger

Faculty of Science and Technology

MASTER'S THESIS

Study program/Specialization: Petroleum Engineering/Reservoir Engineering	Spring semester, 2016 Open / ~~Restricted~~ access
Writer: Sidra Chughtai	…… (Writer's signature)
Faculty supervisor: Prof. Aly Anis Hamouda	
Thesis title: Experimental and numerical simulation of the recovery of oil and the effect of light oil components on CO_2 flooding mechanism using sandstone reservoir.	
Credits (ECTS): 30	
Key words: CO_2 flooding Sandstone PVTSim Live Oil Pore Volume Gas Chromatography	Pages: 93 + enclosure: Stavanger,15/06/2016 Date/year

ACKNOWLEDGEMENT

Foremost, I would like to thank God for always showering his blessings upon me.

I would like to express my deepest appreciation to my supervisor, Professor Aly Anis Hamouda whose expertise, patience and immense knowledge added considerably to my post graduate experience. I received a better technical understanding of lab work and numerical simulation under his guidance. Without his supervision and persistent this dissertation would not have been possible.

I would also like to thank Kryztof for his support and cooperation throughout my work. Last but not the least my family and friends for their wise counsel and sympathetic ear.

Sidra Chughtai

1 *ABSTRACT*

Carbon dioxide (CO_2) flooding is considered as an efficacious method of EOR. It is a complicated process as it involves phase behavior. In order to master the performance of CO_2 flooding, a comprehensive investigation of mass transfer mechanism and compositional changes for gaining miscibility based on laboratory study was conducted.

In this manuscript, CO_2flooding experiments were carried out on Bentheimer Sandstone and Berea Sandstones under three temperature conditions (50°C, 70°C and 90°C). During the flooding, fluid samples were analyzed to elucidate the effect of light components on the recovery of model oils (Live-oil A and Live-oil B) and crude oil from a field in the North Sea. Model oils were prepared using different composition of light components (C_1 and C_3) combined with n-decane.CO_2flooding experiments were also performed with CO_2containing light components (C_1 and C_3) to comprehend the effect of light oil components on the recovery when present in the displacing fluid and displaced fluid.

The experimental and simulation results have highlighted that higher miscible condition provides higher recoveries. Light components also affect the recovery of the oil. The recoveries obtained with the oil consisting of only methane as a light component provided higher recovery than the oil consisting of both methane and propane. However, the incremental recovery was observed when the light components were displacing fluid with CO_2. This may be due to that the presence of light components in the injected fluid in a miscible condition increased the oil mobility. This dissertation addressed material balance of all the studied components and compared the experimental result with the simulated one.

Table of Contents

List of Figures

LIST OF TABLES

Nomenclature

EOR	Enhanced Oil Recovery
GC	Gas Chromatography
H	Reservoir thickness
h_1 & h_2	Bottom & top of perforation interval
HCPV	Hydrocarbon Pore-volume (HCPV)
IFT	Interfacial tension (IFT)
K_x & K_z	Permeability in x & z direction
L	Length of reservoir
P_c	Capillary Pressure
P_L	Pressure at the well location L
P_{nw}	Non-Wetting phase pressure
PV	Pore-volume (PV)
P_w	Wetting phase pressure
q	Flow rate
W	Width of the reservoir

1. INTRODUCTION

With approaching towards the tail production/ declining phase of many mature fields on the Norwegian Continental shelf and worldwide, the field owners are inclined towards opting Enhanced Oil Recovery (EOR) as a possible method for optimizing the production of oil from these fields. CO_2 flooding has been highly regarded as a promising Enhanced Oil Recovery (EOR) technique which can be lined up in both the categories of secondary and tertiary recovery mechanisms (Mungan, 1981). Patents and papers have been written by Beeson and Ortloff, Holm, and Martin on this subject, which have laid the foundation of CO_2 oil recovery processes. Initially when this method was introduced, immiscible flooding was under discussion as an alternative water-based EOR processes (Hamada &Tabrizy, 2013). However, the focus was later placed on miscible processes. The mixing of CO_2 in the oil is ruled by three major mass transfer mechanisms:

1. Solubility;
2. Diffusion and
3. Dispersion.

Other factors also largely affects the displacement efficiency for CO_2 injection which includes density differences between oil and gas, viscosity and mobility ratios of the fluids, relative permeability, wetting properties of the rock and injection and production rates (Rojas et al., 1991)

1.1.Carbon Dioxide Flooding

One of the main characteristic of carbon dioxide is that it is highly soluble in oil and lesser soluble in water. It is important to note that carbon dioxide and its mechanisms play an essential role in improving the overall process of oil recovery. Some of the carbon dioxide mechanisms that positively contribute towards oil recovery are listed as follows:

1. Reduction in oildensity
2. Reduction in crudeoilviscosity
3. Reduction in swelling of crude oil
4. Reduction in miscibility effects(Jarrell et al., 2002; Holm and Josendel, 1982; Orr et al., 1982)

According to Pasala, S. M. interfacial tension and capillary forces are eliminated and residual oil is successfully recovered when complete miscibility exists between the oil and CO2/ hydrocarbon solvents. Another important point to note is that when CO2 and oil are mixed, two important physical changes take place which positively enhance the oil recovery

process. Firstly, due to the lower viscosity of the CO2-oil mixture than the original oil, it becomes considerably easier for the contacted oil to flow into the porous medium. Secondly, the high solubility of CO2 in oil plays a key role in causing swelling and as a result of this expansion; it becomes important for some fluid to migrate. Injection of CO2 into an oil reservoir gives birth to a complex chain of interactions between oil, water and CO2. Lastly, it is worthy to understand that both phase behavior and fluid flow properties of the gas – liquid mixtures play a highly significant role in determining the efficiency with which an injected gas (CO2) displaces a liquid, such as, oil or water.

1.2.CO2 Properties

The process of improving the recovery of oil with the help of CO2 began in the 1950s with Whorton and Brownscombe receiving a patent for a CO2 oil recovery method. After that the use of CO2 for oil recovery started gaining considerable attention and it gained widespread popularity. Following this, the 1970s witnessed a substantial increase in field testing with the help of laboratory and deskwork. Carbon dioxide is defined as a inert, odorless, colorless and non-combustible gas with the following properties under standard conditions: • Molecular weight 44.010 g/mol • Specific gravity with respect to air 1.529 • Density 1.95 kg/m3 • Viscosity 0.0137 mPa/s The phase behavior of pure CO2 is shown on a P-T diagram below.

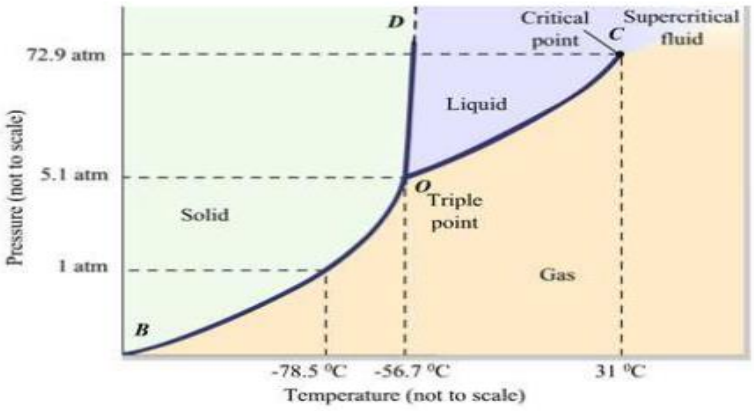

Figure 1.1. CO_2 phase diagram

Yin (2015) is indicated that it is normally solid at low temperature and pressures. At the temperature of -78.5 °C, solid CO2 will evaporate directly to gas. But when the temperature will increase, the liquid phase will emerge and co-exist with the solid and the vapor phases at the triple point. A critical point will be reached and the CO2 will behave as a vapor if the temperature and pressure are increased further. Its critical properties are: Pc =

7.39 MPa (1073 psia) Tc = 304 K (31.1°C, 37.8 °F) Vc = 94 cm3 /mol. According to Klins (1991), CO2 reacts as a supercritical fluid under most reservoir conditions due to this critical temperature and pressure increase. Moreover, at the critical conditions of pressure and temperature, the viscosity of CO2 is 0.0335 cp which is higher than other probable injection gases (N2: 0.016 cp; CH4: 0.009 cp). Once again, it is important to keep in mind that CO2 is normally two to ten times more soluble in oil as compared to water. By dissolving into water, CO2 leads to a substantial increase in water viscosity which forms carbonate acid. As a result of this dissolution of CO2 with water, shale and carbonate rocks enjoy a beneficial effect.

1.2.1. Relative Permeability:

Relative permeability is defined as the ratio of effective permeability of any given phase such as Ko in the presence of other phases such as oil to the absolute permeability(Al-Sayari, S.S., 2009).

$$K_{ro} = \frac{K_o}{k}$$

Relative permeability plays a vital role in injection projects such as CO2 flooding as relative permeability depends upon the other phases in rock like oil & water thereby affecting the injectivity of CO2[(2)]. There is no proper way of measuring CO2-oil relative permeability curves under miscible condition due to slow development of dynamic miscibility [(3)]. Laboratory results have showed that short/conventional core segments leads to early CO2

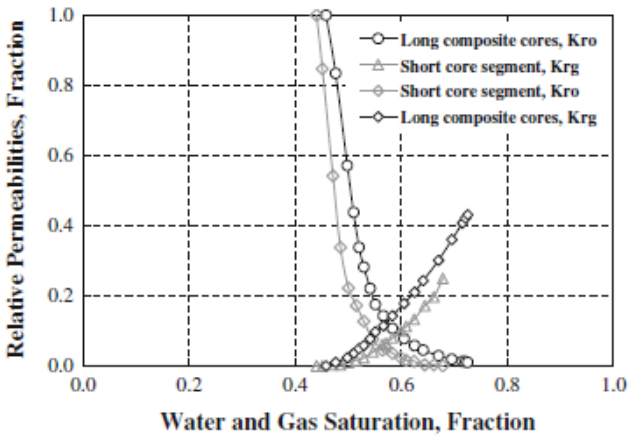

Figure 1.2. Relative permeability of short and long real cores

breakthrough and insufficient vaporizing time & no development of dynamic miscibility whereas, in the case of long cores it leads to better performance and better process of recovery under miscible flooding.

Slim tube experiments in short tubes depicts near miscible features, whereas long slim tube experiments depicts miscible flooding feature above MMP (Minimum Miscibility Pressure).

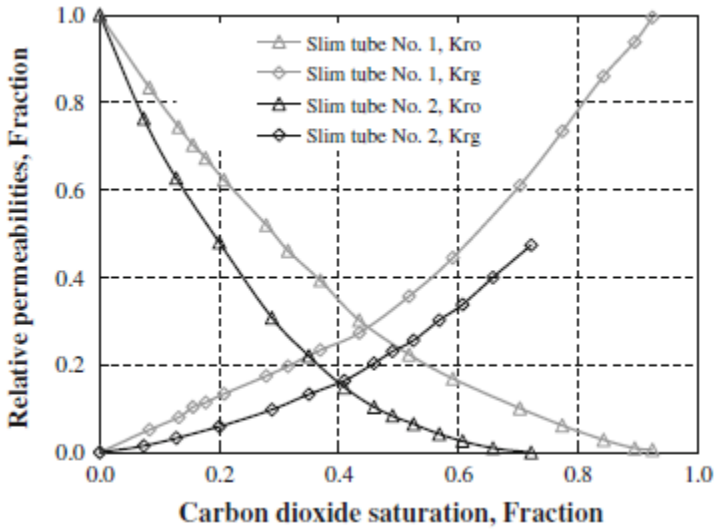

Figure 1.3. Relative permeability curves in long and short slim tube test

Conventional core segment derived relative permeability curves application in reservoir simulators may mislead in predicting performance under miscible conditions(Li, F. F.et al, 2014).

1.2.2. Heterogeneity:

CO2 flooding performance is affected by reservoir heterogeneity. Increasing heterogeneity causes higher unstable flood front and an early breakthrough of injected material can frequently occur. Studies have showed that injectivity in a heterogeneous reservoir is a function of 10 parameters(Pizarro, J.O.S., Lake, L.W., 1998).

$$I = f(K_x, K_z, \mu, P_l, L, h_1, h_2, H, W, q)$$

Where

K_x&K_z= Permeability in x & z direction

P_L = Pressure at the well location L

L = Length of reservoir

h_1 & h_2=Bottom & top of perforation interval

H = Reservoir thickness

W = Width of the reservoir

q = Flow rate

1.2.3. **CapillaryPressure***:*

Capillary pressure is defined as the pressure difference between non-wetting & wetting phase.

$$Pc = Pnw - Pw$$

P_c=Capillary Pressure

P_{nw}= Non-Wetting phase pressure

P_w = Wetting phase pressure

As the capillary pressure increases, non-wetting phase penetrates into the system. Capillary pressure in a porous medium is a function of saturation. When 100% water saturated rock is being displaced by oil reducing the water to its irreducible water saturation, this is called drainage process. Irreducible water saturation is the minimum saturation of wetting phase retained at higher capillary pressure. Similarly, displacement of non-wetting phase by wetting phase thereby reducing the oil to its residual saturation is called imbibition process(Al-Sayari, S.S., 2009).

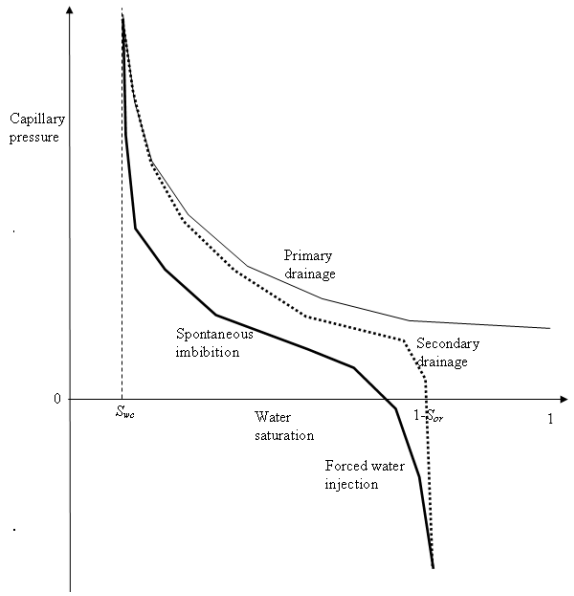

Figure 1.4. Capillary pressure curve for a water-wet system showingdrainage, spontaneous and forced water injection (Al-Sayari, S.S., 2009).

High capillary forces require a high injection pressure for a given injection rate. Higher capillary forces also reduce gravity segregation, and this gives a more homogeneous CO2 plume which improves the dissolution of CO_2 (Alkan,H., Cinar, Y. , Ulker,E. B., 2009)

1.3. Wettability

According to Craig (1971), wettability is defined as "*the tendency of one fluid to spread on or adhere to a solid surface in the presence of other immiscible fluids".* Wettability takes place when two or more immiscible fluids are close to a solid surface and when the molecules of the fluids have an adhesive force that pulls them towards the molecules of the surface. It is important to note that the fluid with the strongest bond or adhesion will preferably stick to the surface and define the wettablity of the solid medium.

Moreover, according to Anderson (1987), wettability is the most crucial parameter during the study of reservoir flow. This is because wettability considerably affects the capillary pressure, water flood behavior, irreducible water saturation, relative permeability, residual oil saturation, simulated tertiary recovery, dispersion and electrical properties (Ydstebø, 2013).

Furthermore, it has been identified that in a rock/oil/brine system, wettability is a preferred method for measuring the preference that the rock has for either oil or water (Anderson, 1986). For example, if the rock is water-wet, then the water will contact majority of the rock surface, especially the small pores. On the other hand, if the rock is oil-wet, then oil will build contact with majority of the rock and the small pores in it. Lastly, if the rock fails to have any wetting preference, then it will be termed as a neutral-wet.

On a different note, Salathiel (1973) has explained wettability through the heterogeneous distribution concept, that is, some of the rock surface is characterized as water-wet, some as oil-wet and some as mixed-wettability of both water and oil. Mixed-wet small pores (MWS) are usually oil-wet in the small pores while mixed-wet large pores (MWL) usually have oil-wet largest pores.

Brown and Fatt (1956) have explained another kind of wettablity, that is, fractional wettability, which according to them, is uncorrelated to pore size. Anderson, (1986b) explains that the term wettability mostly refers to the wetting preference of the rock and does not necessarily refer to the connection or contact between the fluid and the rock at any given time. Anderson (1986) also observes that most of the clean sedimentary rocks are water-wet prior to oil-immigration. But due to the absorption of polar compounds and the deposition of organic matter in the crude oil, the composition of wettability changes from time to time. The polar compounds contain both a polar end and a hydrocarbon end and as a result of this, the polar end absorbs the rock and hydrocarbon end establishes a contact with the fluids. Another

important feature to keep in mind is that some natural surfactants in crude oil are sufficiently soluble in water, and have the ability to adsorb onto the rock.

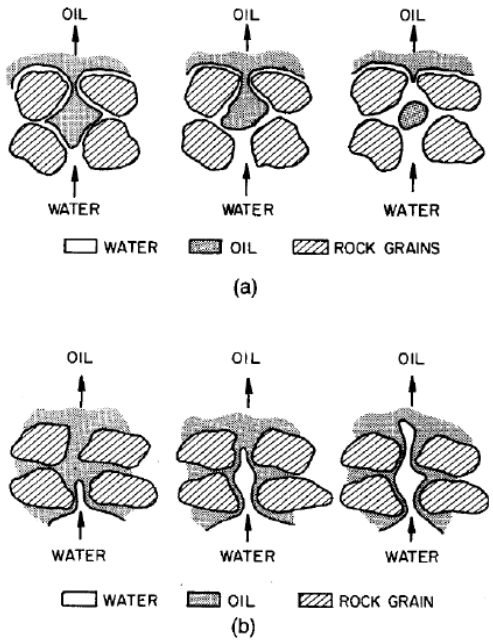

Figure1.5. Water flood in (a) Strongly water wet rock and (b) Strongly oil wet rock

1.4. CO_2Dissolution in Oil

CO2 dissolution in oil also carries great significance because it leads towards enhanced oil recovery. The dissolution solubility of CO2 in oil normally depends on the characteristics of the crude oil, the pressure and the overall temperature. The characteristics of the oil can be seen in the figure 3.2 below:

ADA crude oil has a gravity of 30.3 °API while West Texas crude is of 39 °API. According to Figure 3.2, CO2 has a higher solubility in lighter oil; this value is slightly greater when the temperature is 13 increased. When the pressure increases, solubility will increase and is sometimes limited to a saturation value.

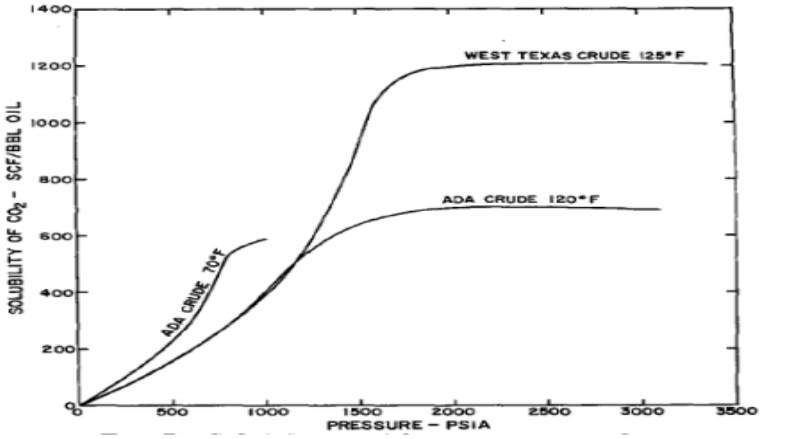

Figure 1.6. CO_2 solubility in crude oil (Crawford et al, 1963)

FIGURE 1 CO2 SOLUBILITY IN CRUDE OIL (CRAWFORD ET AL, 1963)

1.4.1. Oil Swelling

The oil volume tends to increase from 10 to 60 % when CO2 is dissolved into the crude oil. According to Holm (1987), the above phenoemenon takes places more often with light oil and results in lower residual saturation. When a given residual oil saturation increases, oil swelling simultaneously increases the recovery factor. The mass of the oil remaining in the reservoir under standard conditions is lower than residual oil that has not had contact with the CO2.

1.4.2. Viscosity Reduction

Oil viscosity reduction is witnessed due to the dissolution of CO2 in crude oil. Viscosity reduction is the major mechanism for EOR as indicated by calculations. Moreover, according to the results of laboratory experiments, it has been identified that the viscosity reduction is relatively greater for oil with higher original viscosity (Klins and Bardon, 1991).

1.5. Phase Behavior of Oil and Carbon Dioxide

The phase behavior of a CO2-oil system is not an easy process, rather it is a highly complex one. Pasala (2010) points out that when the reservoir oil and injection gas are mixed in a certain ratio, they form a single phase and are referred to as first contact miscible. First contact miscibility is only achieved for hydrocarbon rich gases, or at very high pressures for lean systems. It is important to remember that even at high operating pressures, carbon dioxide is not first contact miscible with most reservoir oils. Specific oil compositions, specific pressure and temperature conditions can play a substantial role in allowing CO2 to

develop miscibility through multiple contacts. Miscibility is usually developed with the help of two mechanisms, which are discussed as follows:

The vaporizing gas drive process (VGD) which enriches the gas phase with the help of extraction of light and intermediate fractions of oil. The original oil is in contact with the vapor phase generated from the previous mixture. The vapor phase becomes fully miscible with the reservoir crude due to the richness of light and the presence of intermediate hydrocarbons. The minimum pressure required to achieve this is called the minimum miscibility pressure (MMP). The CO2 injection process relies on a highly important parameter (MMP) for the screening and selecting of reservoirs. Moreover, a candidate reservoir is required to withstand an average reservoir pressure greater than the CO2 MMP for achieving the highest recovery. Reliable determination of miscibility conditions for a system is achieved through both experimental slim tube measurements and through properly interpreted slim tube simulations. During this process, nothing is assumed about the path of developed miscibility or displacement mechanism (Pasala, 2010). Carbon dioxide flooding is generally a VGD process in which the miscibility generation mechanism is called the condensing gas drive (CGD). In this process, the in situ transfer of the intermediate molecular hydrocarbon fraction from the injected gas into the oil can also generate miscible displacement between reservoir oil and hydrocarbon gases.

Moreover, according to Pasala (2010), it is worthy to note that when reservoir rocks containing oil and water are injected with CO2, then some of the essential components present in the gas usually dissolve better in oil instead of water. At the same time, some components of the oil transfer into vapor phase. As a result of different phase saturations and the imposed pressure gradient, they move at different rates generally. For example, the lower viscosity vapor phase proceeds ahead and establishes a contact with fresh oil in the reservoir. Hence, those phases achieve equilibrium by mixing together and by allowing new liquid and vapor phases to flow ahead and develop a contact with the fluids in the reservoir. This process of interaction between the flow and the phase equiblirium, components are successfully separated as they disseminate through the reservoir.

1.6. Miscible Displacement

L.W. Holm has defined the miscible state in the following words “the ability of two or more substances to form a single homogeneous phase when mixing in all proportions”. On the other hand, with regard to petroleum reservoirs, miscibility is usually defined as the physical form between two or more fluids which allows them to blend in all proportions without the

presence or existence of an interface. If two fluid phases form after some amount of one fluid is added to others, the fluids are considered immiscible. According to Yin (2015), a miscible gas drive involves two main processes. The two processes are they are identified as the first contact miscibility process and the multiple contact miscibility process. First contact miscibility is achieved when both fluids are completely miscible in all proportions without any multiple behaviors. However, it is has been identified that while other solvents are not directly miscible with reservoir oil, miscibility can still be achieved through the in-situ mass transfer between oil and solvent through repeated contacts. This form of miscibility is refered to as dynamic miscibility or multiple contact miscibility. Intense mass transfer between phases takes place when large amounts of CO2 are mixed with oil. Moreover, it is essential to take into account that multiple contact miscibility is sub-divided into two main processes, which are, condensing gas drive and vaporizing gas drive. Both of these processes are based on component transfer. The reservoir oil and injected gas components are usually classified into four groups, which are named as follows:

1. Light components: C1 (methane)
2. Lean components: CO2, N2, and CH4 injection gas
3. Intermediate components: C2-C6
4. Heavy components: C7+ (heptane and heavier fractions)

1.6.1. Vaporizing Gas Drive

Yin (2015) has indicated that one of the most important function of CO2 is related to the extraction and vaporization of hydrocarbons from crude oil. The vaporizing gas drive mechanism is usually defined as the process through which a lean injection gas passes over reservoir oil rich in intermediate components and extracts those fractions from the oil and concentrates at the displacement front where miscibility is achieved.

A schematic of CO2 gas vaporizing and condensing gas drive mechanisms are shown in Figure 1.7 below:

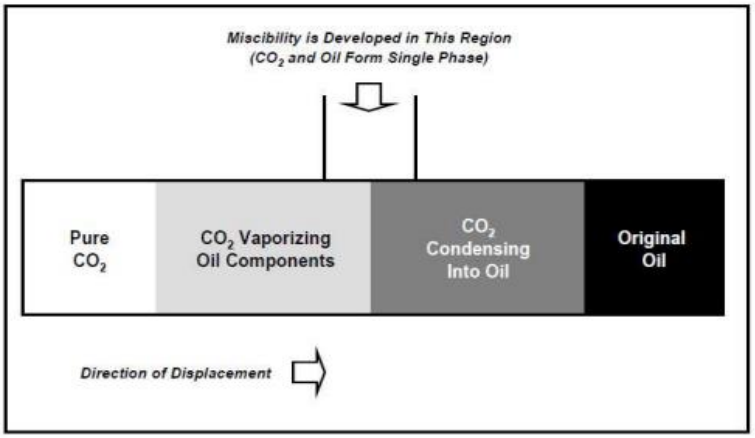

Figure 1.7. One dimensional schematic of CO_2 miscible process (Advanced Resources International, Inc, 2005)

1.6.2. Condensing Gas Drive

Condensing is usually defined as a process that allows transfer through the condensation of intermediate components from rich solvent to intermediate-lean reservoir oil. In CO2 miscible flooding, the intermediates that were stripped from the oil that are present in the gas condense when the gas encounters fresh oil downstream (Yin, 2015).

1.7. Near Miscible Displacement

It is important to keep in mind that CO2 injection is measured as miscible or partial miscible when economic or technical factors hinder the miscibility pressure to be reached effectively or to be maintained. This is referred to as a process between immiscible and miscible displacement. The mechanisms which are used for recovery usually include light component extraction, oil swelling and viscosity reduction. Miscible displacements cases are usually witness lesser oil recovery as compared to the ones under miscible conditions. But Klins and Bardon (1991) have pointed out that on a positive side, the process is highly attractive because the volume of CO2 required to produce additional oil is considerably less.

1.8. Minimum Miscibility Pressure

According to Yin (2015), the minimum miscibility pressure (MMP) is the minimum pressure which allows the injection gas and reservoir oil to can mix together and become one phase. At above MMP, the interfacial tension between reservoir oil and injected gas disappears. Therefore, MMP is an essential parameter for screening and selecting CO2 miscible flooding candidates. Typically, CO2 MMP is greater than 1,400 psia and changes under the influence of several factors.

1.8.1. Factors Influencing MMP

Minimum miscibility pressure (MMP) is defined as a function of temperature and oil composition. It is important to remember that MMP is negatively affected when impurities are injected in the CO2.

1.8.2. Reservoir temperature

CO2 MMP is temperature dependent which means reservoir temperature has a significant effect on CO2 MMP determination for a 18 given reservoir oil. Usually, MMP increases as temperature increases. A simple temperature versus bubble point pressure of CO2 MMP is shown below.

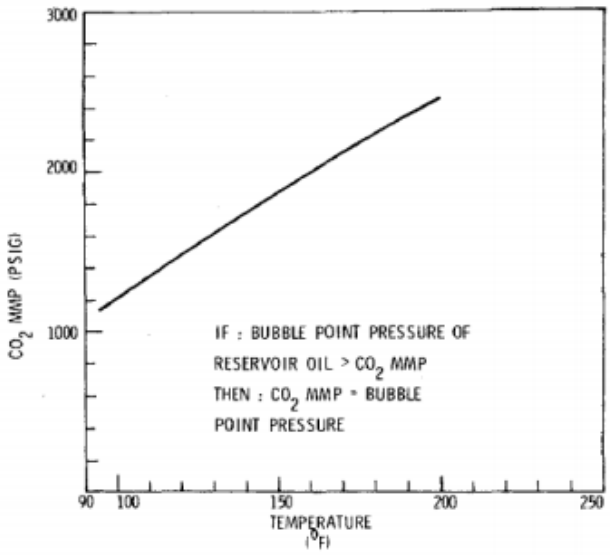

Figure 1.8. Temperature/ bubblepoint pressure of CO_2 MMP correlation (Yellig and Metcalfe, 1980)

1.8.3. Oil Characteristics

For correctly understanding oil characteristics, it is essential to understand that when volatile components in oil such as C1 have a greater fraction, then automatically the MMP between CO2 and oil increases. On the other hand, MMP is usually decreased due to the presence of intermediate components such as C2 – C4 in the reservoir fluid (Yin, 2015). Moreover, Alston et al (1985) indicate that a higher MMP is achieved due to the presence of higher molecular weight components such as C5+ or C7+ fraction in the reservoir oil.

2. OBJECTIVE

The main objective of this work is to study the effect of light oil components (C_1 and C_3) on the recovery of oil through CO_2 flooding. This study addresses the mass transfer mechanism taking place between the components during flooding and the interaction of CO_2 with the oil and the lighter components. Very little work has been done on this subject. The comparison of using lighter components as a displaced fluid and as a displacing fluid is made. Further the effect of temperature on the recovery of oil from sandstone reservoir is also investigated. Three model oils with different composition are utilized for performing the experiments at three temperatures (50^0C, 70^0C and 90^0C) and the results are evaluated.

3. MATERIAL AND METHODS

3.1.Solid Phase

Core flood experiments were performed using outcrop Bentheimer sandstones and Berea sandstones. The cores were 9-10 cm in length and 3.8 cm in diameters. The outcrop haveapproximate porosity of 20-25% and higher permeability of 900-1200 mD. Table 3.1 depicts further characteristics, associated fluid content and flooding conditions in detail.

Table 1. Characteristics of cores along with associated fluid and flooding conditions.

Exp. No.	Core Type	Porosity (%)	Length (cm)	Saturating fluid	Displacing fluid	Flooding Temperature (°C)
1	Bentheimer	21.7	5,07	Live-oil A	CO_2	50
2	Bentheimer	21.25	9.00	Live-oil A	CO_2	70
3	Berea	0.193	8.96	Live-oil A	CO_2	90
4	Bentheimer	23.24	9.00	Live-oil B	CO_2	50
5	Bentheimer	23.30	9.00	Live-oil B	CO_2	70
6	Berea	*19.6*	9.09	Live-oil B	CO_2	90
7	Bentheimer	20.20	8.90	Deadoil	CO_2	50
8	Bentheimer	21.05	9.00	Deadoil	CO_2	70
9	Bentheimer	21.97	8.90	Deadoil	CO_2	90
10	Berea	21.68	9.00	Model oil (Crude)	$CO_2+C_1+C_3$	70
11	Berea	21.88	9.00	Crudeoil	$CO_2+C_1+C_3$	70
12	Berea	21.22	9.00	Crudeoil	CO_2	70

1.1.Live-Oil – A Preparation Procedure

The Live-oil preparation procedure involved a number of steps, which are briefly discussed in this section. Firstly, 200 ml of n-decane was accurately measured into a clean Live-oil cylinder. Secondly, the empty weight of the gas sampling cylinder (m_e) was measured and recorded accurately. Thirdly, the required gas (C_1 or C_3) was injected into the gas sampling cylinder and the weight was measured after the cylinder was filled with the gas (m_f). Once this was done, the gas (C_1 or C_3) was injected into the Live-oil cylinder (m_{ail}) from the gas sampling cylinder. Then, the weight of the empty gas sampling cylinder was accurately measured. Moving ahead, the weight of the gas (C_1 or C_3, m_g) which was injected into the. Live-oil cylinder was calculated ($m_g = m_f - m_{ail}$). In the next step, the residual weight of the g.as (m_{res}) in the gas sampling cylinder was calculated as $m_{res} = m_{ail} - m_e$. Following this, pro.cedurewere repeated until the total amount of the gas was obtained (C_3 must be injected first due to its low pressure before C_1). Proceeding forward, after the required amount of the gas (C_1 or C_3) was injected into the Live-oil cylinder, it was pressurized to approximately 250 bar at a low flow rate of about 0.5 ml/min (but a higher flow rate can be used before the pressure begins to build-up) in order to get the required pressure of about 200 bar during mixing (Rotation). During the rotation period, the pressure drop due to the mixing must be monitored for the first two hours at 30 minutes interval and re-pressurised to the required (200 bar). Then, the Live-oil cylinder is placed into the rotation cell for 24 hours by noting the time of starting the rotation and the expected stopping timenext day. In the next stage, it is important to ensure that after 24 hours, the pressure drop is negligible to Live-oil is ready to be used. Lastly, the prepared Live-oil is mounted in its position in the oven.

Table 2. Composition of the saturating oils

Oil Type	C_1 (Mole %)	C_3 (Mole %)	n-decane (Mole %)
Live Oil A	20.14	-	79.86
Live Oil B	9.86	11.9	78.23
Dead Oil	-	-	100

Table 3. Type of oil with temperatures and MMP

Oil Type	Temperature °C	MMP bar
Live Oil A	50	105.6
Live Oil A	70	138.4
Live Oil A	90	165.3
Live Oil B	50	98.2
Live Oil B	70	132
Live Oil B	90	159.2
Dead Oil	50	96.6
Dead Oil	70	131.31
Dead Oil	90	158.88

1.2.Preparation of Core

Initially a fully saturated core wrapped with teflon tape and then covered with plastic sleeve as shown in figure 3.1. The plastic sleeve was made air tight by using a heat gun. For further prevention of contamination of the core, the core is covered with a thick rubber shown in figure 3.2. Then the core was placed in the core-holder. Lastly, the core holder was mounted in its position in the oven.

.- 

Figure 3.1. Preparation of the core (applying plastic sleeve)

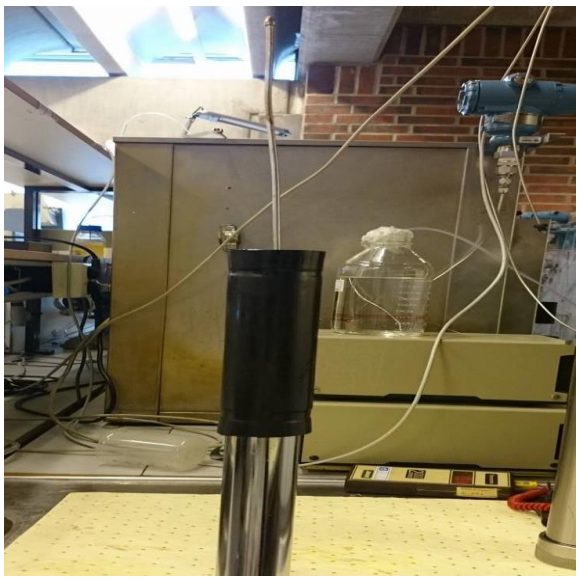

Figure 3.2. Preparation of the core (placing the rubber)

1.3.Before The Start The Experiment

These were some of the essential steps which were followed before the start of the experiment. First of all, it was ensured that the outlet valve OV-1 remained always open while OV-2 must only be opened when required. Secondly, it wasensured that the CO2 cylinder was isolated from both inlet (WV-6) and outlet (IV- 7, IV- 8 & MIV- CO_2). Thirdly, it was ensured that the Live-oil cylinder was also isolated from both inlet (WV-4 & WV- 5) and outlet (IV- 4, IV- 5, IV- 6 & MIV- Oil). Moving ahead, it was further ensured that both the Dead-oil cylinder inlet valve (MWV-Injection, WV2-Oil & WV3) and outlet valve (IV-1, IV-

2, IV-3 & MIV- Oil) were opened. During this time, a confining pressure of 40 bar and core pressure of 10 bar was created. While creating this pressure, all the air from the system was removed. The pressure was further built up to approximately 190 bars confining and 150 bars inlet pressures. After which the oven was turned on to the desired temperature (50^{o}C, 70^{o}C or 90^{o}C).Due to increase in temperature, the confining pressure, inlet pressure, Live oil pressure and dead oil pressure increased. Once the temperature and pressure became stable, the pressures were set to 200 bars inlet pressure and confining pressure to 240 bars. In the next stage, the connections to the three cylinders were secured and it was ensured that they were no leakages by placing tissues at the connection point to detect any kind of liquid leakage. Lastly, before the experiment started, it was ensured that the separator was empty whenever the outlet valves were used especially during the displacement of the Dead-oil with the Live-oil and also during the actual CO_2 flooding so that the exact produced volume could be measured accurately. Figure 3.3 shows the schematic of the setup of the experiments.

1.4.Creating of the Confining and Inlet Pressures in the Core

With the help of the following six steps, the confining and inlet pressures in the core were created: Firstly, an initial confining pressure of 40 bar was created around the core with Dead-oil inlet pressure of 10 bar created inside the core. Secondly, the oven was turned on to the required temperature (50^{o}C, 70^{o}C or 90^{o}C) as dictated by their corresponding Minimum Miscible Pressure (MMP). Thirdly, the confining pressure and the Dead-oil pressure in the core were increased in a step-wise manner with a difference of 40 bar between the confining pressure and the core pressure. In the next step, the temperature of the oven was left to stabilize, the waiting period was depending on the experimental temperature. While stabilizing, the temperature caused the pressure in the Live-oil, dead-oil and the confining pressure to increase. Hence, it was reduced especially the Live-oil to approximately 200 bar since it was initially high.The confining pressure was reduced using its appropriate bleed valve while the pressure in both the Dead-oil and the Live-oil were bleeded off using the water line and valves. Lastly, after a desired confining pressure of 240 bar and dead-oil (Core) pressure of 200 bar was created, both the dead-oil inlets (WV-3) and outlets (IV-1, IV-2, IV-3 & MIV-Oil) were isolated or closed.

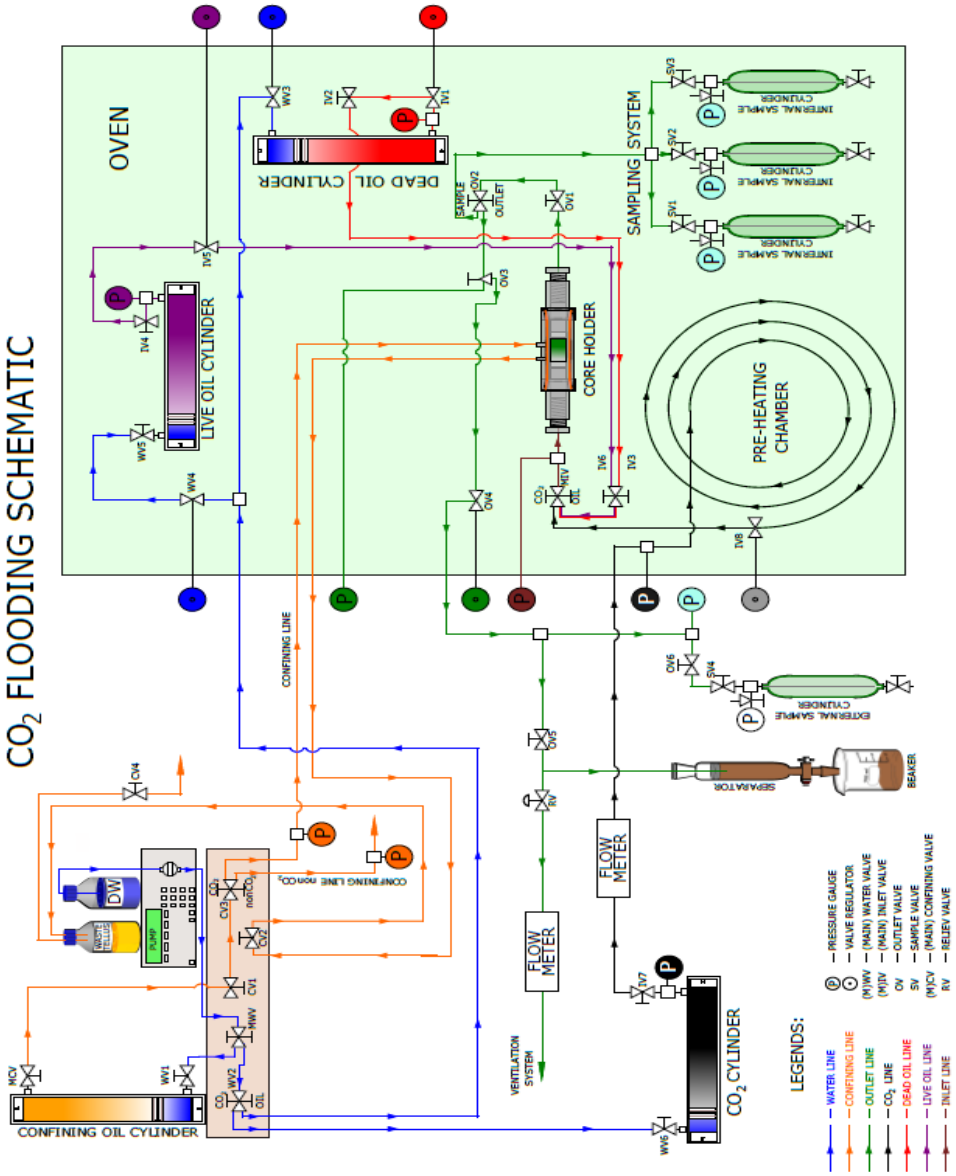

Figure 3.3. CO_2 flooding schematic

1.5.Displacing the Dead-Oil with the Live – Oil

For effectively displacing the Dead-oil with the Live-oil, several steps were taken. First of all, the water flow-line to the Live-oil cylinder was pressurised to approximately the same pressure of the live-oil (i.e. 200 bars) before opening the water line valve (From WV-1 through to WV-2 and to WV- 4) at a flow rate of 0.1 ml/minute. Moving ahead, the water line between MWV-Injection to WV-4 was pressurised to approximately the same pressure as the Live-oil before opening WV- 4. Once this was done, the pump pressuring the piston behind the Live-Oil with water, IV-4 was gently opened for the flow line between IV-4 and IV-5 to

be pressurised to the same pressure as the Live-oil 200 bar. In the next stage, after the pressure equilibrium had been established between IV-4 and IV-5, IV-5 was gently opened for the flow line between IV-5 & IV-6 to be at approximately the same pressure as the Live-oil. Moving ahead, after the pressure in the line hadestabilised, IV-6 was opened for the pressure in the flow line between IV-6 &MIV-A to reach a stable pressure. Next, after a stable flow-line pressure had been established up to MIV-A, MIV-A was opened. Now with both outlet valve OV1 & OV-2 opened, the Live-oil was used to displace at least 1.5 PV. Lastly, after displacing 1.5 PV with the Live-oil, the Live-oil was isolated and the system-up was allowed to achieve equilibrium for approximately 2 hours.

1.6.Producing Two Pore Volume of the Live-Oil

For producing two pore volume of the Live-oil, the following five steps were followed. Firstly, after a minimum of 2 hours were elapsed for the live-oil to attain equilibrium in the core, 2 PV of the Live–oil were produced at a low flow rate (0.05ml/in to 0.1ml/min) to ensure efficient displacement of the Dead-oil with the Live-oil. Secondly, the OV-2 was opened to a small volume and its pressure drop was monitored between the inlet and the outlet which was kept as small as possible (not more than 2 bar). Thirdly, after producing two PV of the Live-Oil, the outlet (OV-2) and the inlet valves of the Live-oil were closed (MIV-Oil, IV-6, IV-5 & IV-4) but OV-1 remained open always. In the fourth step, the Live-oil water inlet (WV-5 & WV-4) was isolated. Lastly, the WV-2 was directed towards the CO_2 water flow- line.

1.7.Actual CO_2Flooding

During actual CO2 flooding, in the first step, it was ensured that both the Dead-oil and the Live-oil cylinder inlets (WV-3 and WV-4, WV-5 respectively) and outlets (IV-1, IV-2, IV-3 and IV-4, IV-5, IV-6 respectively) and the MIV-Oil were isolated. In the second step, the flow line between MWV and WV-6 was pressurised to approximately the desired pressure of the CO2 (200bar) before the WV-6 was opened. In the third step, it was necessary to wait for the pressure equilibrium to be established between the CO2 and the water behind the piston of the CO2 cylinder before opening IV-7. Moving ahead, in the next step, once the IV-7 was opened, it was important to wait for the pressure in the CO2 flow line (Pre-heating chamber) to reach equilibrium for about 1 hour before opening IV-8. Once this had been done, the MIV-CO2 was opened to allow equilibrium to be achieved between the inlet and the

outlet of the core which usually takes not less than 3 hours preferably overnight. During this time, with the water valves to the CO2 cylinder were still opened at a low flow rate of 0.2 to 0.5ml/min , the outlet valve (OV-2) was opened very slowly and to a small capacity (OV-1 was always kept opened). In the last stage, it was ensured that the pressure drop between the inlet and the outlet was very small (<= 0.1) to ensure piston-like displacement.

Figure 3.4. CO_2 flooding set up

1.8.Sampling

During the experiment three sets of samples were taken. One set of sample was taken in the very initial stage of the experiment to capture the state of the core in the initial time. In the first set of sample. The first sample was taken inside the oven at the specified temperature (50°C, 70°C and 90°C) and 200 bar. Similarly the second set of samples were taken close to or before breakthrough. The second internal sample was taken inside the oven at the specified temperature (50°C, 70°C and 90°C) and 200 bar. The second external sample was taken outside at the room temperature and pressure. The final set of samples were taken after the breakthrough was acheived and the core was at its decline phase. The thrid internal sample was taken at the specified temperature (50°C, 70°C and 90°C) and 200 bar whereas, the external sample was taken outside the oven at the room temperature and pressure.

1.8.1. Analysing the samples

After the collection of six samples for each experiment, CO_2 absorption method was applied on each sample. The maximum amount of CO_2 was absorbed in NaOH as shown in the CO_2 set up in figure 3.6 and the light gases/components were collected in balloons for further analysis through GC. Titration was performed on the NaOH absorbing CO_2 for estimating the mass of CO_2.

Figure 3.5. GC for analysing the gas samples

Figure 3.6. CO_2 absorbtion apparat

2. MAIN RESULTS AND DISCUSSION

In this section, the main results and discussion are presented in detail. The section is divided in two parts. In the first part experimental results are discussed, the recoveries of oil by saturating the core from different model oils and crude oil with both, light components as a part of the composition of the oil (Live Oil A and Live Oil B) and light oil components injected along with CO_2. Whereas in the second part these experimental results are compared with the results achieved from numerical simulation in order to verify the results.

4.1. Experimental Results

4.1.1. Model Oils

A total number of three model oils with the composition described in table 2were used for performing these experiments. The first three experiments discussed are for Live Oil A. Live Oil A consists of only 20.14% of methane and 79.86% of n-decane. The first experiment was performed at 50°C and 200 bars. The core used for this experiment was Bentheimer sandstone which was initially saturated with n-decane and then aged for approximately two weeks in the aging cell. With the PV of 13ml and porosity 0.217, length of the core was 5.07cm.The core was mounted in the core holder and placed inside the oven. The confining pressure in all the experiments was kept 40 bars above the inlet pressure. In this case, it was kept at 240 bars with the inlet pressures of 200 bars. The first inlet pressure was build up by injecting 2 PV of dead oil (only n-decane) in the core. This injection took around a day. After producing 2 PV of dead oil, Live Oil A was injected in the core. 4 pore-volume of Live Oil A was produced, 2 pore-volume with a slow rate injection and 2 pore-volume with fast rate in order to fully saturate the core with Live Oil A. The range of rates for this experiment remained in between 0.005ml/min to 0.5ml/min. At this point of the experiment, the initial oil saturation of the core was 100%. All these experiments were performed without water. Finally the main CO_2 flooding experiment was performed. $CO_2$was injected in the core at 200 bars above the MMP which was 105.6 bars and the first two samples were taken immediately after stabilizing the pressures of the experiment. The analysis of the composition of oil obtained through samples will be discussed in detail, later in this chapter. Following the steps described in section 3.8, the other two samples were taken before the breakthrough. The final set of samples was taken at the decline phase after the breakthrough. Keeping the rate constant, the pressure inside the core was allowed to decline. Throughout the process the readings were recorded after every hour. These reading included the time, inlet and out pressures provided

by flow view, the pump rate, confining pressure and volume of the produced oil in the separator. For Live Oil A, the calculations performed are described in the table 4.1.

Table 4.1: Calculated recovery for the Live Oil- An experiment at 50°C

Time min	Pinlet bars	Poutlet bars	Density g/cm3	Pconfining bars	Qpump ml/min	injected PV	Cum Vol ml	Recovery
0			0			0	0	0
36	209.78	209.75	0.79415	240	0.2	0.21515	2.5	19.23077
51	208.2	208.17	0.79257	240	0.2	0.304975	4.5	34.61538
438	202.49	202.46	0.78686	240	0.3	7.657808	6	46.15385
498	202.35	202.33	0.78673	240	0.3	8.79797	7.5	61.53846
589	203.97	203.95	0.78835	240	0.3	10.52366	8	63.84615
626	203.42	203.42	0.78782	240	0.3	11.22579	8.3	63.84615
650	204.06	204.04	0.78844	240	0.3	11.68087	8.5	65.38462
692	198.42	198.4	0.781693	240	0.3	12.48412	8.8	67.69231
724	199.41	199.34	0.783283	240	0.3	13.09489	9	69.23077
746	176.23	176.18	0.744097	240	0.3	13.5369	9.15	70.38462
826	6.21	6.24	0.10505	50	0.3	24.92195	9.18	70.61538
							13.68	

The density of the Live Oil A at 50°C was 0.7515 g/cm^{3,} the molar volume was 146.69 cm³/mol and the viscosity of the oil at 50°C was 0.5845 cP. The total recovery including all the samples was 70.61% which means the residual oil for this experiment was approximately 29.39%.

A similar experiment was performed at 70°C to observe the effect of temperature on the recovery of oil as well as the effect of light component on mass transfer mechanism. In the case of Live Oil A, the only lighter component involved was methane. The core used for this experiment wasBentheimer sandstone. Both Bentheimer and Berea sandstone are not widely different from each other; therefore, both of the sandstones were used in performing different experiments by neglecting their differences. The length of the core was 9cm and the diameter was 3.78cm. Using the weight before and after saturation of the core, pore-volumewas calculated to be 21.745ml and the porosity was 0.215. The pressures for this experiment were

kept to be within the miscibility condition. The MMP for this experiment was 138.4bars. The density of the oil at 200 bars and 70°C was calculated to be 0.7375 g/cm³ with the molar volume 149.48 cm³/mol and viscosity of 0.4928 cP. It can be seen that the viscosity and density are reduced at 70°C with an increase in the molar volume which reflects the effect of temperature on the experiment. The increase in temperature enhances the recovery by 10%. The total recovery for this experiment was 80.01%.

The final experiment performed using Live Oil A was at 90°C. The core used for this experiment wasBentheimer sandstone with the length of 9.01cm and diameter of 3.78cm. Most of the cores used in the further experiments were of the same dimensions. The porosity of this core was 0.197 and the pore-volumewas 20.18ml.Keeping the temperature constant at 90°C, the pressures were kept above the MMP of 165.3bars. The molar volume for this experiment was 152.54cm³/mol. Density and viscosity of Live Oil A at 90°C were determined to be 0.7227g/cm³ and 0.4026cP respectively. A further decrease in the density and viscosity is observed with the increase in the temperature causing the recovery to increase with further 4% from the previous temperature. The recovery for Live Oil A at 90°C was calculated to be 84.24%.

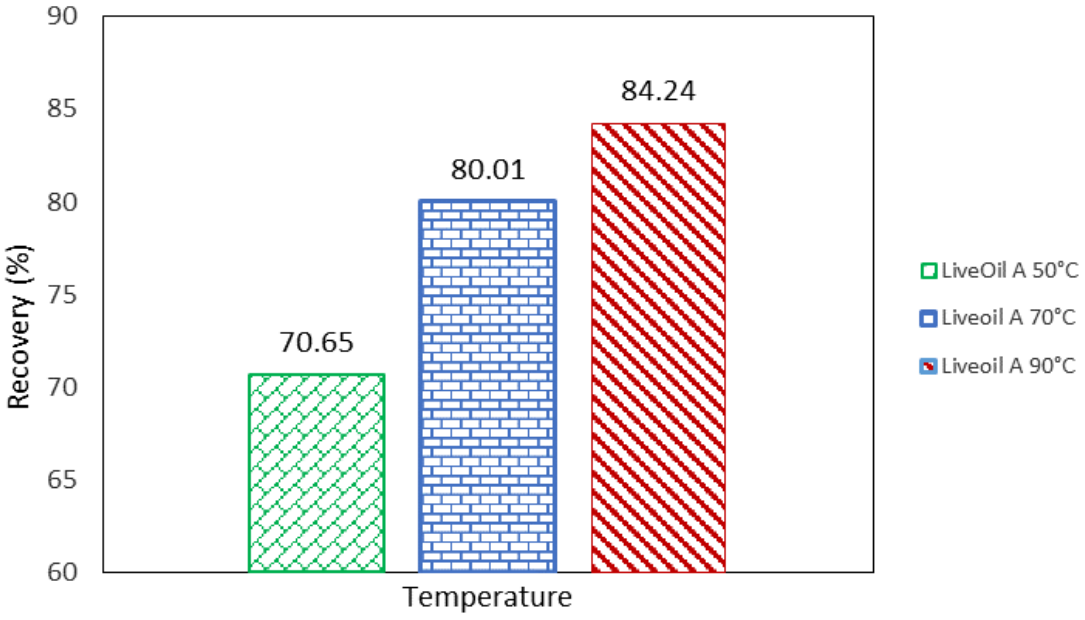

Figure 4.1. Comparison of oil recoveries with Live Oil A at 50°C, 70°C and 90°C

The main mechanism ruling the oil recoveries are usually diffusion, capillary forces, gravity drainage and total pore compressibility. Any of the mechanism can be dominant

depending on the reservoir properties. Gravity drainage is because of the density difference between the injected gas and the oil. Viscous flow can also be prominent in the high permeable matrix media. Figure 4.1shows a gradual increase in the recovery with the increase in the temperature. Highest recovery is obtained at the highest miscible conditions (90°C and 200 bars).

All the experiments are conducted at approximately 200 bars but with different respective temperatures. The viscous stability enhances with the increase in the flooding conditions due to which the highest recovery is obtained at the maximum temperature used in the experiments. Figure 4.2 shows that thepore-volume of CO_2 injected during the three experiments for Live Oil A decreases with the increasing miscibility conditions of the experiments. The experiment for Live Oil A with the lowest temperature that is 50°C shows the highest pore-volume of CO_2 injected. However, the earliest breakthrough is observed in the experiment conducted at 90°C. The density of CO_2 decreases with the increasing temperature, as in this case it decreases from 0.794g/cm^3 at 50°C and 200 bars to 0.535 g/cm^3 at 90°C and 200 bars. Therefore, at lower density the CO_2 becomes comparatively more mobile and less viscous, the process of viscous fingering becomes prominent and occurs at the CO_2 front where part of CO_2 get saturated in oil and part of it displaces oil.

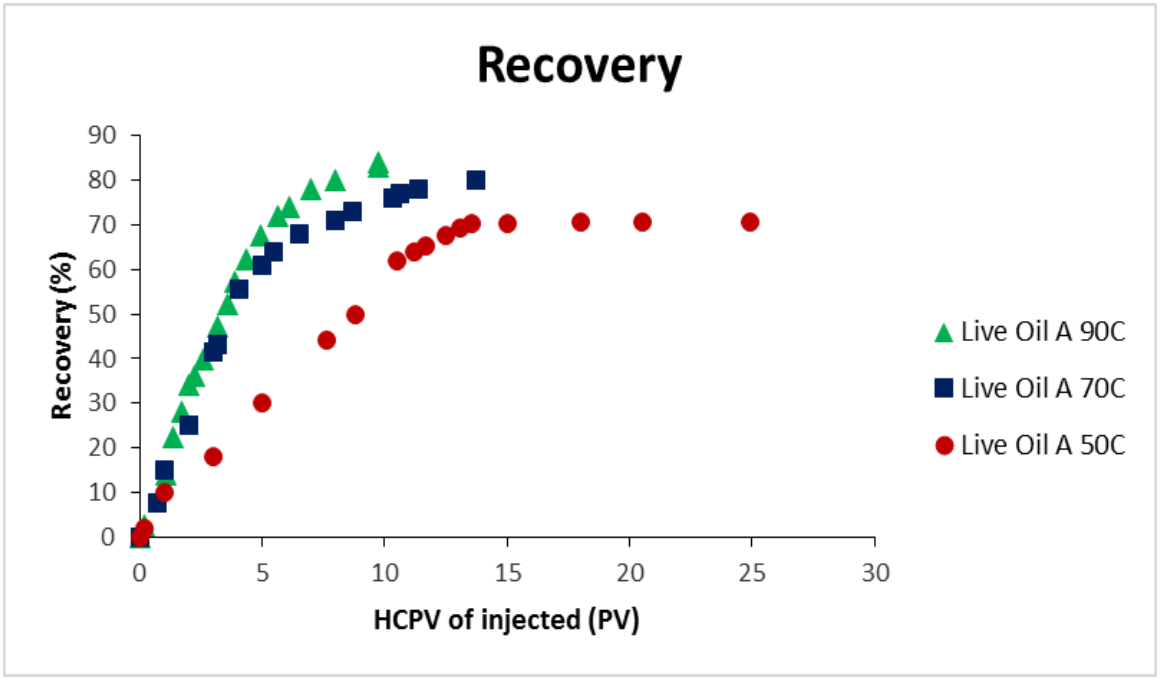

Figure 4.2. Comparison of oil recoveries as a function of injected pore-volume of CO_2 for Live Oil A at 50°C, 70°C and 90°C

Further, three sets of experiments were performed for Live Oil B at 50°C, 70°C, and 90°C. Live Oil B consists of two lighter components, methane, and propane. Methane was about 9.87%, propane was 11.9% and n-decane is 78.23%. The first experiment was performed at 50°Cwith a Bentheimer sandstone. The length and diameter of the core were similar to the previous core as well as the porosity. The experiment was performed above the MMP of Live-oil B at 50°C which was 98.2bars. The results obtained by this experiment were presented in table 4.2. The molar volume for this experiment was estimated to be 147.91 cm^3/mol. The density of oil at 50°C was 0.755 g/cm^3 and viscosity of the oil was 0.604cP. The recovery obtained after performing this experiment was the least recovery of all the experiments performed. 66.34% of the oil was recovered in this case. Another experiment was performed at 70°C with same dimensions of the Bentheimer sandstone. The PV for the experiment was 22.53ml. The MMP for this experiment was 132 bars. The molar volume noted for this oil was 150.65cm^3/mol and the density measured was 0.7412g/cm^3. The viscosity of the oil decreased to 0.5147cP with the increase in the temperature. The recovery achieved in this experiment was 77.67%. The final experiment performed using this oil was at 90°C using Bentheimer sandstone with nearly same dimensions and PV of 20ml. The molar volume of oil was 153.66cm^3/mol and density of oil was 0.7267g/cm^3. The viscosity of the oil had decreased to 0.4217cP. The recovery obtained at 90°C was 81.5%.

Table 4.2: Calculated recovery for the Live Oil B experiment at 50°C

Time min	Pinlet bars	Poutlet bars	Density g/cm3	Pconfining bars	Qpump ml/min	injected PV	Cum Vol ml	Recovery
0			0			0	0	0
58,18333	204,6	204,61	0,7376	240	0,5	1,614341	0,5	2,22618
105,1833	192,75	192,8	0,7189	240	0,25	1,987002	1	4,45236
141,1833	195,71	195,72	0,7237	240	0,1	2,164186	2	8,90472
415,1833	194,13	194,15	0,7212	240	0,175	2,646912	4,5	20,03562
441,1833	192,156	192,109	0,7179	240	0,175	2,692929	5,5	24,48798
503,1833	190,136	190,115	0,7144	240	0,175	2,803199	6,5	28,94034
563,1833	190,763	190,786	0,7155	240	0,175	2,909747	11	48,97596
664,1833	187,15	187,17	0,7093	240	0,3	4,141905	13	57,88068
1224,183	184,91	184,91	0,7053	240	0,3	11,01241	14	62,33304
1282,183	178,49	178,46	0,6934	240	0,3	11,73621	14,4	64,11398
1344,183	149,76	149,74	0,6279	240	0,3	12,59064	14,6	65,00445
1402,183	153,87	153,89	0,6391	240	0,3	13,37594	14,8	65,89492
1432,183	127,89	127,91	0,5529	240	0,3	13,84546	14,9	66,34016
1451,183	112,32	112,34	0,4668	240	0,3	14,19766	14,9	66,34016
1465,183	99,86	99,83	0,3615	240	0,3	14,53278	14,9	66,34016
1476,183	11,73	11,73	0,0202	240	0,3	19,2449	14,9	66,34016

Similar trends are observed in the case of Live Oil B and Dead Oil. Figure 4.3 shows the trend of increasing recovery with the increase in temperature and the opposite trend is observed in figure 4.4 decrease in injected PV of CO2 with the increase in temperature. Live Oil B consists of higher content of lighter components as compared to other model oils. The mass transfer mechanism taking place during the experiment will be discussed later in this section. The recoveries from Dead Oil with no lighter component are shown in figure 4.5 and the injected PV of CO2 is presented in figure 4.6. It was also observed in all the experiments of model oils that the amount of injected PVwas highest for Dead Oil at different temperatures and then Live Oil A and the least PV of $CO_2$was injected for Live Oil B.

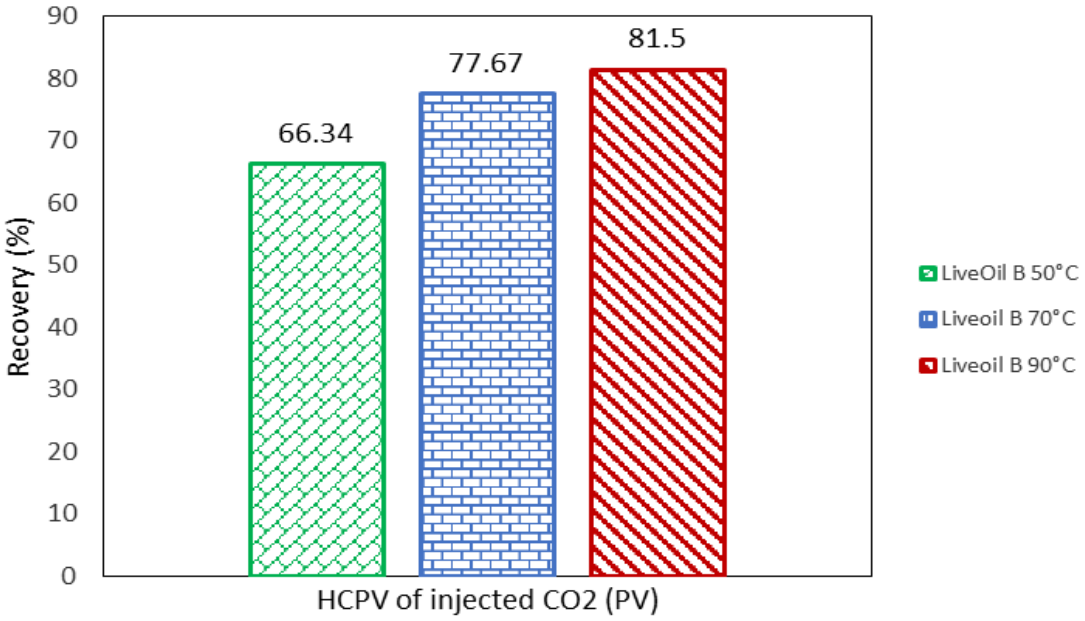

Figure 4.3. Comparison of oil recoveries with Live Oil B at 50°C, 70°C and 90°C

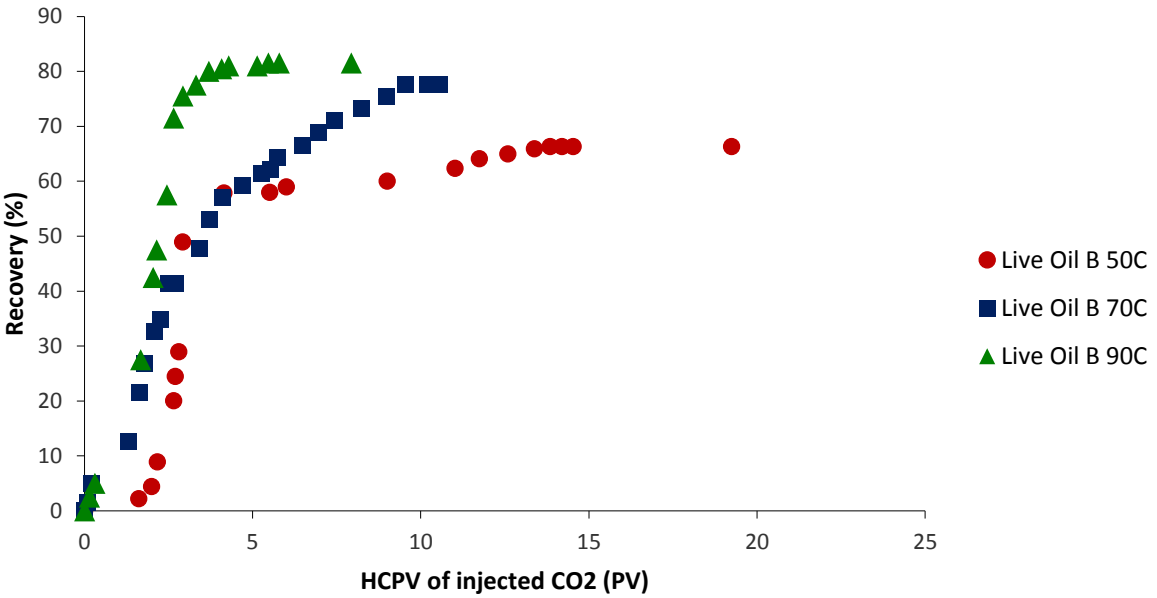

Figure 4.4. Comparison of oil recoveries as a function of injected PV of CO_2 for Live Oil B at 50°C, 70°C and 90°C

Another set of three experiments were performed for Dead Oil at 50°C, 70°C and 90°C. The composition of Dead Oil only included n-decane and no lighter components. The first experiment was performed at 50°C. The process of the experiment for Dead Oil was very much similar to the experiments of Live Oil A and B but with a slight difference in the

preparation stage. In these experiments 4 PV of Dead Oil was injected and then directly the main experiment of CO_2 injection was performed. Rest all the steps were similar to the previous experiments. The core used for the experiment of Dead Oil at 50°C was Bentheimer sandstone with the PV of 22.6ml. The molar volume for this experiment was 169.76 cm^3/mol whereas the density of the oil was 0.7894g/cm^3 and viscosity was 0.8457 cP. The next experiment for Dead Oil was performed at 70°C using Bentheimer sandstone with the PV of 22.28ml. The molar volume was estimated to be 172.33 cm^3/mol, density of the oil decreased to 0.7776 g/cm^3 and viscosity decreased to 0.7145 cP. The final experiment was conducted at 90°C. The core used was Bentheimer sandstone with the PV of 21.93ml. The molar volume was 175.13 cm^3/mol, density of the oil was 0.7652 g/cm^3 and the viscosity was 0.6175cP.

Table 4.2: Calculated recovery for the Dead Oil experiment at 50°C

Time min	Pinlet bars	Poutlet bars	Density g/cm3	Pconfining bars	Qpump ml/min	injected PV	Cum Vol ml	Recovery
0			0			0	0	0
43	208,06	208,8	0,79246	230	0,5	1,103596	0,259	1,146018
57	198,82	198,8	0,782403	235	0,3	1,257472	0,259	1,146018
101	198,69	198,68	0,782183	250	0,28	1,675187	0,859	3,800885
281	198,7	198,7	0,7822	230	0,15	2,886881	4,259	18,84513
369	197,91	197,9	0. 78086372	250	0,13	3,400474	5,259	23,26991
417	198,45	198,48	0,781777	230	0,125	3,669432	6,259	27,69469
482	198,91	198,89	0,782556	250	0,125	4,033284	7,759	34,33186
553	197,31	197,31	0,779849	255	0,125	4,432102	9,159	40,52655
618	198,21	198,22	0,781371	250	0,125	4,796506	10,259	45,39381
674	197,12	197,15	0. 77952704	260	0,125	5,111196	11,259	49,81858
752	196,64	196,64	0,778715	230	0,1	5,463103	12,059	53,35841
778	197,54	197,55	0,780238	230	0,09	5,568455	12,159	53,80088
1402	195,13	195,1	0,77616	230	0,09	8,110171	12,259	54,24336
1768	194,76	194,73	0,775534	260	0,085	9,519706	12,859	56,89823
1830	194,18	194,2	0,774553	240	0,12	9,857246	13,759	60,88053
1872	194,45	194,46	0,775009	240	0,12	10,08577	14,359	63,5354
1907	195,13	195,13	0,77616	240	0,15	10,32321	15,259	67,5177
1932	195,93	195,93	0,777514	240	0,15	10,49251	15,759	69,73009
2002	193,94	193,97	0,774146	240	0,22	11,19268	16	70,79646
2020	193,22	193,22	0,772928	240	0,22	11,37301	16,5	73,00885
2124	51	55	0,10784	100	0,41	25,26281	17	75,22124
							21,5	

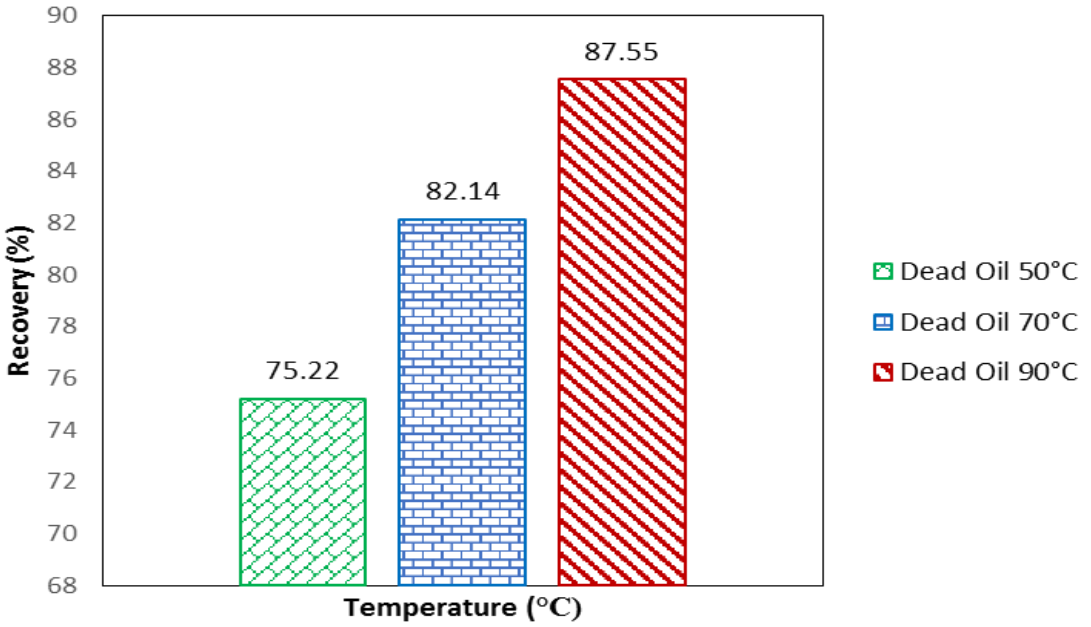

Figure 4.5. Comparison of oil recoveries with Dead Oil at 50°C, 70°C and 90°C

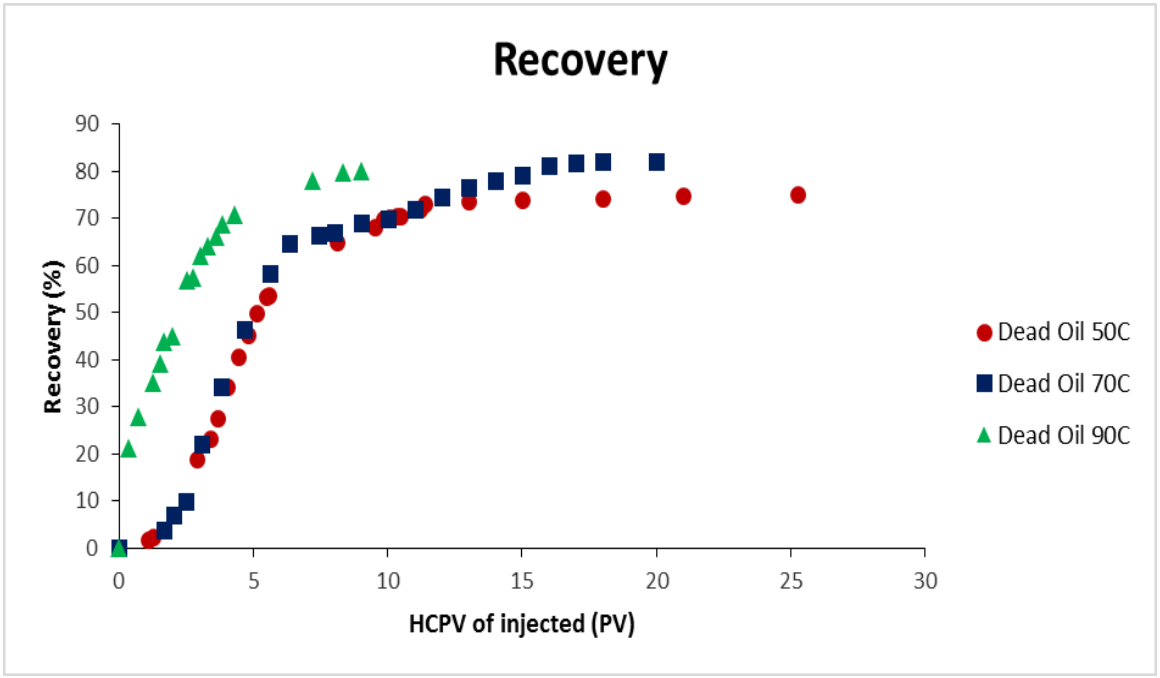

Figure 4.6. Comparison of oil recoveries with respect to injected PV of CO_2 for Dead Oil at 50°C, 70°C and 90°C

4.1.2. Comparison of the Results of Model Oils

CO_2 flooding experiments were carried out using different miscibility conditions and different composition of oils in order to determine the influence of light oil components on the oil recovery. The cores were saturated with Live oil A, Live oil B and Dead oil respectively and the CO_2 flooding was performed at 50°C, 70°C and 90°C. It can be easily observed that the higher the miscibility condition, the higher the recovery was achieved. The highest recoveries were obtained at 90°C for all the three oils. The results also show that the recovery decreased in the presence of the lighter components. Highest recovery was recorded with dead oil and the lowest was recorded with live oil B. This trend of decreasing recovery in the presence of the light components occurs due to the reduction in the mass transfer between oil and CO_2. This causes a decrease in the diffusion and solubility of CO_2 in the oil. Therefore, in the absence of the intermediate or light components, CO_2 flooding provides higher recoveries.

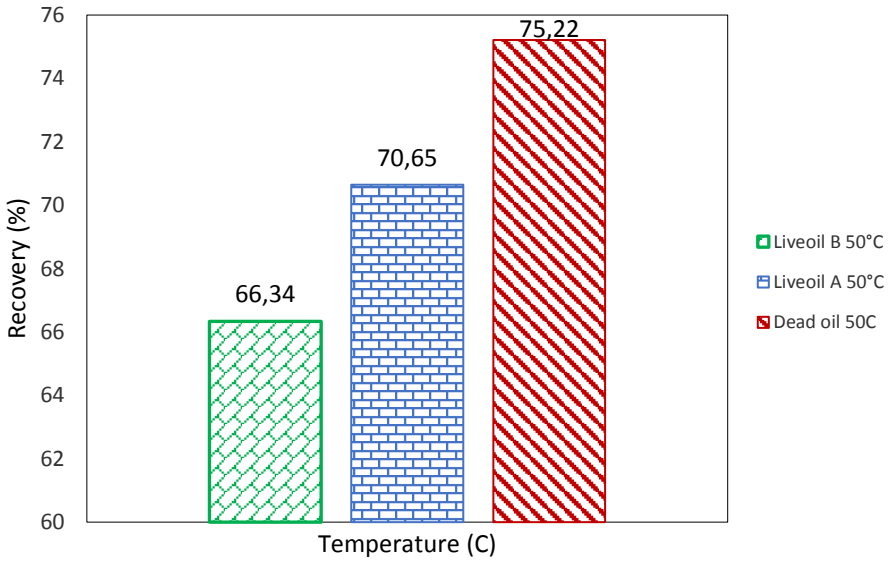

Figure 4.7. Comparison between the recoveries of Live-oil A, Live-oil B and Dead Oil at 50°C

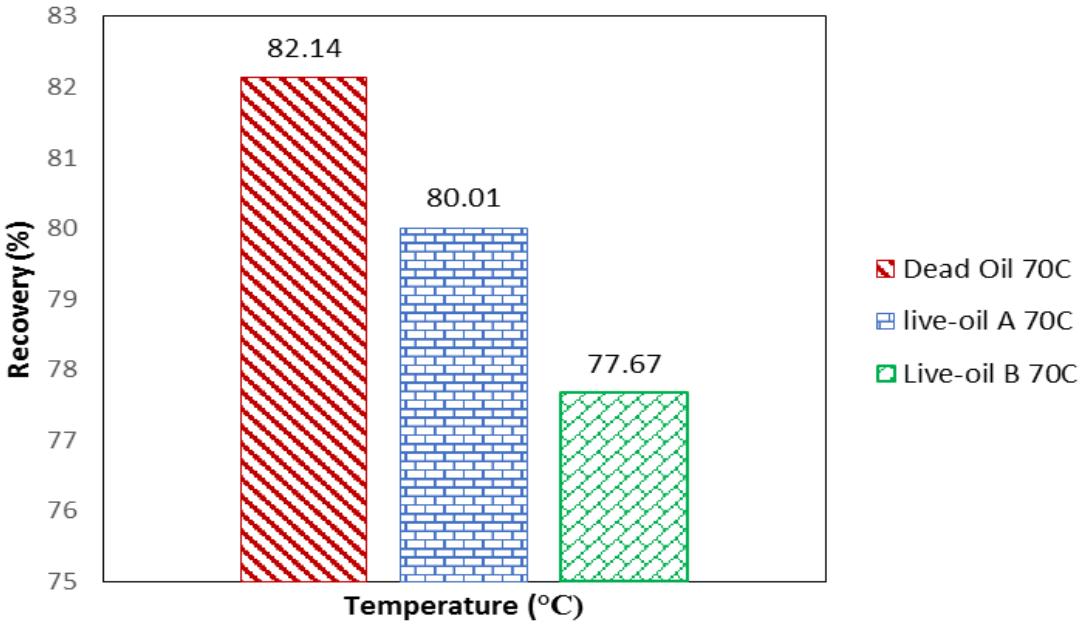

Figure 4.8. Comparison between the recoveries of Live-oil A, Live-oil B and Dead Oil at 70°C

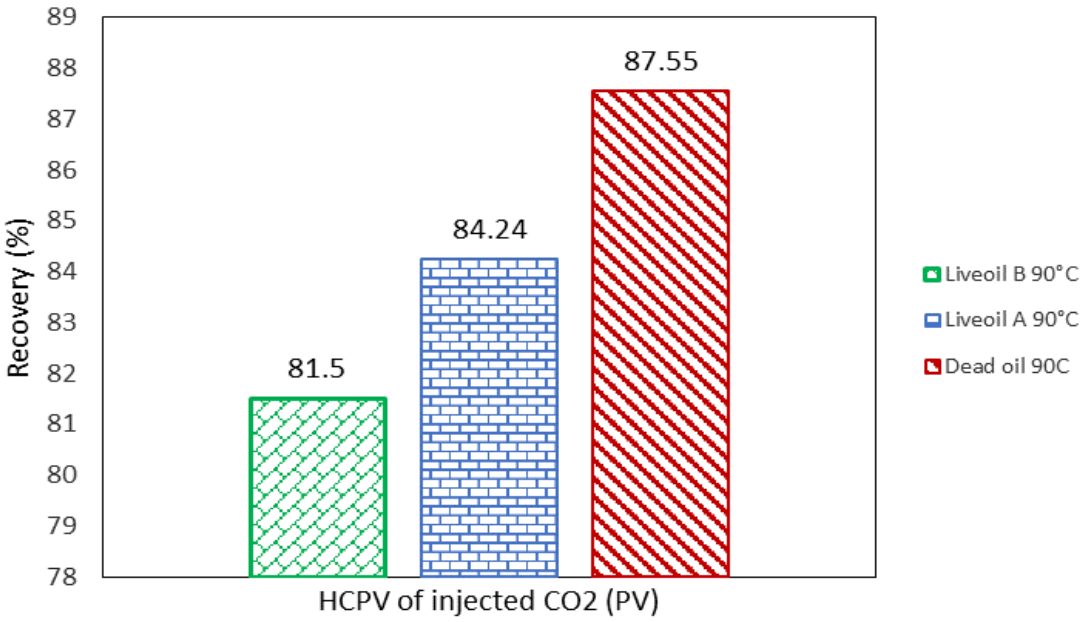

Figure 4.9. Comparison between the recoveries of Live-oil A, Live Oil B and Dead Oil at 90°C

4.1.3. Comparison of the Results of Model Oil and Crude Oil

The model oil used here for making a comparison with crude oil experiments was Dead Oil (n-decane only) without any lighter component. The core used for conducting this

experiment was Berea sandstone with a PV of 21.89ml. The core was initially saturated with Dead Oil and then aged for approximately two weeks. In this experiment, $CO_2$was injected with C_1 and C_3. The composition of this injected fluid was similar to the Live Oil B composition but in place of n-decane $CO_2$was used. CO_2 with C_1 and C_3were injected in the core at temperature and pressure above the miscibility condition that was at 70°C and 200 bars. The same process was repeated for this experiment. Three sets of samples were taken during the experiment at three different time intervals. The molar volume estimated for this experiment was 173 cm^3/mol, density of the oil was 0.78g/cm^3 and the viscosity of the oil was 0.699 cP. The recovery obtained in this casewas 84.51%.Model oils were compared with crude oil by conducting two experiments using crude oil. In one experiment, the core was initially saturated with crude oil and aged for two weeks and then CO_2 flooding was performed. The injected gas in this experiment was 99.99% CO_2which was flooded in a Berea sandstone of 22.24ml PV. The molar volume was 169.68 cm^3/mol, density was 0.7749 g/cm^3 and viscosity was 0.6942 cP. The recovery achieved in this case was 77.99%. The final experiment was performed on Berea sandstone with the PV 22.32 ml. The core was saturated with crude oil and then flooded with CO_2 with lighter components (C_1 and C_3). Same mole fraction of CO_2, C_1 and $C_3$was used as used in the dead oil experiment. The molar volume estimated was 170 cm^3/mol. The density of the oil was 0.732 g/cm^3 and viscosity was 0.653 cP. The recovery obtained was 80.20% in this experiment.

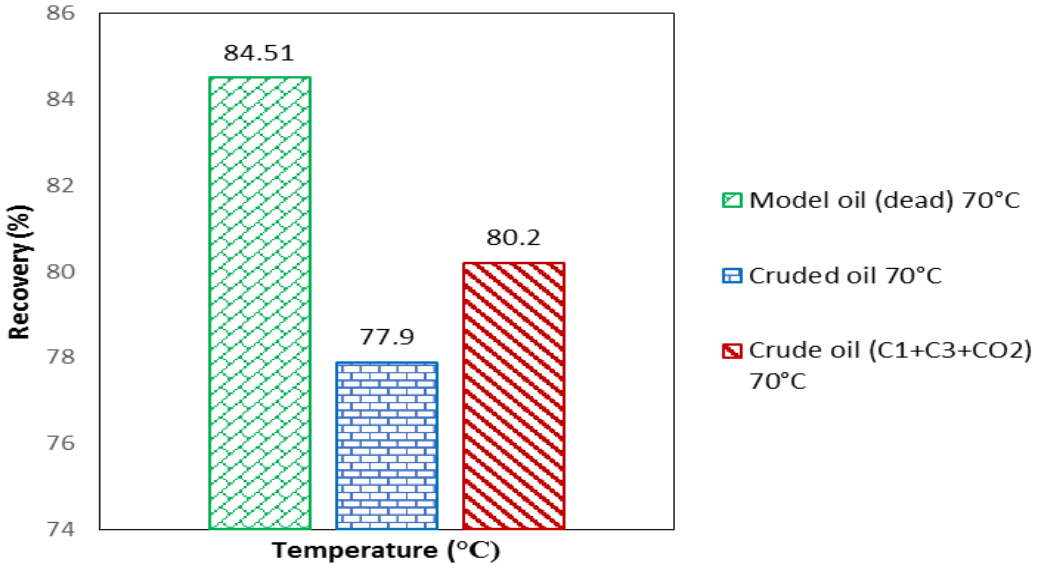

Figure 4.10. Comparison between the recoveries of Crude Oil flooded with CO_2 only, crude Oil flooded with CO_2 mixture(C1 and C3) and Model Oil (dead oil) flooded with CO_2 mixture(C1 and C3) at 70°C

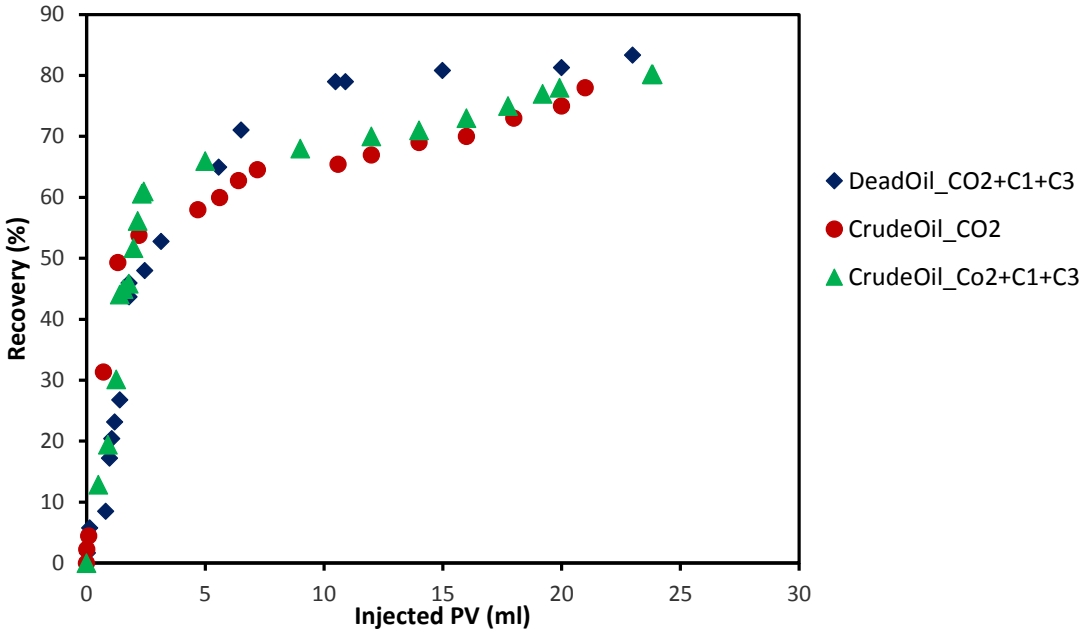

Figure 4.11: Comparison between the recoveries of Crude Oil flooded with CO_2 only, crude Oil flooded with CO_2, C1 and C3 and Dead Oil flooded with CO_2, C1 and C3 with respect to injected pore-volume of CO_2 at 70°C

Comparing these three experiments, it is quite evident that lighter components do have a huge impact on the results.

4.2. Numerical Simulation Results

In order to verify the results obtained from experiments, a numerical simulation model was developed using PVTSim Nova. The model created was then compared with the experimental results.

4.2.1. Effect of Light Oil Component on the Recovery of Oil

As mentioned earlier that while performing the experiments, six samples were taken in each experiment. Four samples before the break through and two after the breakthrough during the decline phase. Three samples were taken at these three times outside the oven that was at standard conditions while the rest three were taken inside the oven at the temperature and pressure set for the respective experiments. CO_2 from the samples wasabsorbed by using

Noah and the rest of the sample gas was evaluated through the Gas chromatograph which provides the mole percentages of different components present in the sample gas. The weight of CO_2 was calculated by performing titration of the NaOH in which CO_2 was absorbed. Further flash calculations were also performed using PVTSim to verify the results and study the mass transfer mechanism taking place inside the core during CO_2 flooding.

4.2.2. Vaporization of Light Oil Component

The injected CO_2 after coming in contact with the core matrix starts diffusing into the oil phase. It can be due to the concentration as well as a chemical potential gradient. With the passage of time, the CO_2 concentration in the oil phase starts increasing while releasing the intermediate and/or light components for gaining thermodynamic equilibrium. This mechanism is called vaporization. Then occurs the condensation process of these vaporized hydrocarbons and finally drive towards the production well (outlet). Due to the high mobility of the injected gas, the oil keep coming in contact with the fresh CO_2. In this process it keeps losing its light components and become saturated with CO_2. CO_2 being heavier than methane and propane continuously diffuses into the oil phase making it further denser and viscous. Thus in the Model Oil experiments, we have observed that Dead Oil has provided better recovery than Live Oils. In the absence of lighter components, CO_2 directly aid the oil in making it less viscous and less dense.

4.2.3. Effect of injected gas composition on the light oil component vaporization

The factors affecting the composition of the vaporized gas are temperature, pressure, injected gas and type of oil. The effect of the composition of injected gas on the vaporized process of oil is studied by varying the composition of the injected gas. For this purpose, two experiments are performed using a mixture of CO_2, C_1 and C_3. Figure 4.9 shows that the oil production is accelerated by richer gas injection. It is seen through the results that oil phase get lighter after coming in contact with this gas composition. The initial oil viscosity is reduced during gas injection. Vaporization of the components of oil phase is prevented by the lighter component in the injected gas phase. Because of this phenomenon, oil keeps losing its intermediate components and receives a lighter component from the injected gas to come into thermodynamic equilibrium phase with the injected gas. This yield higher mobility, lower viscosity and lower density for crude oil in the matrix.

4.2.4. Live Oil B Experiment at 70°C

Compositional profiles from experimental and simulation results predict the generation of miscibility. Normalized compositions of the different components of oil as well as of CO_2 (molar compositions of the components) as a function of hydrocarbon PV of CO_2 injected in the core are plotted in figure 4.12. The normalized molar compositions are used to show the trend of different components during the experiment. The experimental results show that NC10 with the highest composition (78.23) with respect to other components decreases throughout the experiment to its residual composition (0.4%). C_3 being originally higher in composition (11.9%) compared to C_1 (9.86%) also decreases with the injection of CO_2 but the residual is higher than C_1 probably because C_1 tends to finger through the reservoir ahead of the miscible bank (Holm, L.W. &Josendal, V. A., 1982). But methane has the potential to affect the MMP if it is present in an enough amount to raise the bubble-point pressure above what would otherwise be the MMP. Bubble-point pressure would then be regarded as the MMP, as Yellig and Metcalfe found in their experiments. The simulation results are comparatively a good match with the experimental results and are showing similar trends as experimental results.

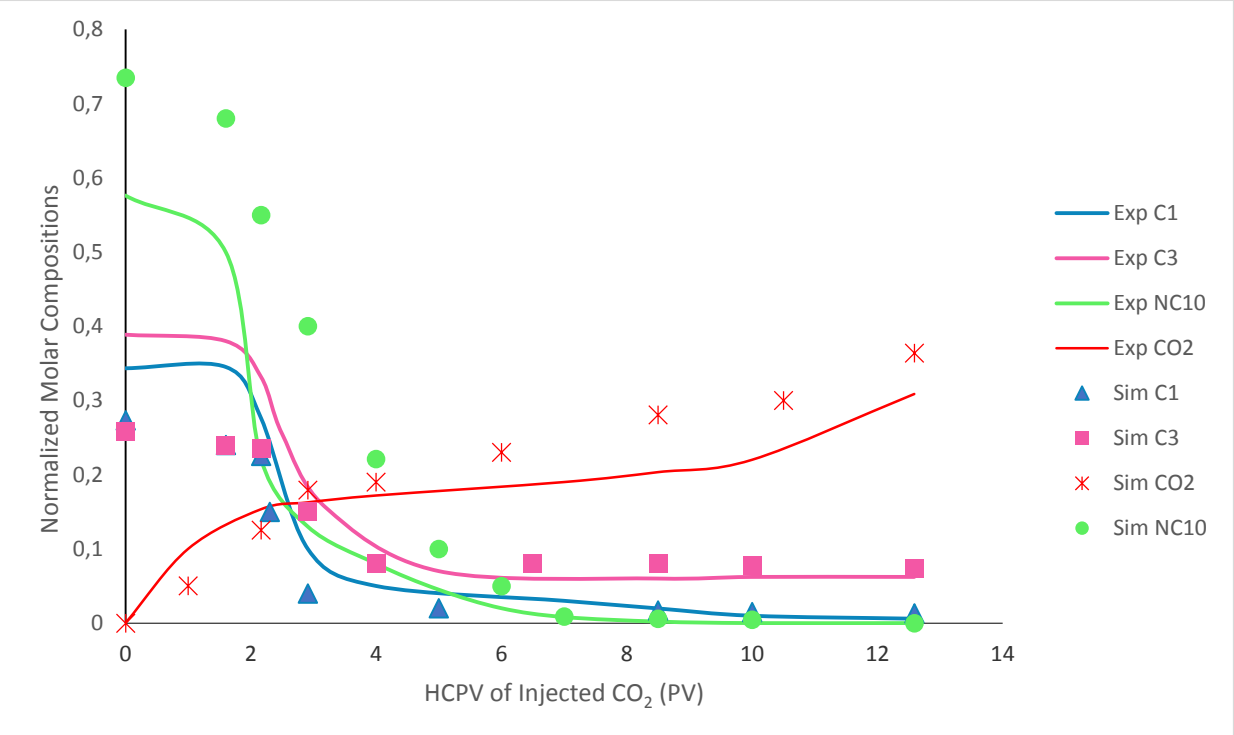

Figure 4.12. Comparison of simulation and experimental normalized molar composition as a function of injected PV of CO_2 for Live Oil B experiment at 70°C (displacing fluid, CO_2).

Figure 4.13 and 4.14 shows the GC and flash results of the sample cylinders. The flash calculation is performed in PVTSim using Peng-Robinson equation of state. The sample A1 (internal) was taken during the initial stages of the experiment at 2.164 PV of CO_2 injected. The sample cylinder A1 was connected inside the oven under 70°C. It can be observed from the figure 4.12 that during the collection of the first sample there is no CO_2 production may be because CO_2 has not mixed with the oil yet. Comparatively mass percentage of oil is the highest than other components i.e. 73.10 %. The produced mass percentages (C_1=7.74%, C_3=19.16% and n-decane=73.1%) of the components is quite similar to the actual composition of the oil (C_1=9.86%, C_3=11.9% and n-decane=78.23%). The sample B1 (external) was also taken at approximately at the same PV of CO_2 injected (2.164 PV) but the sample cylinder in this case was connected outside the oven at the room temperature and pressure. GC results of the sample B1 show differences than sample A1 because of the components flashed at the room temperature from 70°C and atmospheric pressure from 200 bars. Due to the time difference between the first external and first internal samples, their results were not a good match, similarly the simulation result in case of sample B1 for oil composition appears to be higher than experimental composition because the simulation results depict the condition of the core. The experimental results depend on the volume/mass of oil collected in each sample, which then affect the mass percentages of all other components due to which some differences can be observed in the experimental and simulation result for the sample B1. It can be seen that CO_2 has started to produce in the experimental result (16.66%), this may be due to the viscous fingering phenomenon taking place inside the core.

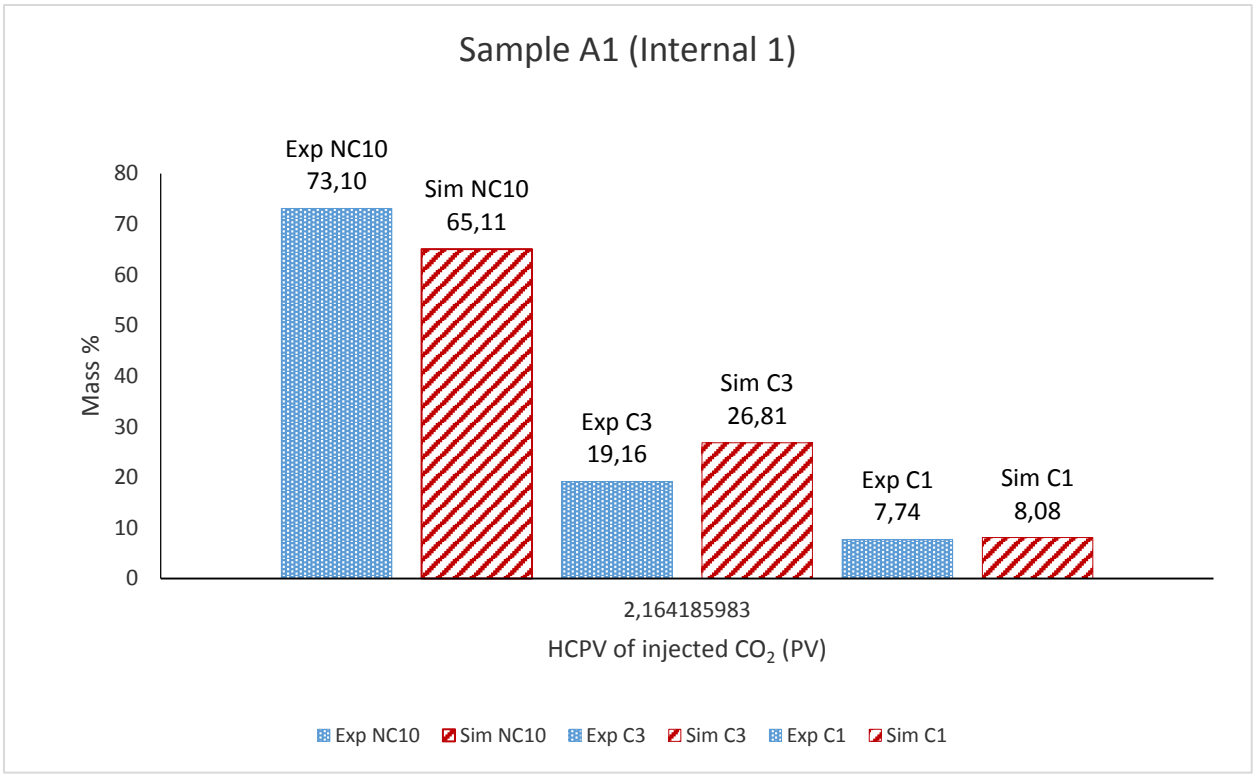

Figure 4.13. Comparison between the composition of the oil and CO_2 analyzed by experiments and numerical simulation for Sample A1 (Internal)

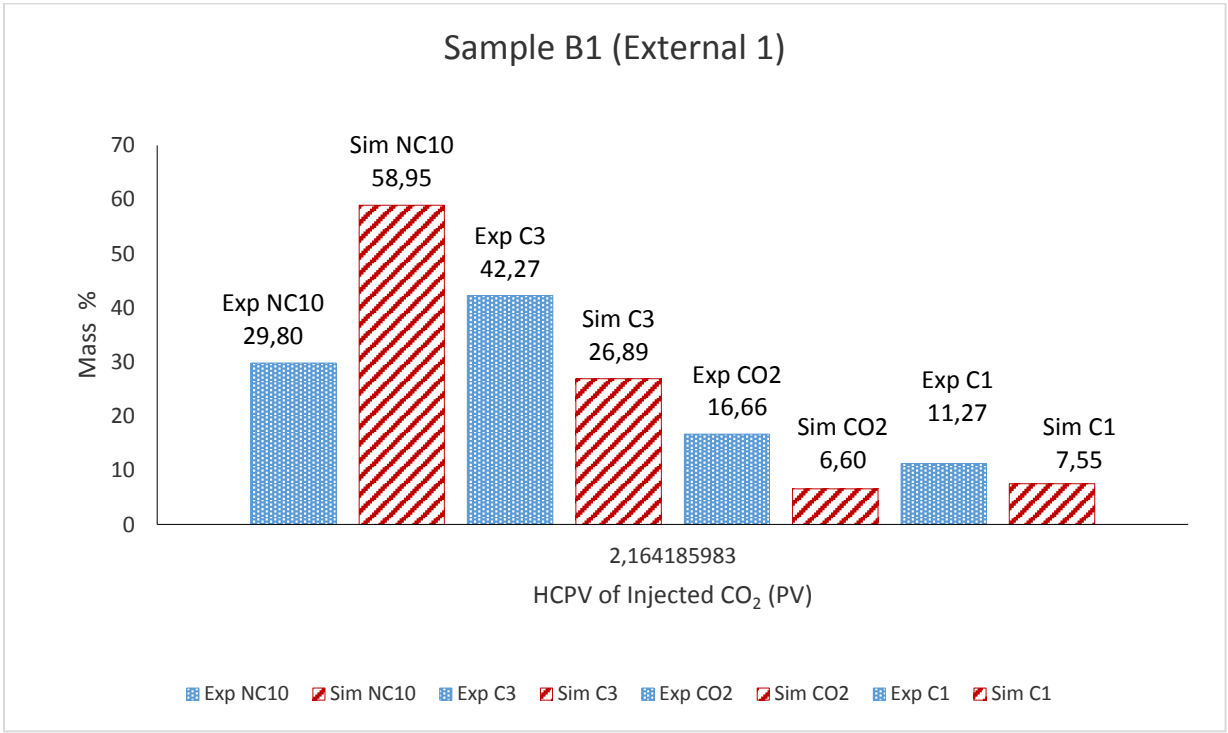

Figure 4.14. Comparison between the composition of the oil and CO_2 analyzed by experiments and numerical simulation for Sample B1 (External)

Sample A2 (internal) was collected inside the oven, before breakthrough at 4 PV. At 2.9 PV, CO_2 became an integrated part of the system. Figure 4.15 shows the mass percentages of different components in the system before breakthrough. The material balance of the experimental results for sample A2 explicates the increment in the CO_2 production to 25.7% which signifies that the injected CO_2 comes in contact with the oil and may start to diffuse into the oil phase because of the concentration and potential chemical gradient. With the passage of time the concentration of CO_2 starts to increase in the oil phase causing the oil to release its intermediate and light components which is called vaporization process for obtaining a thermal equilibrium in the system. The simulation and numerical results are in a close range for sample A2. Sample B2 (external) shows the nearly the same trend as sample A2, as it was collected right after sample A2 (15 minutes) and approximately the similar PV (2.909 PV). Figure 4.16 exhibits a considerable difference between the simulation and experimental result for C_1. The differences are possible because of the flashing of C_1 from higher temperature and pressure to atmospheric temperature and pressure or experimental errors in collecting the sample. As the produced CO_2 increased further, oil production was reduced to 4%.

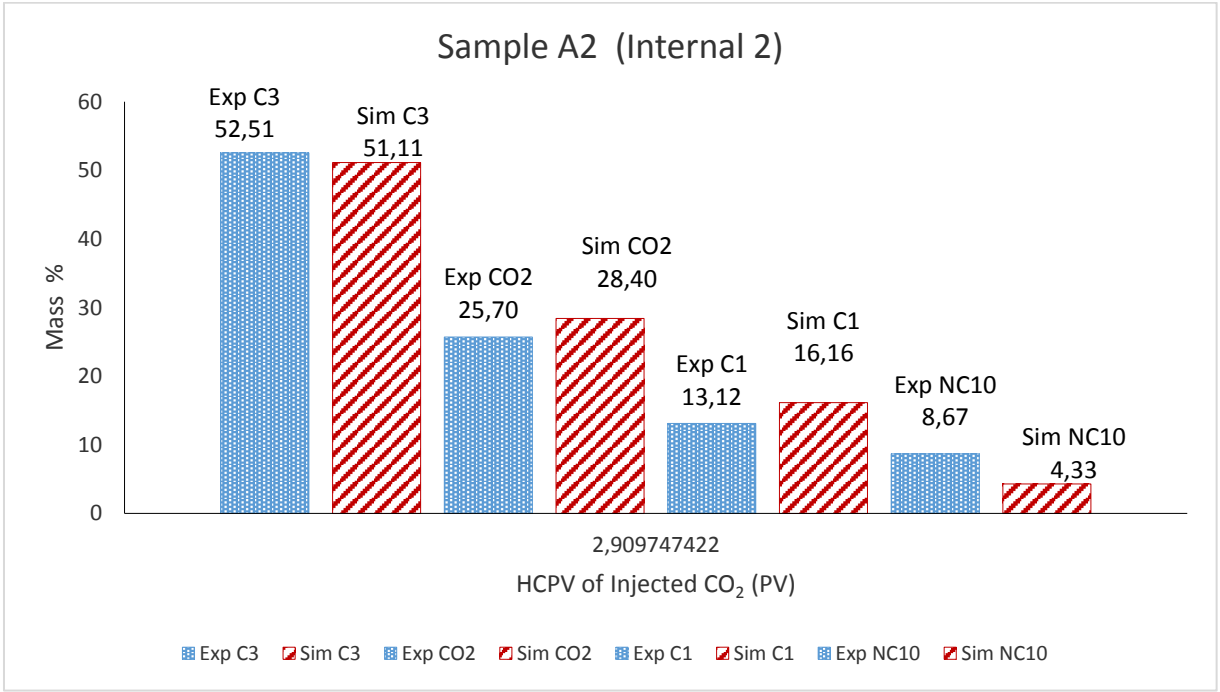

Figure 4.15. Comparison between the composition of the oil and CO_2 analyzed by experiments and numerical simulation for Sample A2 (Internal)

A3 (internal) was the third set of the sample collected during the experiment. This sample was collected inside the oven at 70°C after the breakthrough at 12.6 PV and the experiment was almost at its decline phase. In figure 4.16, we can see that the experimental results show only CO_2, C_3 and a very low composition of C_1. It means for the span of time this sample was collected, there was no produced oil (NC10). The experimental results are highlighting the production part of the experiment. In the decline phase mostly CO_2 is being produced (82.55%) with a very low C_1 and C_3 (16.66% and 0.79% respectively). Whereas, the simulation result are depicting the state of the core inside the oven. In the simulation result, highest mass percent was of CO_2 (64.7%) and comparatively lower masses of oil (2.12%), methane (17.53%) and propane (15.65%). After the experiment, this mass of oil represented by simulation result also includes residual oil left inside the core too. Sample B3 (external) sample is collected at the room conditions after a small difference of time (10 minutes).

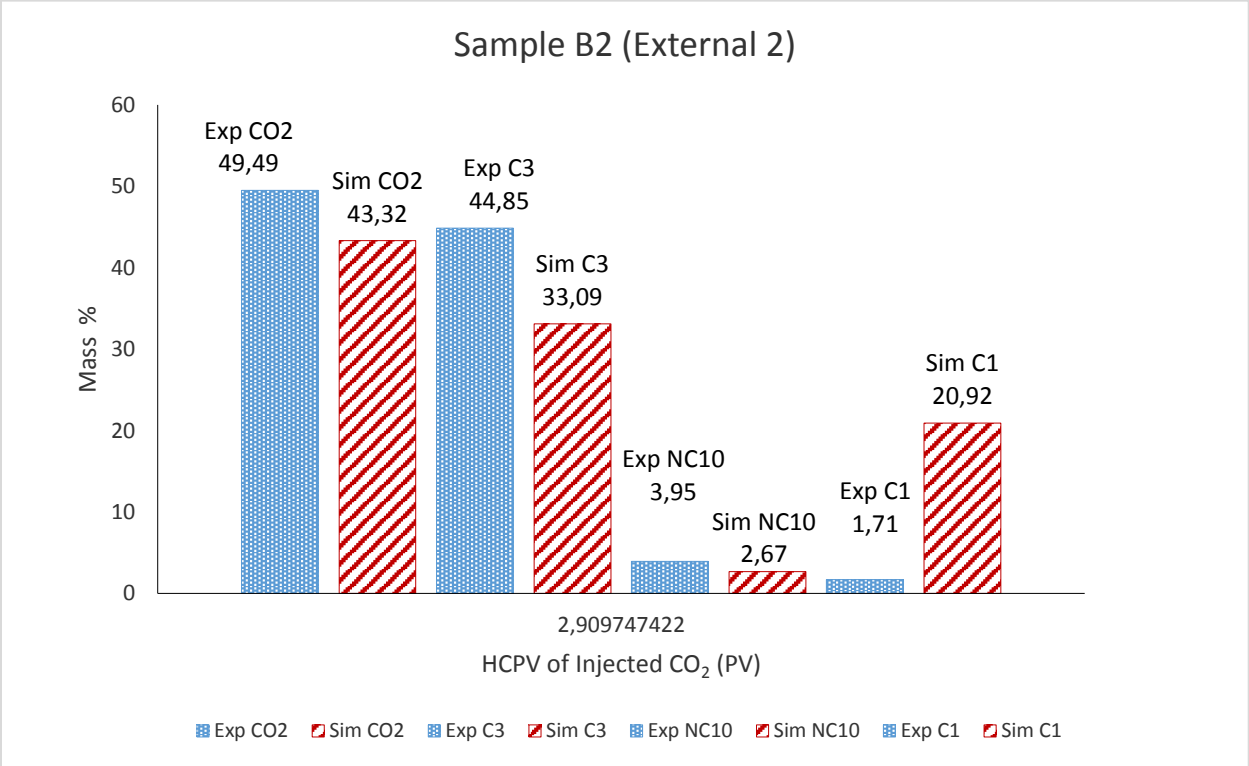

Figure 4.16. Comparison between the composition of the oil and CO_2 analyzed by experiments and numerical simulation for Sample B2 (External)

Figure 4.17 may represent the final compositions. Numerical simulation represents that 65% of CO_2 is present inside the core 4.14% is of oil and 0.74% and 30.64% of methane and propane respectively. The experimental results show what was being produced at the end stage of the experiment. As there is no oil produced in the end because the oil in the core has

reached to its residual saturation, it shows 71% of the CO_2 and 0.8% and 28% of methane and propane respectively. The compositions analyzed through experiments using GC and numerical simulation using PVT Sim reflects the mass transfer taking place inside the core during the experiment. Throughout the experiment, it can be seen that the lighter components are consumed during the experiment on the reaction with CO_2. Methane is the first component to be consumed as compared to propane.

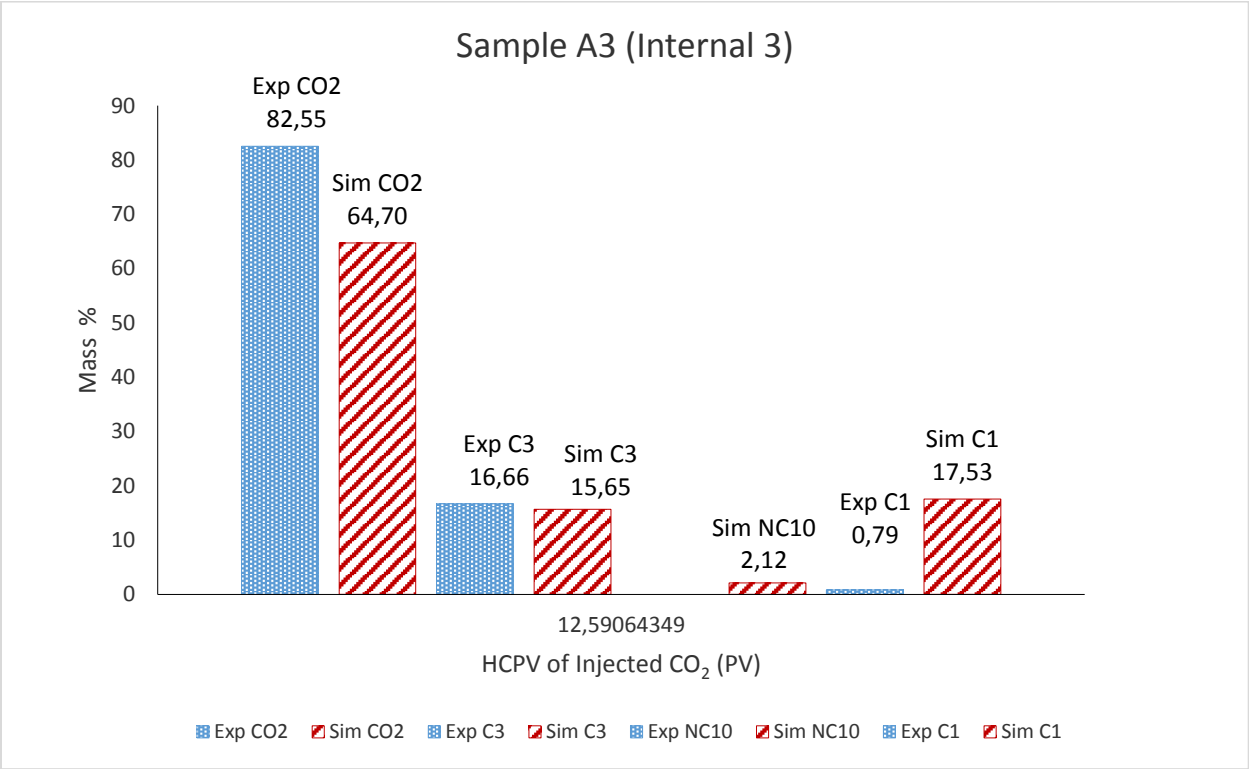

Figure 4.17. Comparison between the composition of the oil and CO_2 analyzed by experiments and numerical simulation for Sample A3 (Internal)

The overall mass change throughout the experiment provides an understanding of the selective extraction of the components from a solution of hydrocarbons (Live Oil B) because these selective components are more readily soluble in CO_2 than other components. The separation of hydrocarbons by the process of vaporization is severely affected by CO_2. According to the experiments performed on crude oil by Holm, L.W. &Josendal, V. A., 1982, the gaseous CO_2 is able to remove C6 and lighter hydrocarbon from the reservoir oil. In this, C_1 and C_3 are the lighter components extracted by CO_2. Dense gas or liquid CO_2 may extract and solubilize hydrocarbons as heavy as C_{30} and probably heavier than that. CO_2 first swells the oil by condensing into it and then shrinks the oil by extracting the lighter components

from it. It is also observed during the experiment that the light components particularly C_1 is initially produced and the heavy components in the later production stage which is also supported by the experiments conducted by Darvish G.R. (2007). The variation observed in the produced oil and gases composition is proposing the domination of the diffusion mechanism.

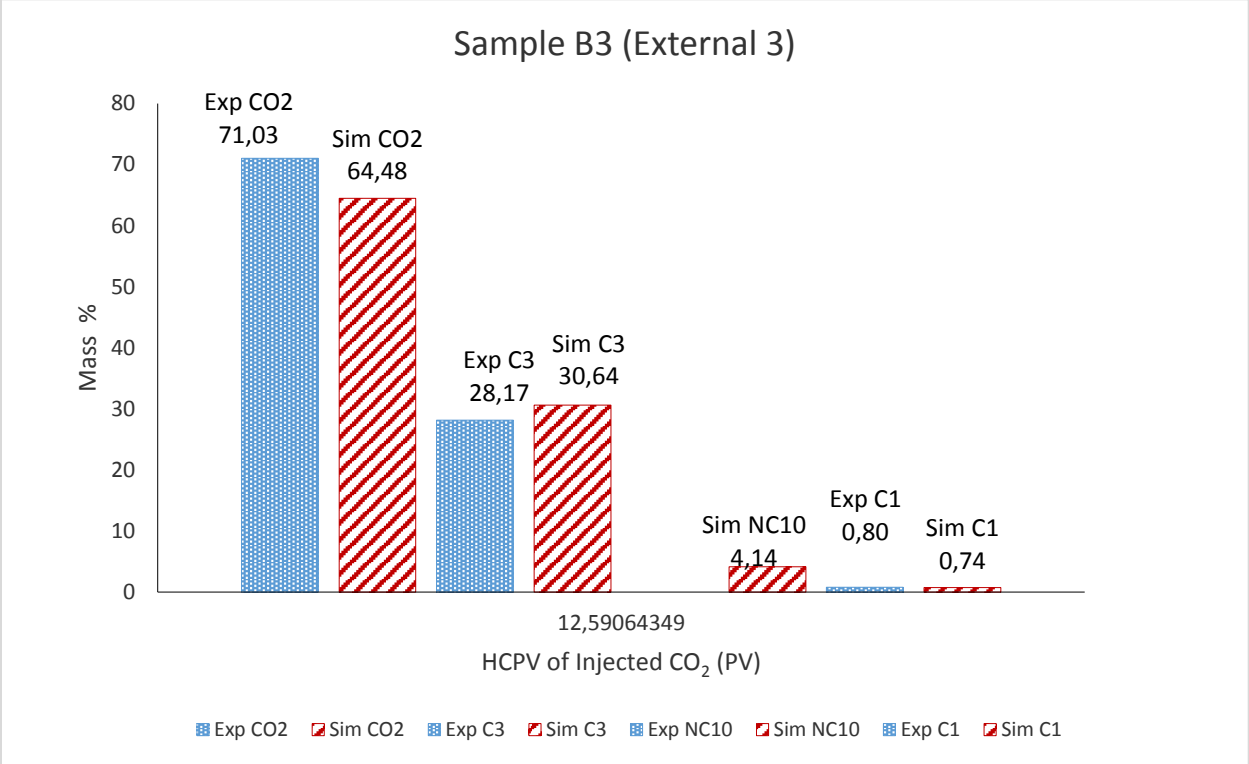

Figure 4.18. Comparison between the compositions of the oil and CO_2 analyzed by experiments and numerical simulation for Sample B3 (External)

4.2.5. Live Oil A at 70°C

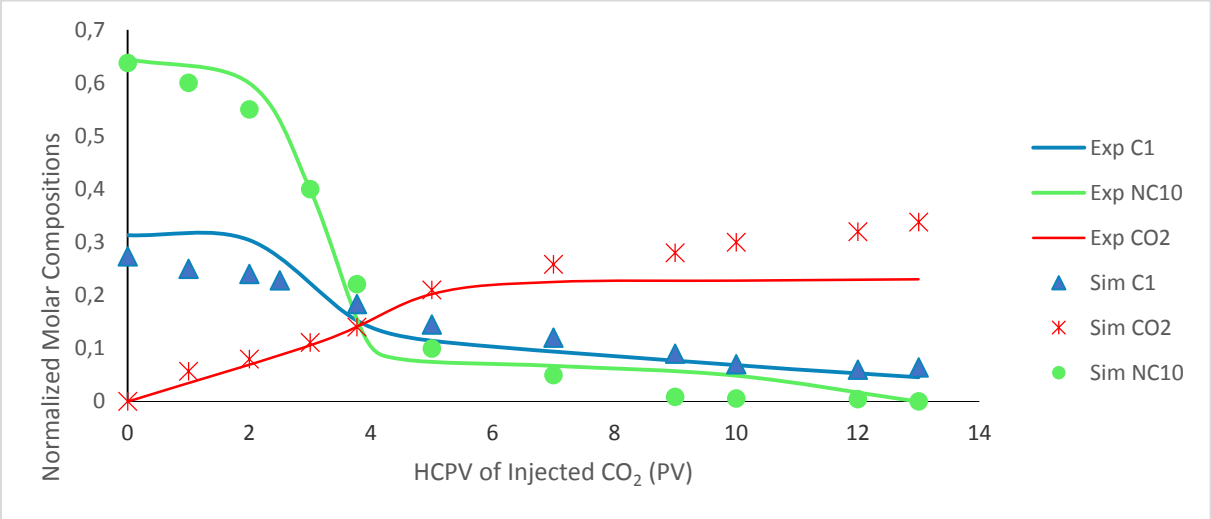

Figure 4.19. Comparison of simulation and experimental normalized molar composition as a function of injected PV of CO_2 for Live-oil A experiment at 70°C (displacing fluid, CO_2).

In this experiment, the saturating fluid was live-oil A with only one intermediate component i.e. C_1 and the displacing fluid is CO_2. The trend of the consumption of different components is highlighted in the figure 4.19. It shows the comparison between the experimental result and simulation results. The decrease in the composition of n-decane and methane is shown both in the experimental and simulation graphs whereas, the increase in the composition of the CO_2 with the increase in the hydrocarbon pore-volume of injected CO_2 are also noticeable.

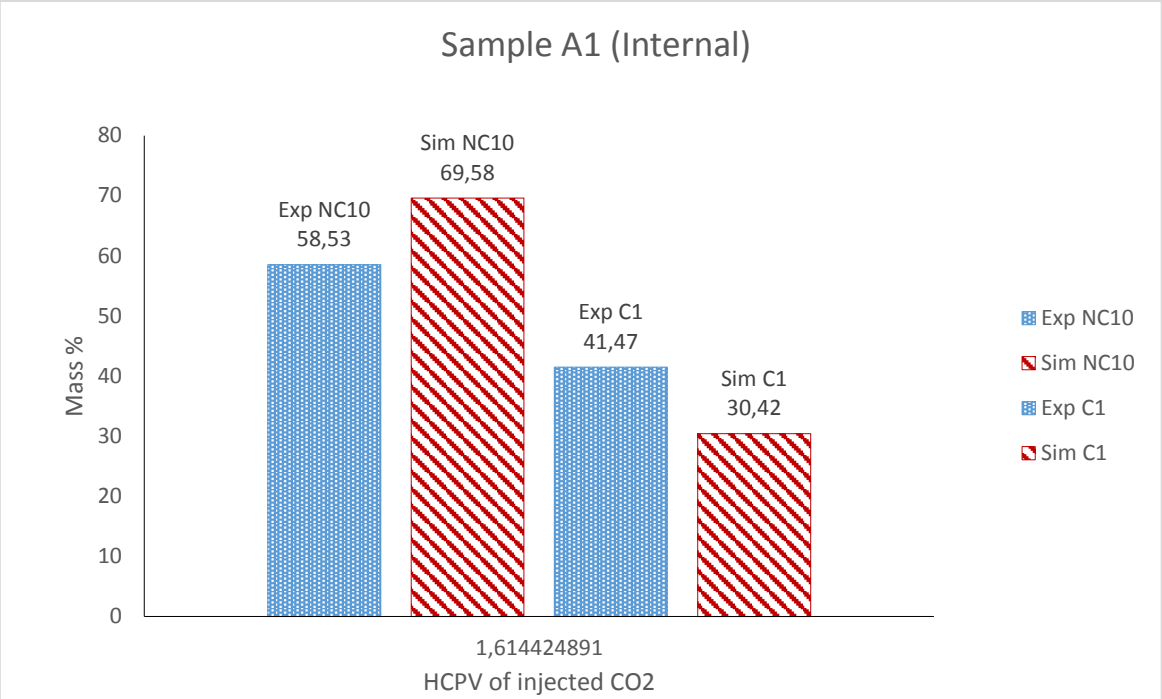

Figure 4.20. Comparison between the compositions of the Live-oil A and CO_2 analyzed by experiments and numerical simulation for Sample A1 (Internal)

The sampling procedure was same in all the experiments. The first internal sample A1 collected inside the oven at 70°C and 200 bars at the initial stage of the experiment (1.614 PV) displays the higher composition (58.53 %) of the n-decane comparatively lower percentage of methane (41.47 %) and zero mass percentage of CO_2 as shown in figure 4.20. This maybe because a low PV (1.614 PV) of CO_2 was injected into the core which means not enough CO_2 has mixed with the oil phase. The simulation result also reflects nearly the same trend. The second sample B2 is collected outside the oven at the atmospheric condition. The collected oil is flashed from 70°C and 200 bars to 25°C and 1 bar. This sample also highlights the same trend as Sample A1 because it is taken nearly after the first internal sample (1.614 PV). But still there is an increase in the amount of CO_2 (14.1 %) as compared to A1 because with the increase in time, the CO_2 injection increases too. Simulation results in the figure 4.21 also support the experimental results. Similar injected PV of CO_2 is considered in these two samples because both the samples are taken simultaneously one after another. There is a time difference (15 minutes) between both the samples but it is neglected and assumed that the same PV of CO_2 is injected for both the samples. Thus, we see the change in the composition for the same PVof CO_2 injected.

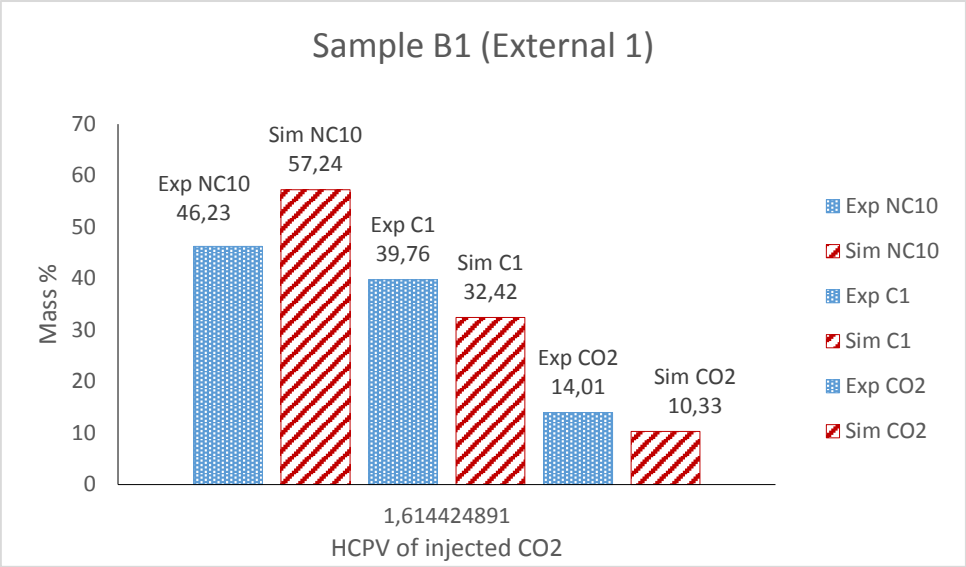

Figure 4.21. Comparison between the compositions of the Live-oil A and CO_2 analyzed by experiments and numerical simulation for Sample B2 (External)

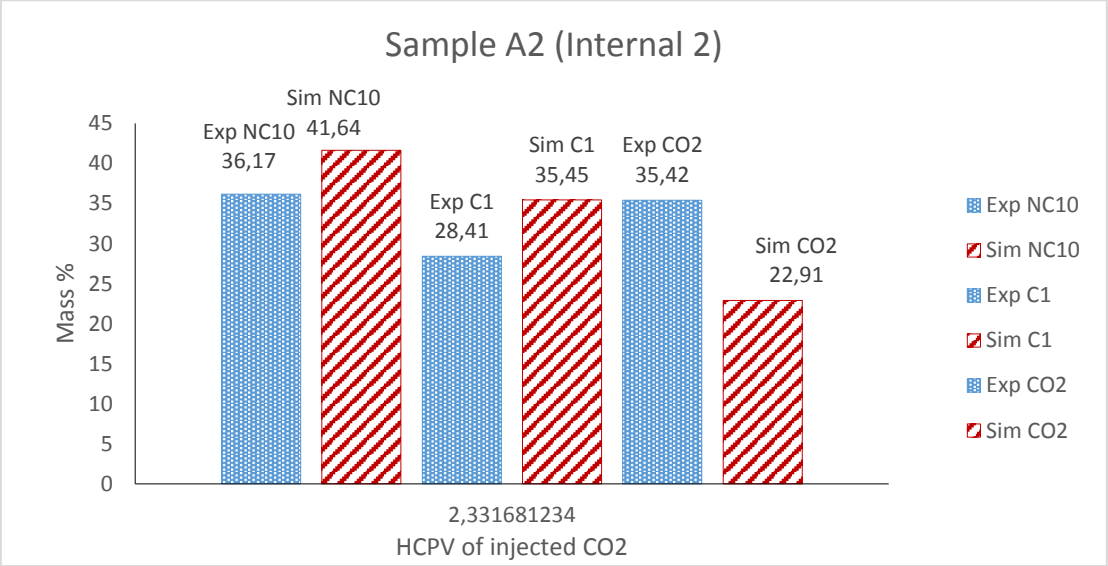

Figure 4.22. Comparison between the compositions of the Live-oil A and CO_2 analyzed by experiments and numerical simulation for Sample A2 (Internal)

Another set of samples were taken just before breakthrough at 2.33 PV. Figure 4.22 shows the mass percentages of the compositions collected in sample A2 inside the oven at 70°C and 200 bars. Still, a higher amount is of oil (NC10) i.e. 36.17 % but probably the CO_2 has invaded further in the core which reacts with the oil to release C_1. A considerable amount of CO_2 (35.42 %) is observed in the figure. Another sample B2 from the same set and PV (2.33 PV) was taken outside the oven after sample A2 at atmospheric conditions. The

experimental results show that CO_2 (45.28 %) has increased than n-decane (30.23 %) and C_1 (24.49 %). But simulation results shows a higher amount of n-decane (48.21 %) than CO_2 (35.07 %) and C_1 (45.28 %).

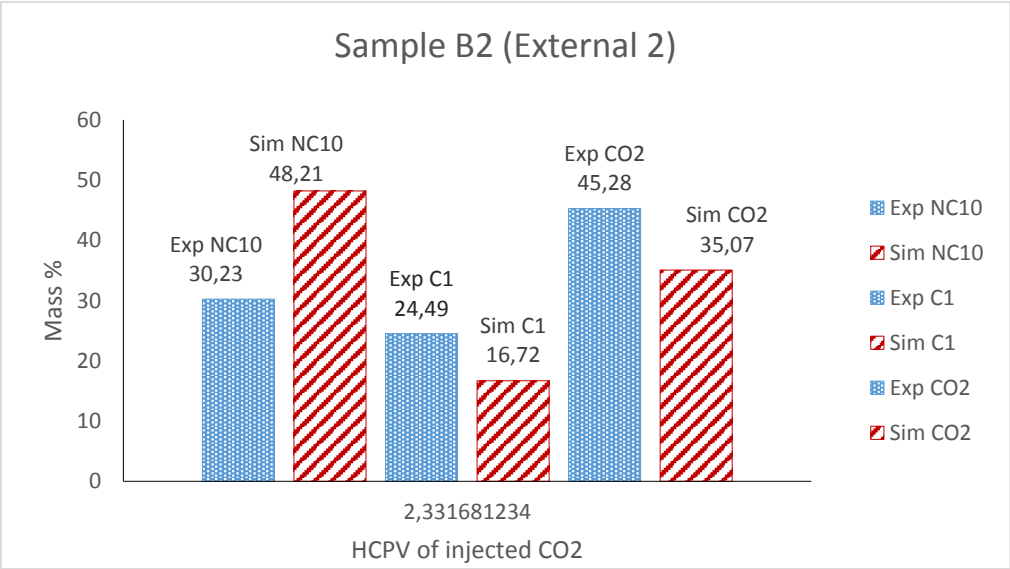

Figure 4.23. Comparison between the compositions of the Live-oil A and CO_2 analyzed by experiments and numerical simulation for Sample B2 (External)

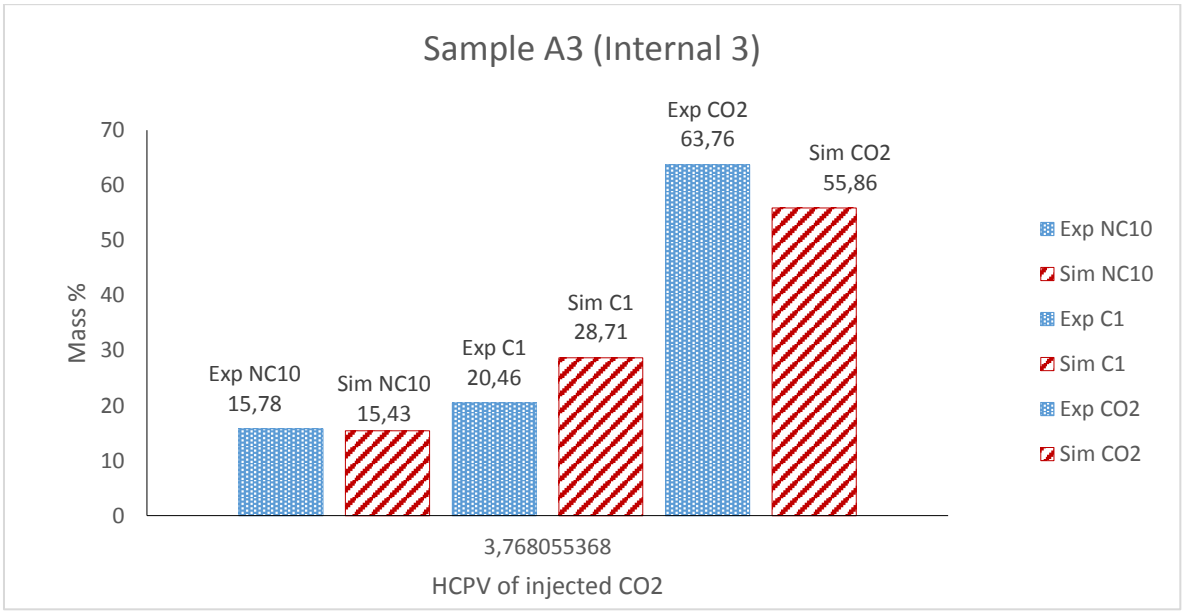

Figure 4.24. Comparison between the compositions of the Live-oil B and CO_2 analyzed by experiments and numerical simulation for Sample A3 (Internal)

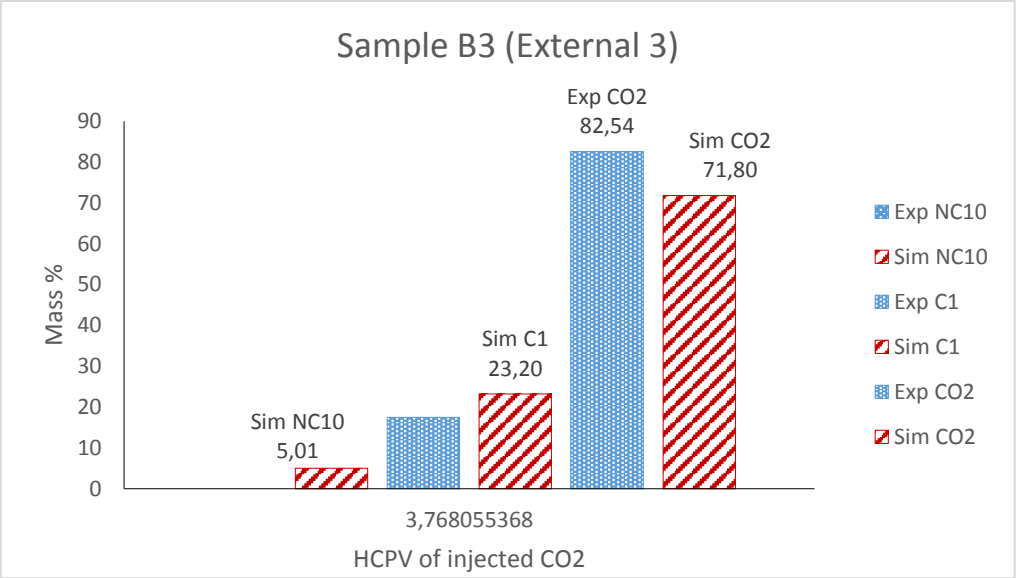

Figure 4.25. Comparison between the compositions of the Live-oil A and CO_2 analyzed by experiments and numerical simulation for Sample B3 (External)

The final set of sample for this experiment was taken after the breakthrough was achieved at 2.5 PV of injected CO_2. Figure 4.24 explains the compositions obtained from sample A3 taken inside the oven at 70°C and 200 bar. The trend shown in this figure highlights the end stage of the experiment where CO_2 is the highest (63.76 %) probably because 3.76 PV of $CO_2$is injected in the core and CO_2 is already mixed with the oil phase while most of the oil is produced. 20.46 % of C_1 is still present in the core. Simulation result supports the experimental results. In case of the externals sample B3 taken outside of the oven at the room temperature, similar trend is observed in both experimental and simulation results as compared to sample A3.The recovery obtained from this experiment is 80.01 % which is 3% higher than Live-oil B at 70°C. This reflects that the addition of richer component C_3 in the oil composition is adversely affecting the recovery.

4.2.6. Model Oil flooded with CO_2 containing C_1 and C_3 at 70°C

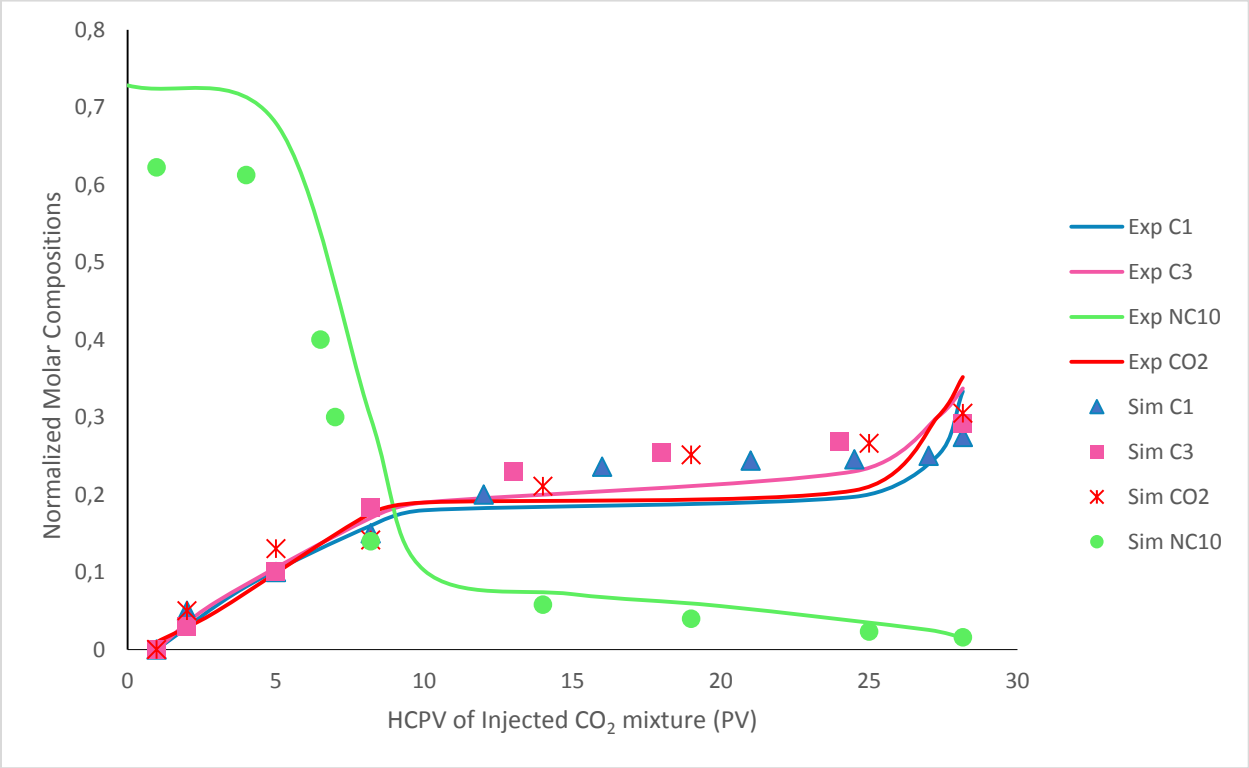

Figure 4.26. Comparison of simulation and experimental normalized composition as a function of injected PV of CO_2 for model saturated core flooded with CO_2 along with C_1 and C_3.

In the case of Model Oil (Dead Oil) experiment conducted at 70°C, the core was initially saturated with Dead Oil and then flooded with the mixture of CO_2 (9.8 mole % of C_1 and 11.9% mole % of C_3 and 78.23 mole % of CO_2). The normalized composition of the different components involved in the experiment is represented in figure 4.26. It can easily be observed that the trend of NC10 is decreasing while the components of the injected gas mixture are increasing during the experiment. From the injected gas mixture, C_3 present in the highest composition (0.4 %), with a slight difference C_1 (0.396 l %) is slightly lesser and the least of all is CO_2 (0.394 %) but again with a small difference. The content of the injected components is lower in the model oil case than crude oil's case. Similar to other experiments, the residual concentration of C_3 is higher by the end of the experiment as compared to C_1. According to Alston (1998) the reason behind the differences in the composition could be that when CO_2 is contaminated or mixed with lighter component like C_1 or N_2, MMP gets adversely affected. Conversely, when CO_2 is contaminated with C_2, C_3, C_4, it was observed that these components lower the MMP.

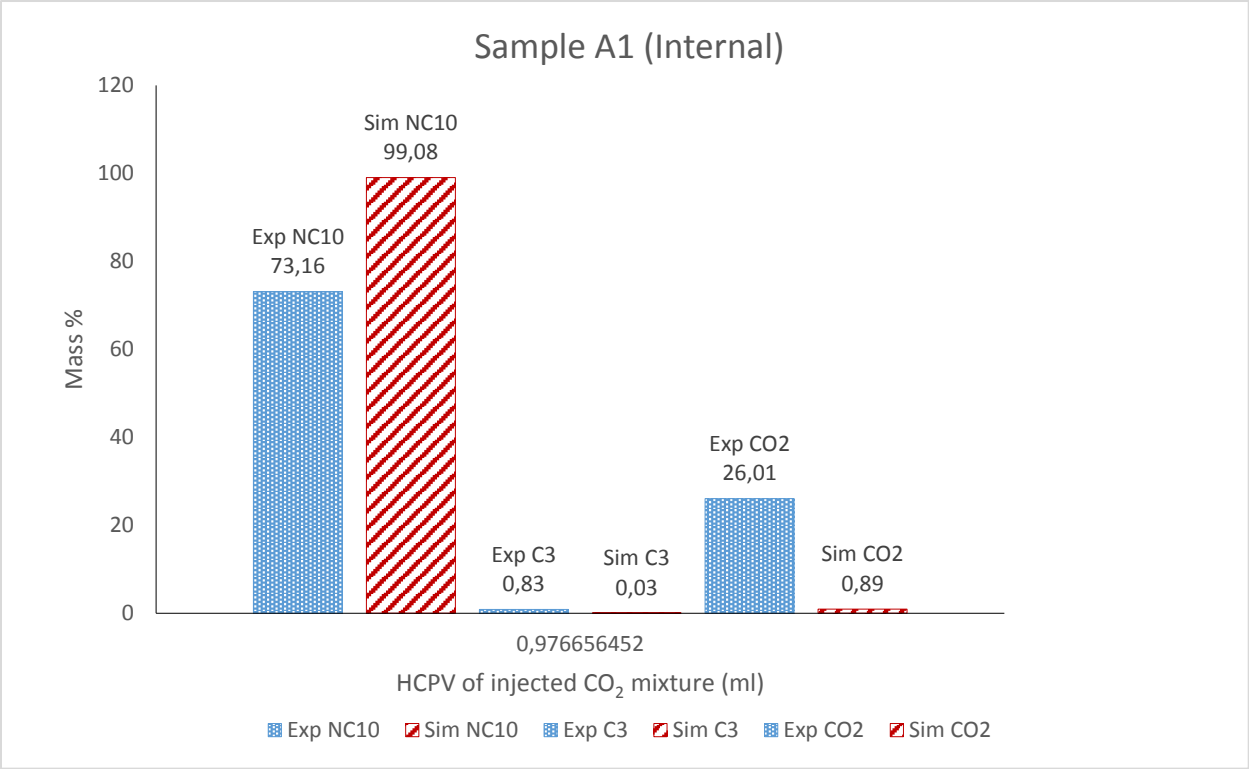

Figure 4.27. Comparison between the composition of the oil and CO_2 mixture analyzed by experiments and numerical simulation for Sample A1 (Internal)

Numerical simulation results, as well as the experimental results,exhibits the same trends in figure 4.27. First sample A1 of Model Oil (Dead Oil) experiment was taken inside the oven at the 70°C and 200 bars in the initial period of the experiment after injecting 0.977 PV of CO_2. As predicted, the composition of NC10 in the experimental results is the highest (73.16 %) maybe because the production has just started and the injected gas has not yet come in contact with most of the oil. But CO_2 is being collected in the sample cylinder (26 %) probably because of the fingering phenomenon of the gas. A slight amount of mass percentage of C_3 (0.83 %) was also observed whereas, C_1 is completely absent in the first internal sample. The results from the first sample were quite convincing as it very well depicts the initial condition of the core during the start of the experiment. Simulation results also support the experimental result in the case of this sample. Another set of the first sample B1 taken outside the oven at the room temperature is shown in figure 4.28. With a small time difference, PV of 0.977 PV and flashing from 70°C and 200 bars to room temperature and pressure, the compositions showed nearly the similar trends as the previous sample taken inside the oven. Oil composition was the highest (93 %) and then CO_2 (6.84 %) but in this case, no light components were collected in the sample.

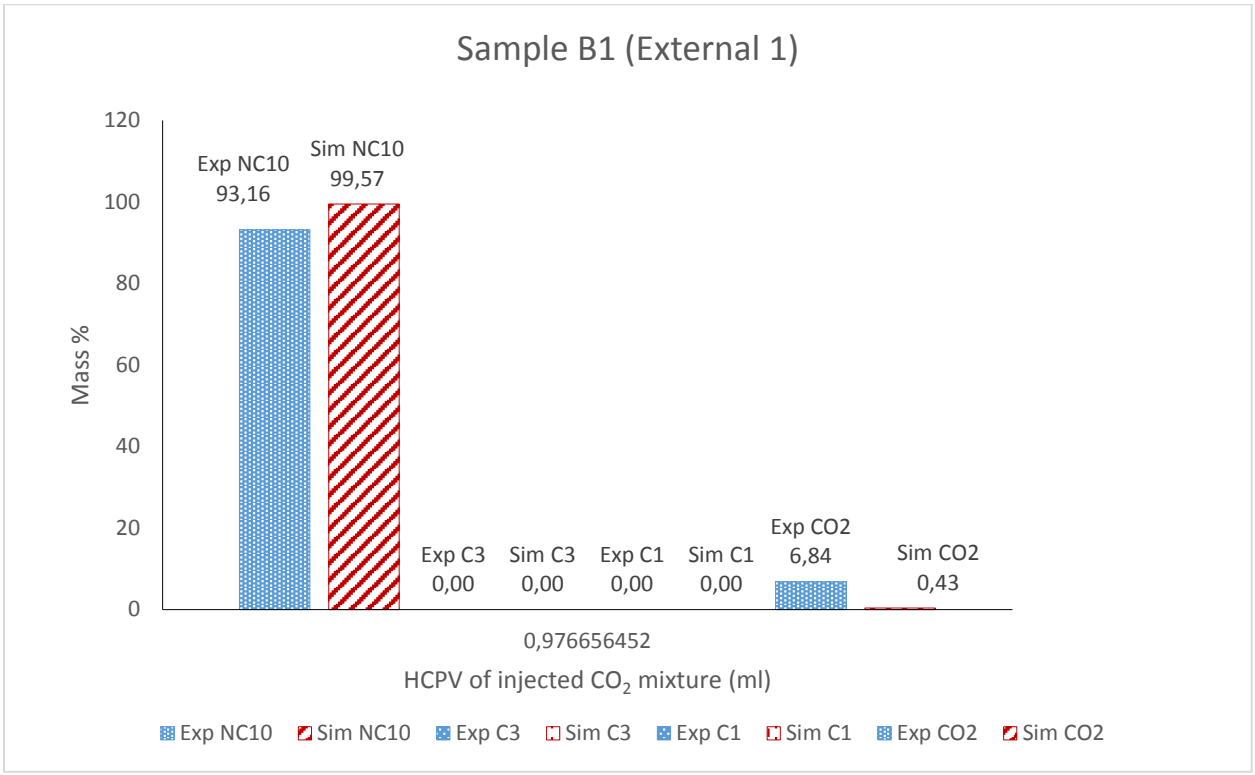

Figure 4.28. Comparison between the composition of the oil and CO_2 mixtureanalyzed by experiments and numerical simulation for Sample B1 (External)

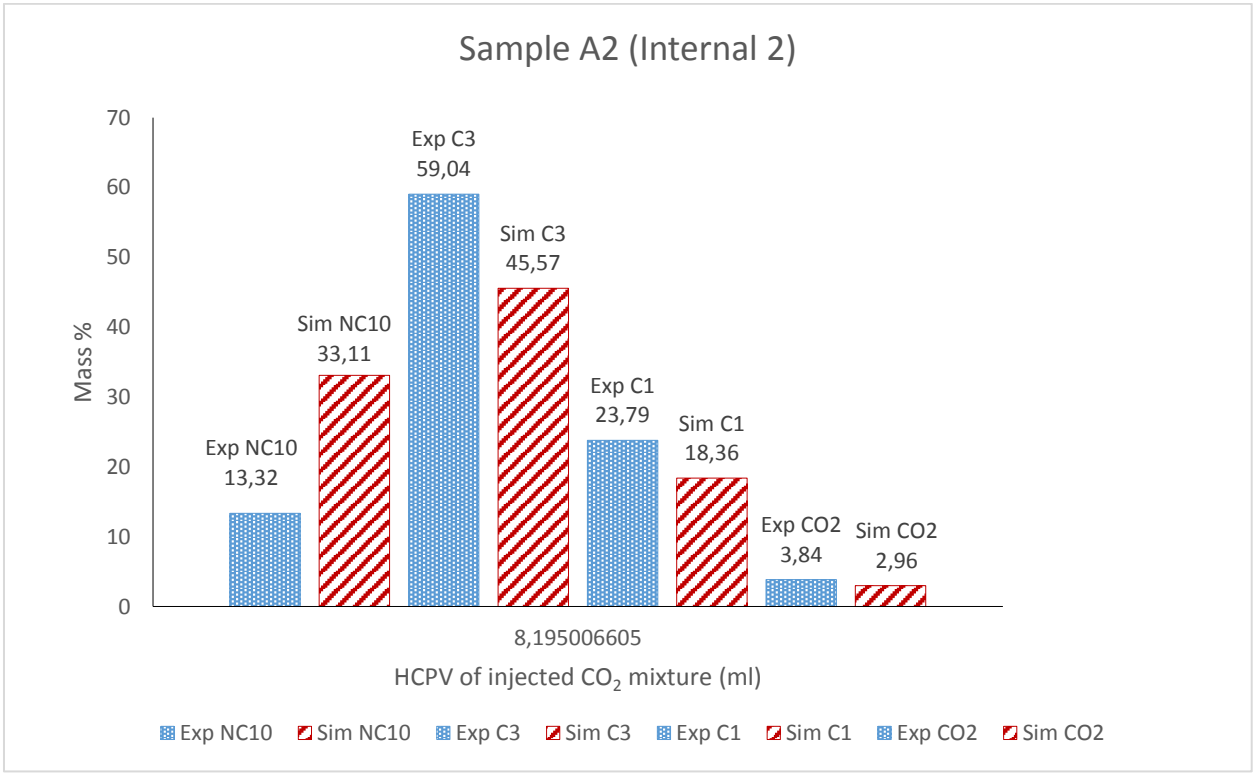

Figure 4.29. Comparison between the composition of the oil and CO_2 mixture analyzed by experiments and numerical simulation for Sample A2 (Internal)

The second set of samples was taken close to a breakthrough which occurred at 10.89 PV. 8.195 PV of the CO_2 mixture was injected into the core. The second sample A2 in figure 4.29 highlights the invasion of the injected gas mixture in the system. The lighter components are in the highest concentration than oil and CO_2 i.e. C_3 is 59.04 % and C_1 is 23.79 %. Lighter components being less dense than CO_2 may pass through the oil faster than CO_2. When CO_2 comes in contact with the oil (NC10), it reduces its density and viscosity whereas the lighter components in this case also aid in reducing the viscosity. The difference in the oil composition presented by the experiment and simulation result could be because the simulation result considers the composition of NC10 present inside the core at the mentioned PV. Sensitivity with respect to the oil produced is performed on the simulation results to create the best match between the experimental and simulation results. On the contrary, the experimental result of NC10 only shows the produced oil for the above PV.

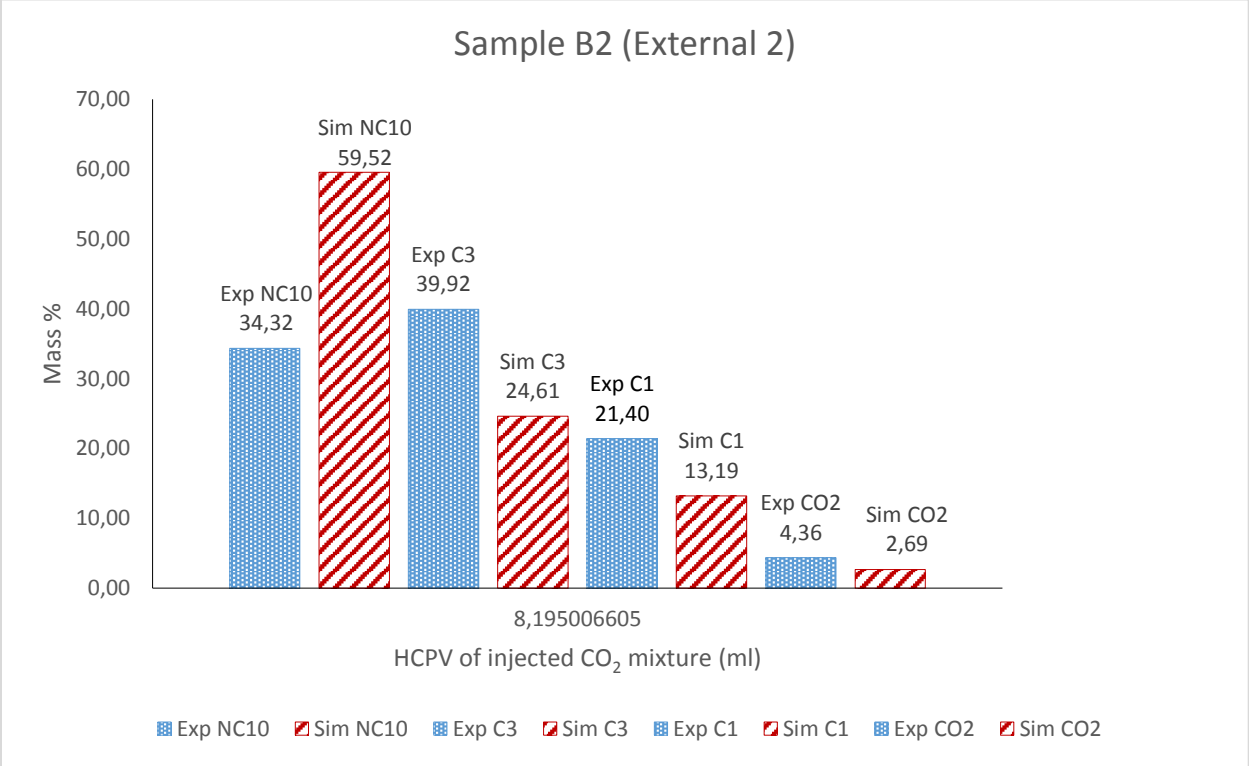

Figure 4.30. Comparison between the composition of the oil and CO_2mixtureanalyzed by experiments and numerical simulation for Sample B2 (External)

Sample B2 was taken outside the oven at the room temperature and pressure. The experimental results in figure 4.30 signify the same trend as sample A2. Oil recovered (34.32 %) is lesser than C_3 (39.92 %) which means that the composition of C_3 is the highest in the core at 10.89 PV of injected gas. The concentration of the injected gas is increasing with the increasing PV and oil is reaching to its depletion phase. But the simulation results shows that at the mentioned PV of injected CO_2 mixture, Oil composition is highest as compared to the injected gas. The oil mass percentage represents the volume of oil present in the core according to the simulation. As mentioned above the mass percentages are widely affected by the volume of oil collected in the sample. The experimental value of oil composition is not depicting the true percentage of oil in the core. The injected gas follows the same trend as experimental, C_3 (24.61 %) being the highest and then C_1 (13.19 %) and least is CO_2 (2.69).

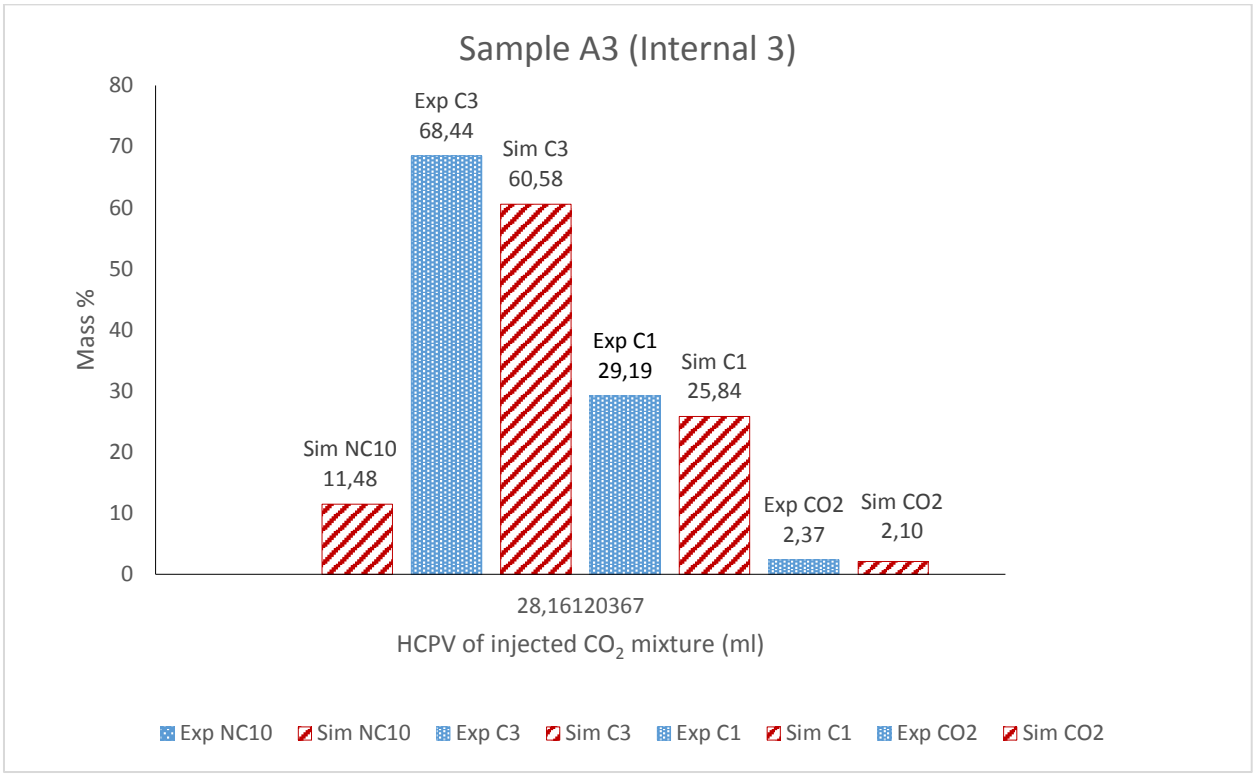

Figure 4.31. Comparison between the composition of the oil and CO_2 mixture analyzed by experiments and numerical simulation for Sample A3 (External)

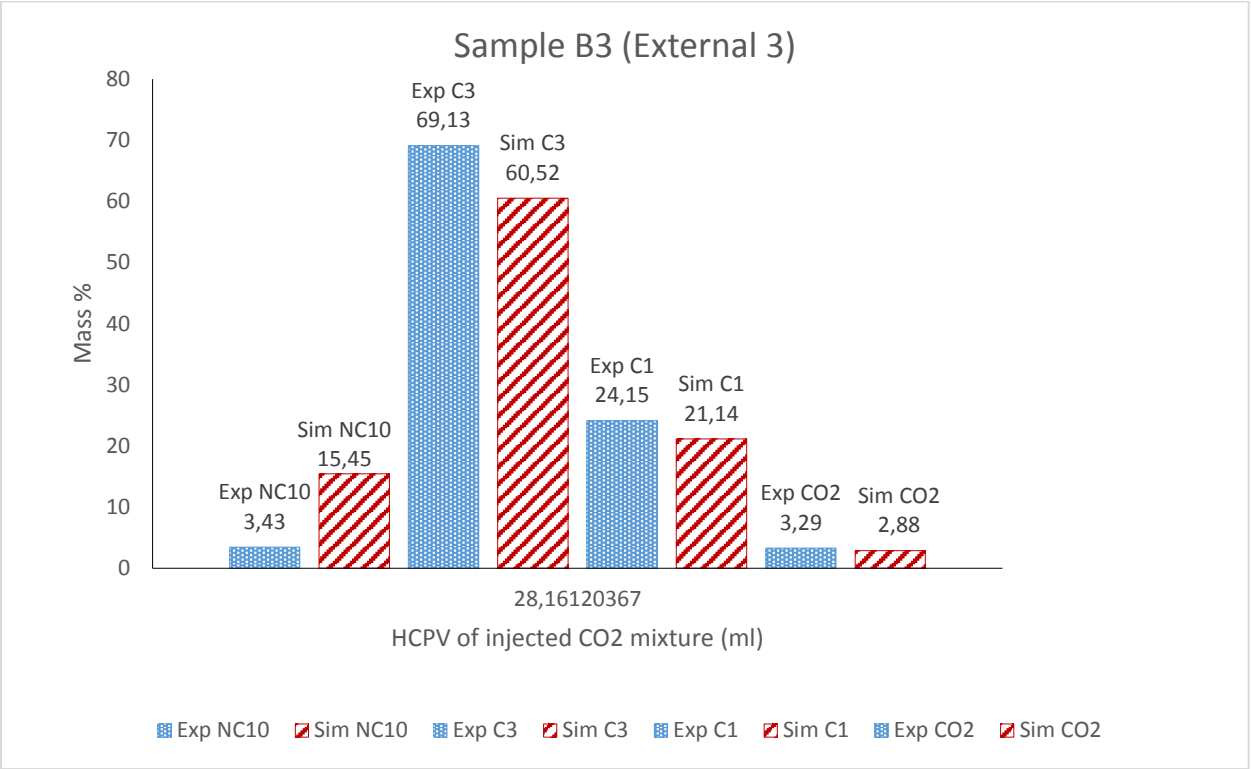

Figure 4.32. Comparison between the composition of the oil and CO_2mixtureanalyzed by experiments and numerical simulation for Sample B3 (External)

Lastly, the third set of samples shows the condition of the core after the breakthrough. According to figure 4.31 for sample A3 (internal) taken inside the oven at 70°C, the composition of C_3 is the most prominent (68.44 %) and oil is reaching its residual saturation (11.48 %). Same is the case for Sample B3 (external) outside the oven at the room temperature and pressure shown in figure 4.32. The simulation results and experimental results are supporting each other in both the cases. The results from this experiment explicate that injection of richer gas accelerates the oil production (Fai-Yengo&Rahnema, 2014). This is in support of the highest oil recovery obtained from this experiment i.e. 84% not only highest recovery among all the performed experiments but also in comparison with the Model Oil (Dead Oil) flooded only with CO_2. The recovery obtained from the Model Oil (Dead Oil) flooded with CO_2 only is 82.14%. The reason behind the increase in the recovery in case of the experiment with CO_2 mixture could be that the lighter components from the injected gas after coming in contact with NC10 solubilizes in the oil along with CO_2 and reduces its viscosity and density. The oil will become less dense in the case of injected CO_2 mixture than

simply CO_2. The density and viscosity differences discussed in the later section between these experiments also provide a better understanding of the efficiency of the different cases.

4.2.7. Crude Oil flooded with CO_2 along with C_1 and C_3 at 70°C

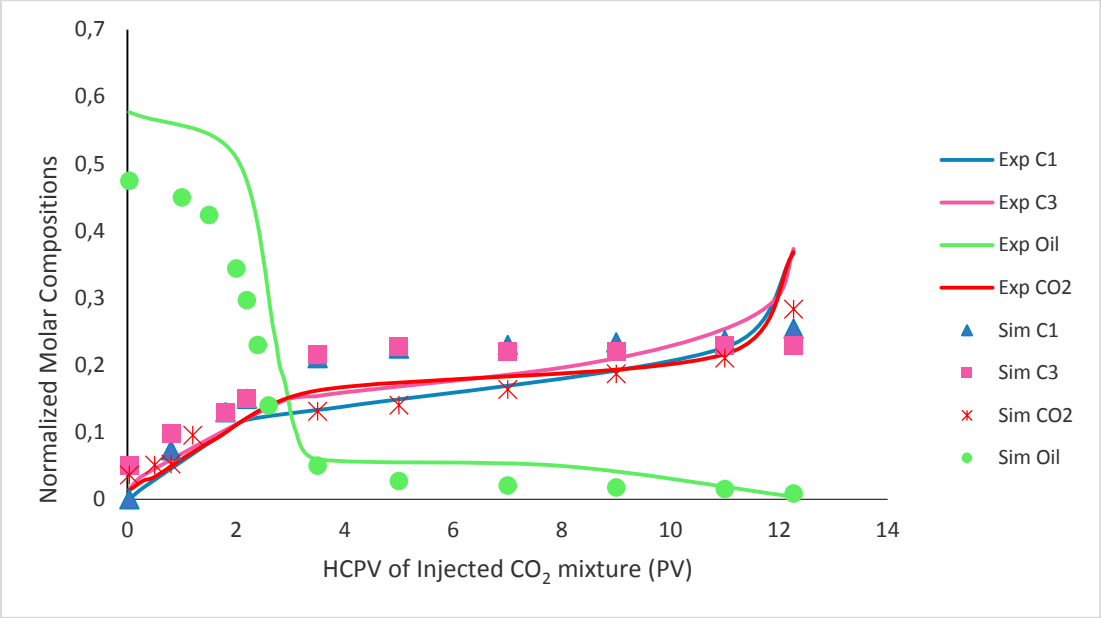

Figure 4.33. Comparison of simulation and experimental normalized composition as a function of injected PV of CO_2 for Crude oil saturated core flooded with CO_2 mixture (C_1 and C_3).

Figure 4.33 demonstrates the normalized composition profile of each of the oil component and injected gas composition at 70°. The core is saturated with crude oil and flooded with the mixture of CO_2 (78.23 mole %), C_1 (9.8 mole %) and C_3 (11.9 mole %). The GC analysis of these samples provides the results represented as an experimental result. The degradation of the components during the experiment is easily comprehendible through the figure 4.33. Oil present in the core decreased during the production whereas the injected gas, CO_2, C_1 and C_3 increases in the core with the injection of the PV of the injected gas mixture in the core. The total PV injected in this experiment is 23.84 PV. The simulation results are also comparable with the experimental results in this case. Figure 4.34 elucidates the mass transfer between the injected gas and the crude oil during the experiment. When the crude oil comes in contact with the injected gas, CO_2 causes the vaporization of the intermediate components from the oil phase but the lighter component present in the injected gas help bringing a thermodynamic equilibrium between the injected gas and the crude oil (Fai-Yengo&Rahnema, 2014). These lighter components condense in the oil and take places of the vaporized intermediate components which ultimately reduces the viscosity and density of the

crude oil. At 0.031 PV of the injected CO_2mixture 84.55 % of oil is produced while 14.20 % C_3 and 1.25 % of CO_2 has entered the core. The simulation results are in good agreement with experimental results. Both results witnessed zero percentage of C_1 in this sample.

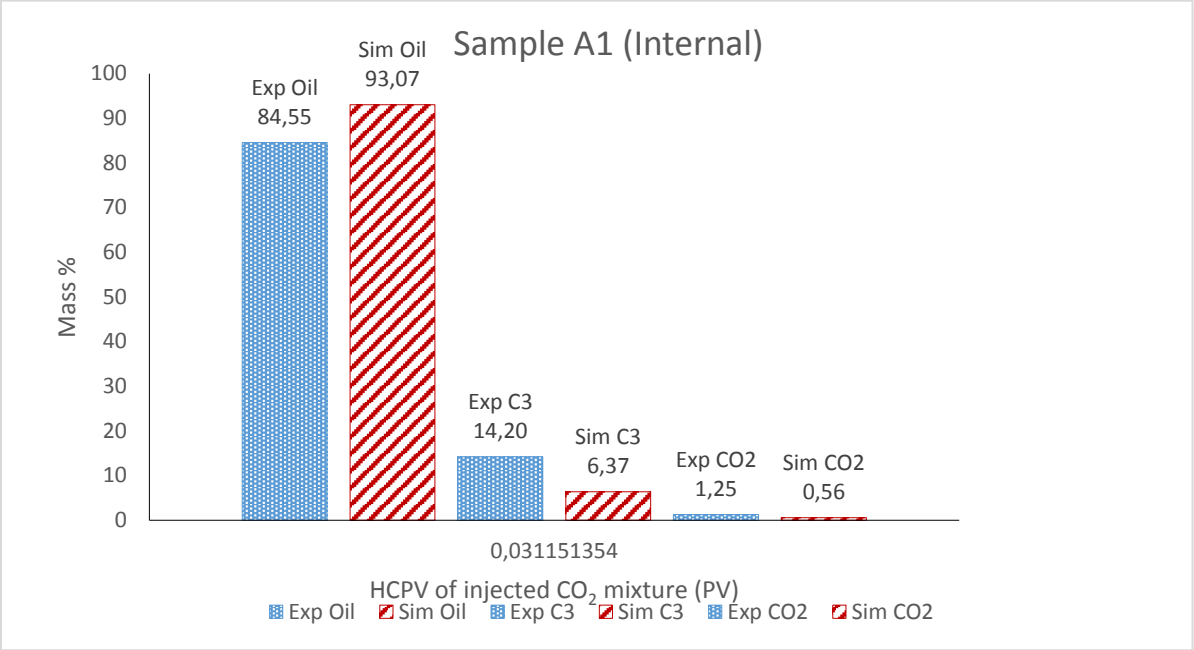

Figure 4.34. Comparison of simulation and experimental mass % with respect to injected pore-volume of CO_2 for Crude oil saturated core flooded with CO_2 mixture (C_1 and C_3).

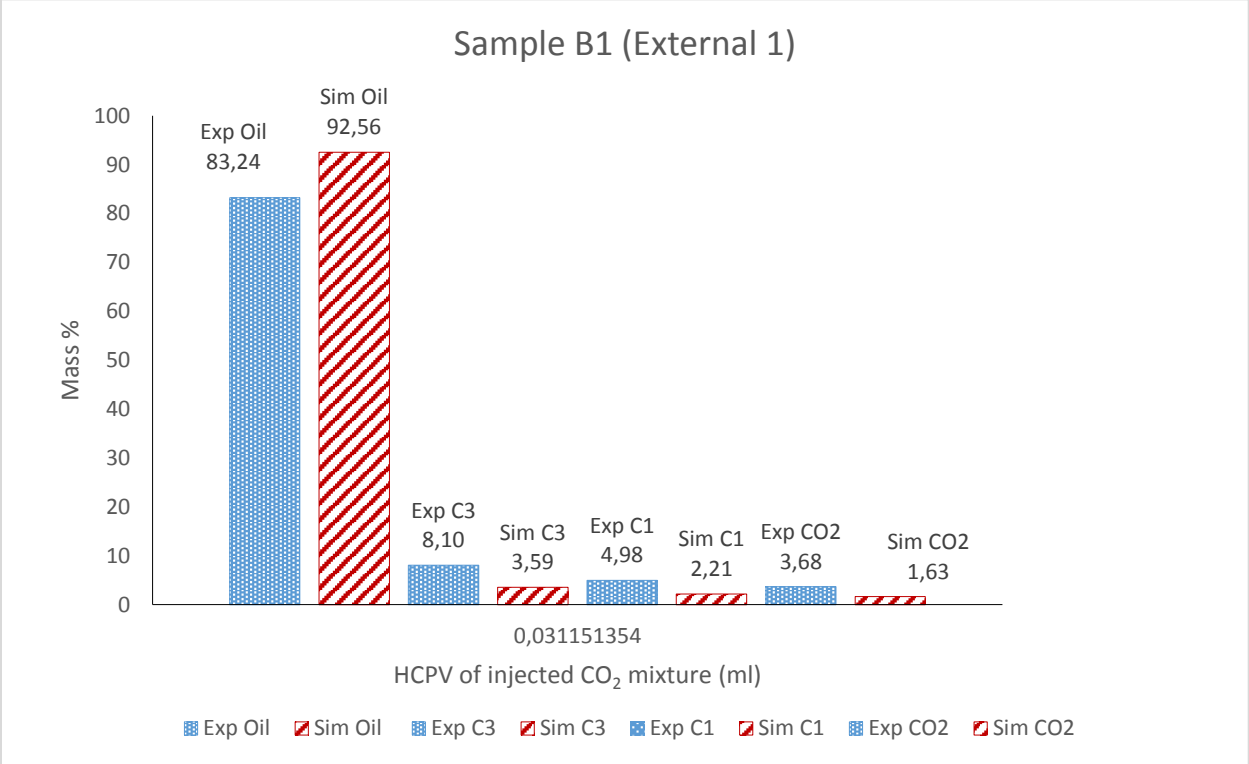

Figure 4.35. Comparison of simulation and experimental mass % with respect to injected pore-volume of CO_2 for Crude oil saturated core flooded with CO_2 mixture (C_1 and C_3).

The sample A2 was collected inside the oven, before the breakthrough at 3.497 PV of CO_2 mixture as shown in figure 4.36. The breakthrough was achieved at 4.5 PV. As the breakthrough is close at this stage of the experiment, hence, the injected gas composition can be observed reaching their peaks. According to the experimental results5, 9 % C_3 and 29 % C_1 are produced in the experiment. CO_2 is observed to be only 3.34 % in the core which indicates that most of the CO_2 is being condensed in the oil. Simulation results are supporting the experimental results with a slight variance in the composition. Sample B2 (external) in figure 4.29 expresses a very similar trend as the internal sample A2. It is collected at nearly the same or a little higher PV of the injected CO_2 mixture and a very small time difference.

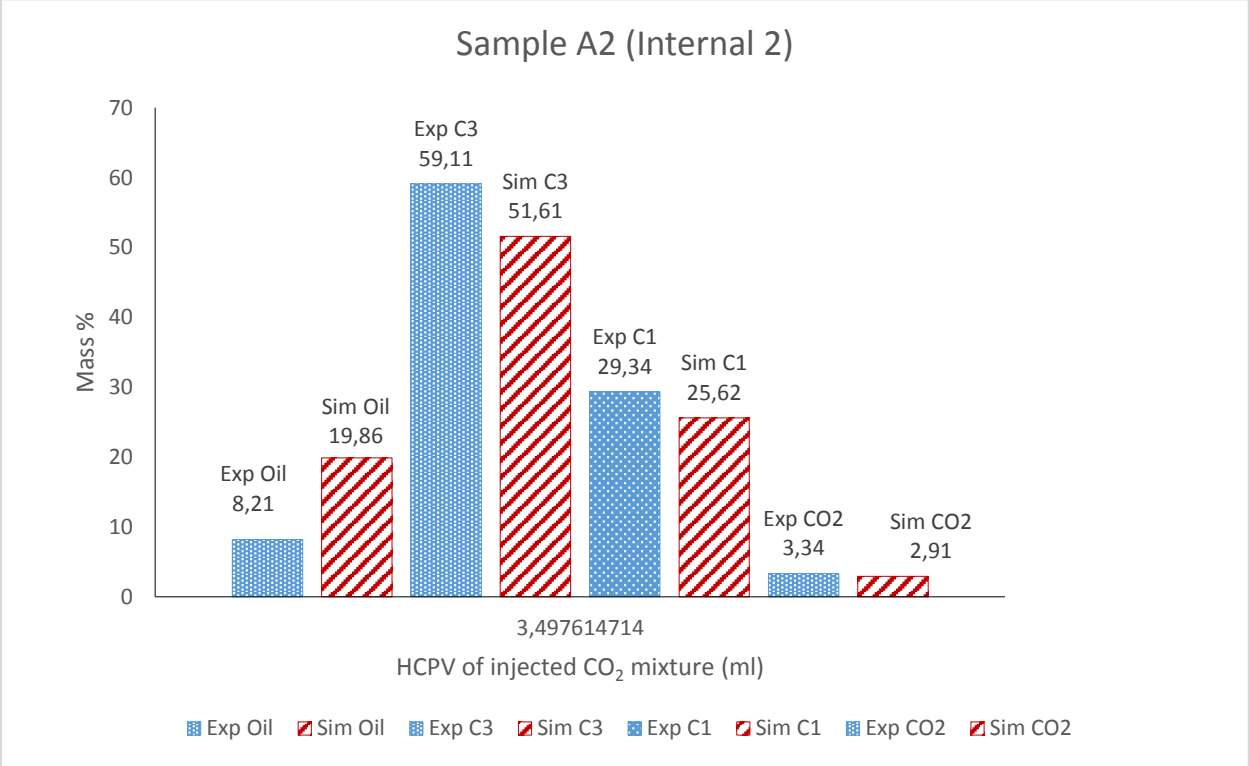

Figure 4.36: Comparison of simulation and experimental mass % with respect to injected pore-volume of CO_2 for Crude oil saturated core flooded with CO_2 mixture (C_1 and C_3).

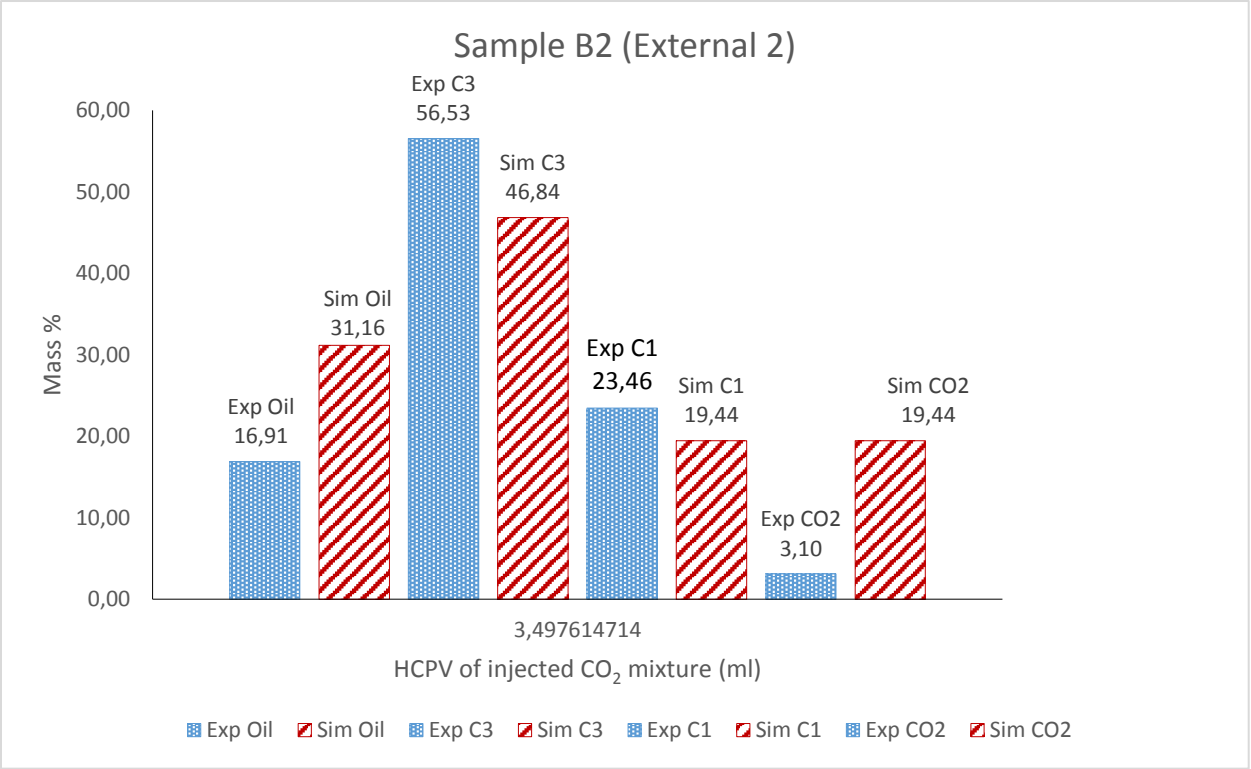

Figure 4.37. Comparison of simulation and experimental mass % with respect to injected pore-volume of CO_2 for Crude oil saturated core flooded with CO_2 mixture (C_1 and C_3).

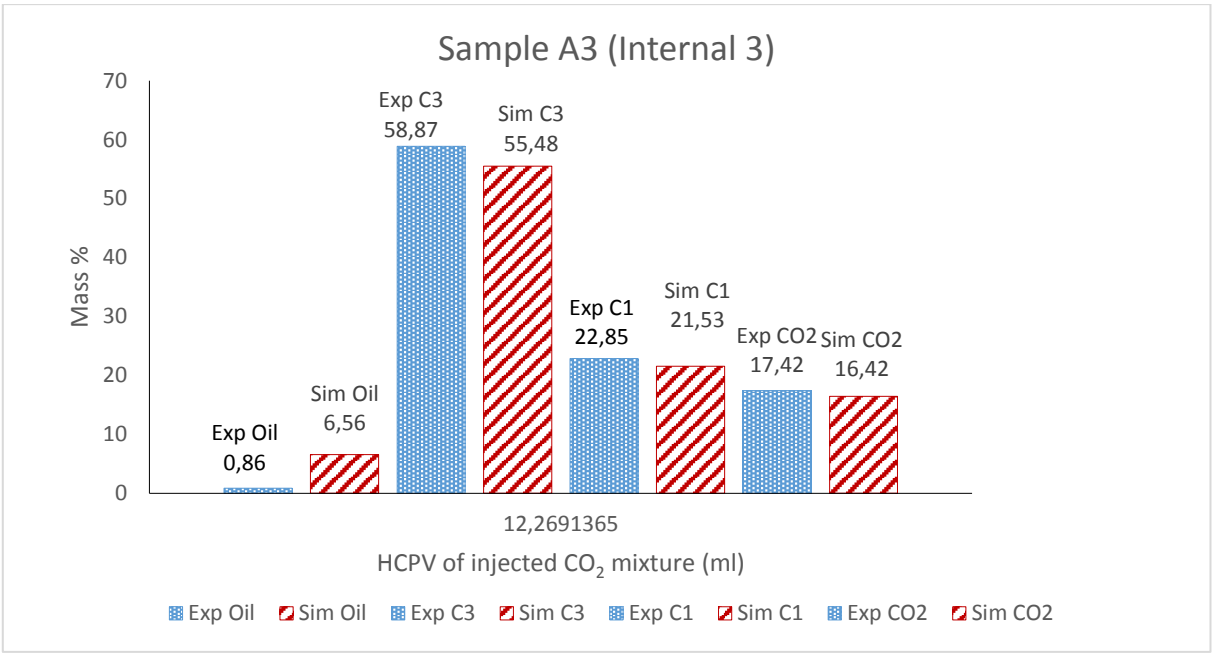

Figure 4.38. Comparison of simulation and experimental mass % with respect to injected pore-volume of CO_2 for Crude oil saturated core flooded with CO_2 mixture (C_1 and C_3).

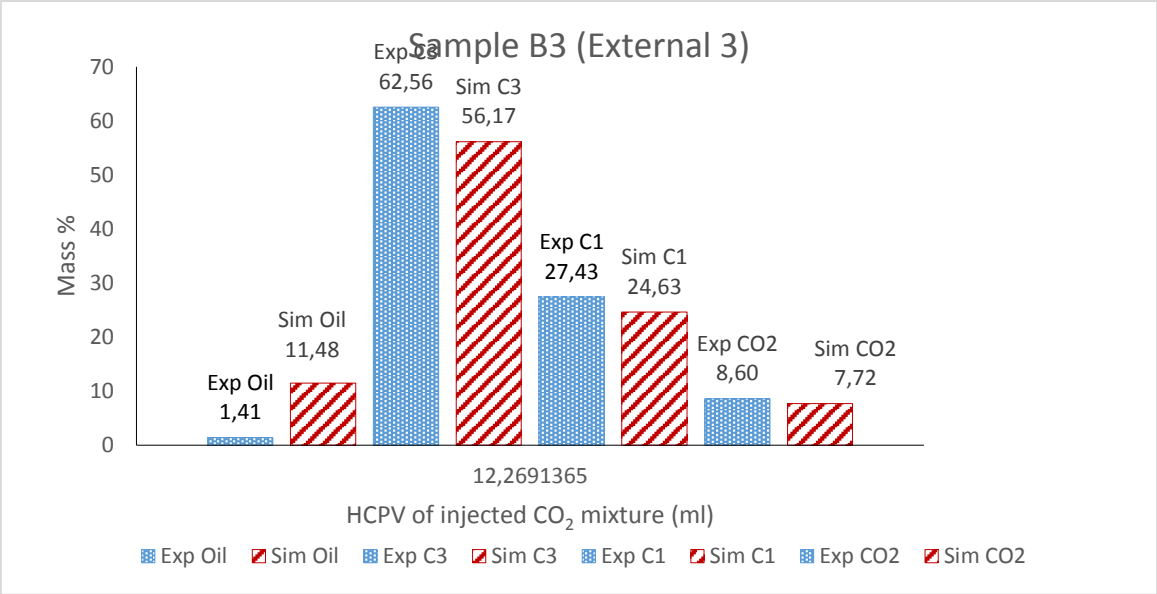

Figure 4.39. Comparison of simulation and experimental mass % with respect to injected pore-volume of CO_2 for Crude oil saturated core flooded with CO_2 mixture (C_1 and C_3).

After viewing the mass changes during the experiment, it is evident that lighter components widely affect the recovery of the crude oil. Compare to the experiment of crude oil conducted with only CO_2 injected gas, the experiment of crude oil flooded with CO_2 and lighter components stimulates the recovery by 2 %. The recovery obtained from crude oil flooded with only CO_2 is 77.99 % while the recovery obtained from crude oil saturated core flooded with CO_2 and lighter components is 80.2 %. In the case of crude oil flooded with CO_2 along with lighter components, crude oil loses its intermediate components from iC_5 to C_{10+} after interacting with CO_2 while the lighter components in the injected gas are condensed in the oil for maintaining the thermodynamic equilibrium between the oil and the injected gas. The lighter components in the injected gas prevent the vaporization of the intermediate components from the oil yielding lower viscosity, lower density and higher mobility of the crude oil. This results in higher recovery. In the case of crude oil flooded with only CO_2, after coming in contact with CO_2 the concentration of CO_2 increases in the oil phase which cause the oil to release its intermediate and light components. These components vaporize on the condensation of CO_2 in the oil phase for obtaining thermodynamic equilibrium. These vaporized hydrocarbons condense into the matrix of the core and are driven out from the core during the production period. CO_2 being heavier than the light components when diffuses into the oil phase, it reduces the mobility of the oil by increasing the density and viscosity of the oil. This maybe the reason behind the comparatively low recovery of oil from crude oil

experiment flooded with CO_2 only than CO_2 mixture with light components (Fai-Yen go &Rahnema, 2014).

4.2.8. Live Oil B at 50C

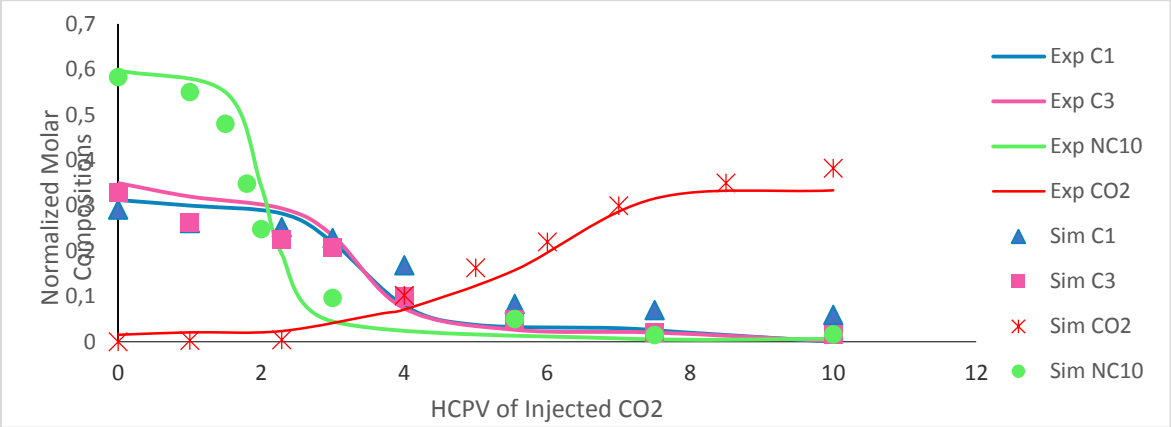

Figure 4.40. Comparison of simulation and experimental normalized composition as a function of injected PV of CO_2 for Crude oil saturated core flooded with CO_2 mixture (C_1 and C_3).

The same analysis was performed for all the experiments. The core saturated with Live-oil B was flooded at 50°C and 200 bar to observe the effect of temperature on the mass transfer mechanism. First sample A1 was taken at 0.2087 PV of injected CO_2 inside the oven at 50°C and 200 bar. The results observed through experimental analysis and simulation are presented in the figure 4.40. The trend of the components is similar to the Live-oil B at 70°C. Sample A1 in figure 4.41shows no invasion of CO_2 with the highest mass percentage of C_3 (62.7 %) and n-decane with 28 % and C_1 with 8.87 %. CO_2 production starts by the time sample B2 is taken (0.79 %). Figure 4.41 represents that CO_2 has started to mix with the oil phase when 0.2087 PV of gas is injected.

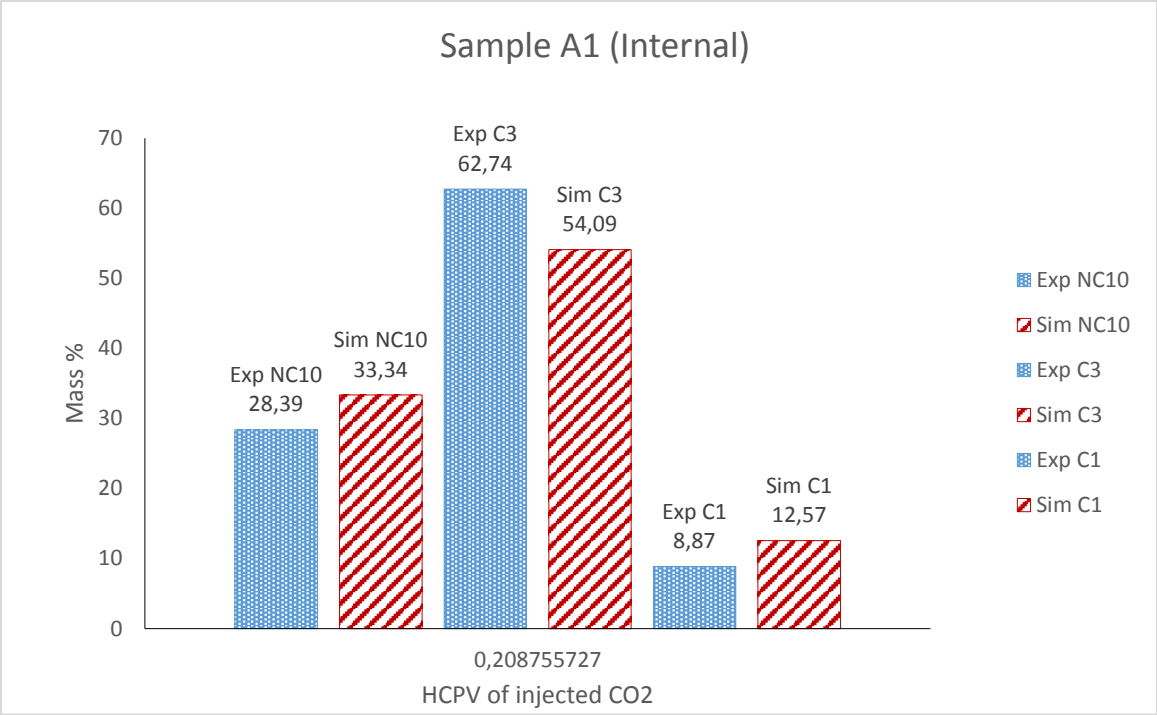

Figure 4.41. Comparison between the composition of the oil and CO_2 mixture analyzed by experiments and numerical simulation for Sample A1 (Internal)

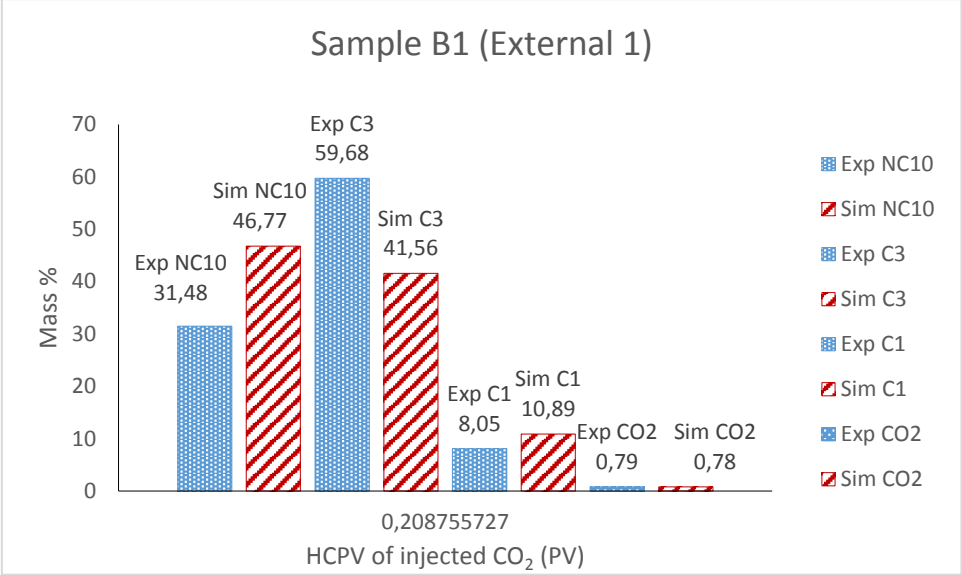

Figure 4.42. Comparison between the composition of the oil and CO_2 mixture analyzed by experiments and numerical simulation for Sample B1 (External)

At 2.29 PV of injected CO_2, sample A2 was collected outside the oven presented in figure 4.43. 66.58 % of C_3 is produced in the sample. CO_2 mole percentage was increased by 15 % in sample A2 as compared to Sample B1. C_1 production was low (5.09 %) with a small production of oil (13.58 %). In figure 4.44 sample B2 taken outside the oven at the room temperature and pressure also represents the same trend shown by sample A2.

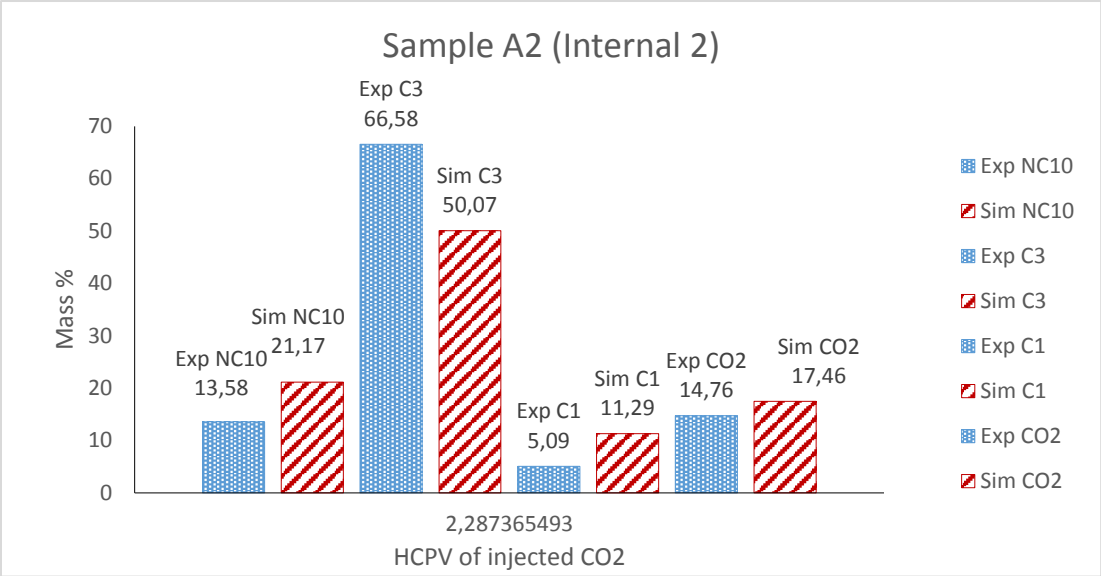

Figure 4.43. Comparison between the composition of the oil and CO_2 mixture analyzed by experiments and numerical simulation for Sample A2 (Internal)

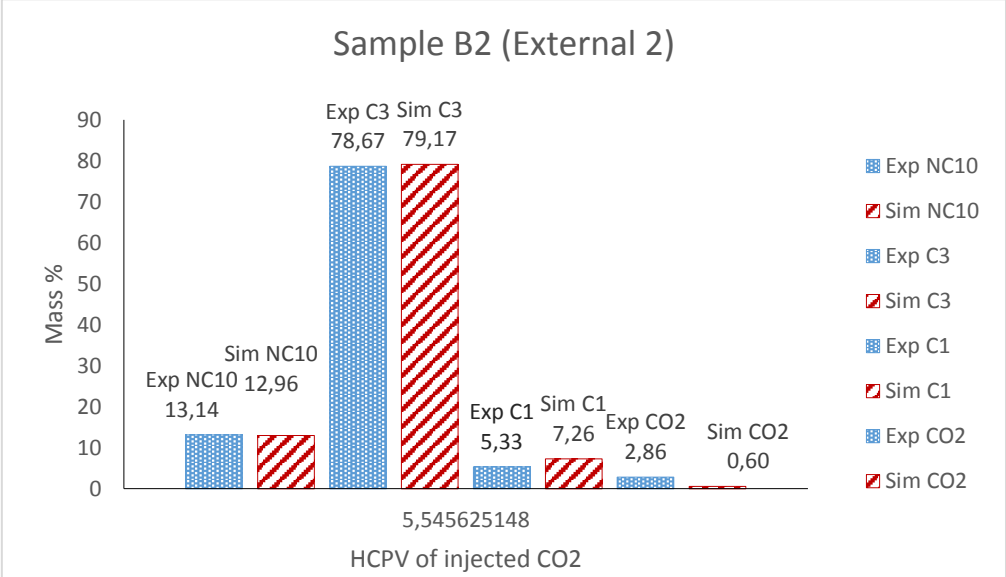

Figure 4.44. Comparison between the composition of the oil and CO_2 mixture analyzed by experiments and numerical simulation for Sample B2 (External)

The last set of sample for this experiment was taken after the breakthrough was achieved at 5.54 PV of the injected CO_2. In figure 4.45 (sample A3) shows that the CO_2 production has increased after the breakthrough. Probably because after breakthrough, the channels or fingers were developed and a higher amount of CO_2 was being produced. Figure 4.46 is showing 75 % of CO_2.

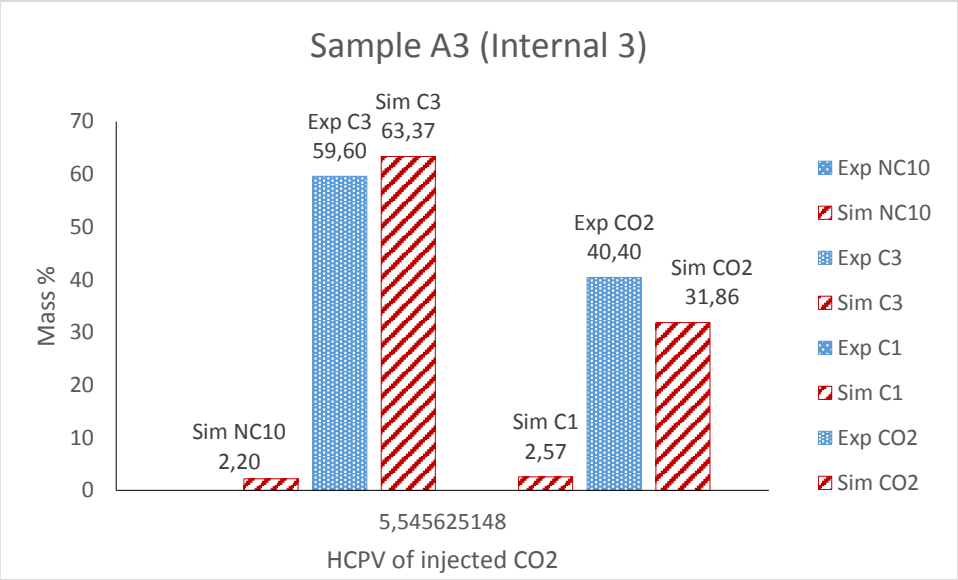

Figure 4.45: Comparison between the composition of the oil and CO_2 mixture analyzed by experiments and numerical simulation for Sample A3 (Internal)

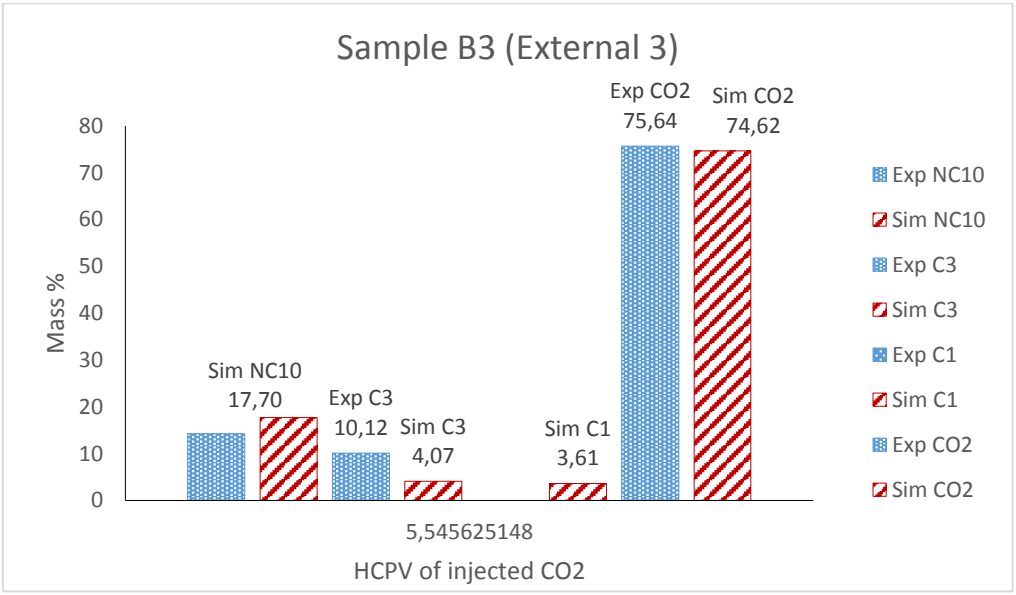

Figure 4.46. Comparison between the composition of the oil and CO_2 mixture analyzed by experiments and numerical simulation for Sample B3 (External)

4.2.9. Live-Oil B at 90°C

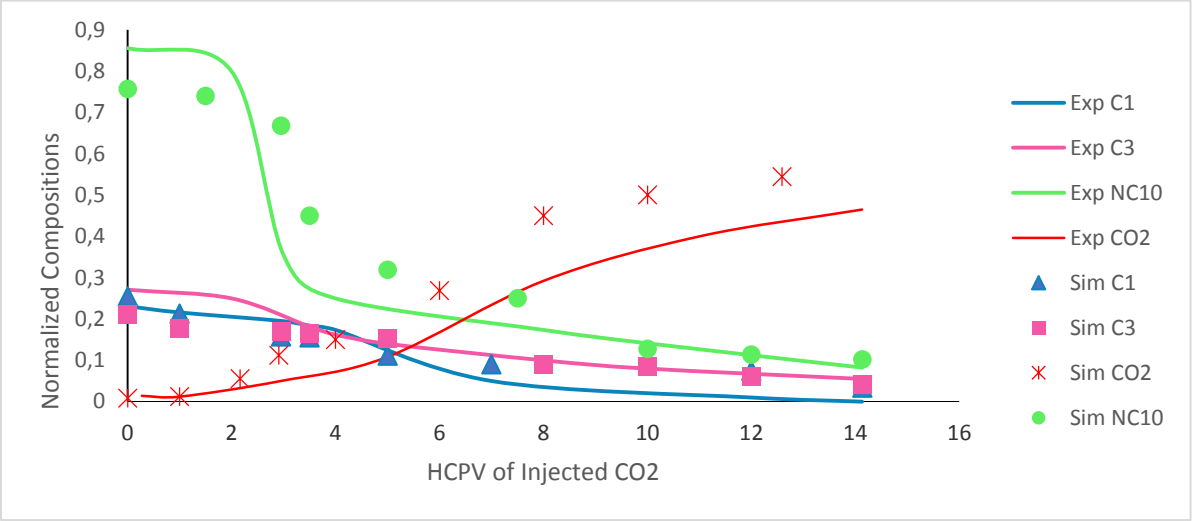

Figure 4.47. Comparison of simulation and experimental normalized composition as a function of injected PV of CO_2 for Live-oil B saturated core flooded with CO_2.

This experiment was conducted at 90°C on the core saturated with Live-oil B. Highest recovery wass obtained at 90°C for live-oil B (81.5 %). Figure 4.47 is representing the degradation of the components of Live-oil B and increment of CO_2 during the flooding of CO_2. The trends are similar at the all the temperature for Live-oil B. In figure 4.48, it can be

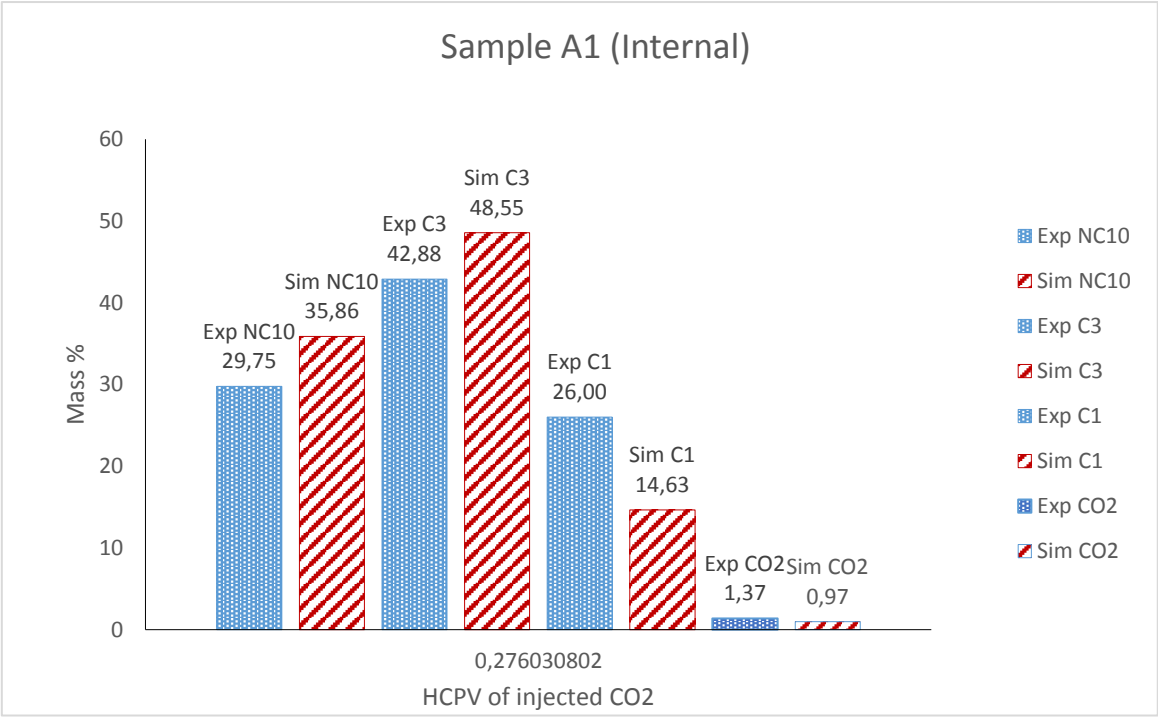

Figure 4.48. Comparison between the composition of the oil and CO_2 analyzed by experiment and numerical simulation for Sample A1 (Internal)

observed that CO_2 production starts earlier at 0.27 PV of injected CO_2. Whereas, in figure 4.49, the mass percentages of all the components is similar to sample A1 as it was collected at approximately 0.27 PV but outside the oven at the room temperature and pressure.

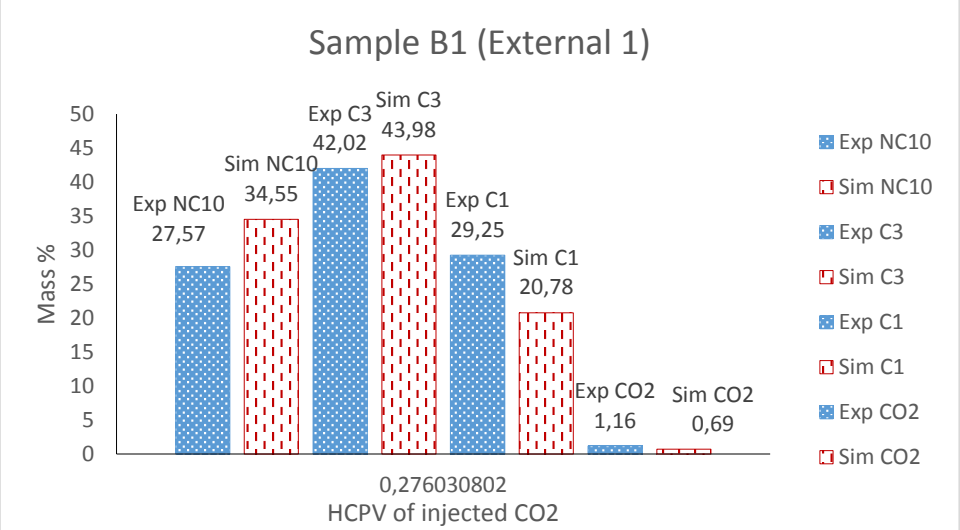

Figure 4.49. Comparison between the composition of the oil and CO_2 analyzed by experiment and numerical simulation for Sample B1 (External)

Second set of samples were taken close to breakthrough 2.95 PV. Figure 4.50 shows the amount of compositions collected in sample A2, inside the oven. It can be observed that C_3 is the highest in mass percentage (48 %) at this PV of CO_2 and the second highest is C_1 (35.47 %). Lighter components were produced in higher amount at 90°C. This maybe because CO_2 after mixing with oil phase extract the lighter components and vaporize them. Similarly, in figure 4.51 for sample B2 taken outside the oven at 2.95 PV, the similar trends can be seen.

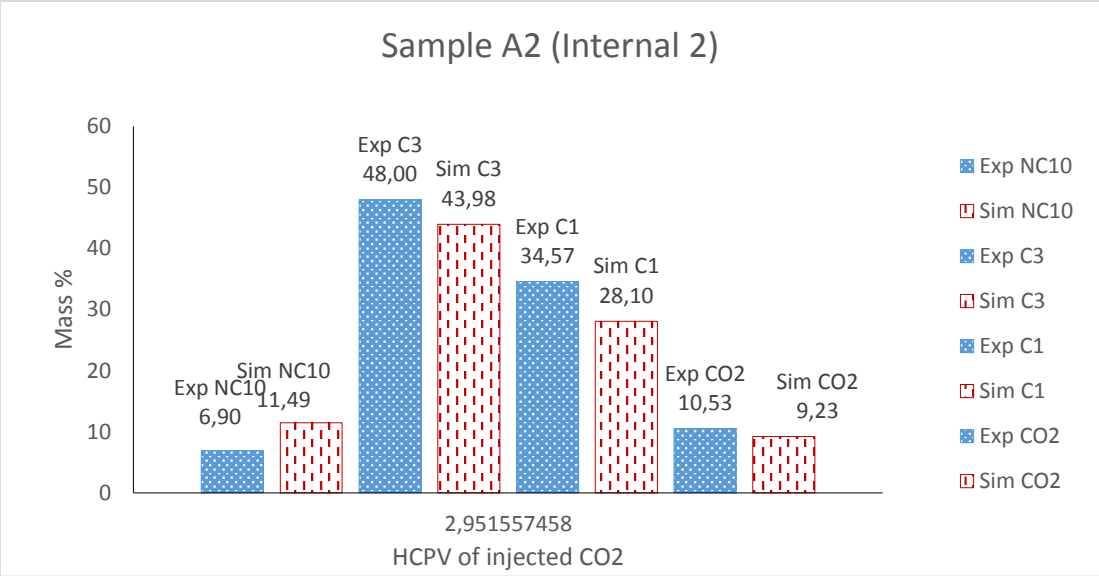

Figure 4.50. Comparison between the composition of the oil and CO_2 analyzed by experiment and numerical simulation for Sample A2 (Internal)

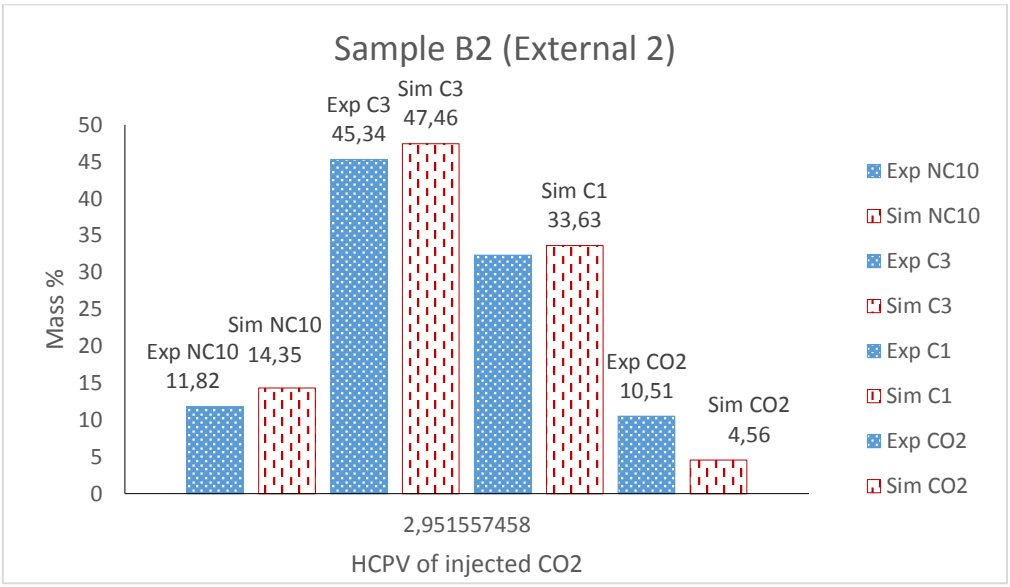

Figure 4.51. Comparison between the composition of the oil and CO_2 analyzed by experiment and numerical simulation for Sample B2 (External)

Sample A3 was taken inside the oven after the breakthrough at 14.13 PV of injected CO_2. Figure 4.52 and figure 4.53 shows the simulation and experimental results of the composition obtained for this set of sample. In sample B3 we can observe the mass percentage of CO_2 is comparatively higher than all other components which shows that the breakthrough has already achieved.

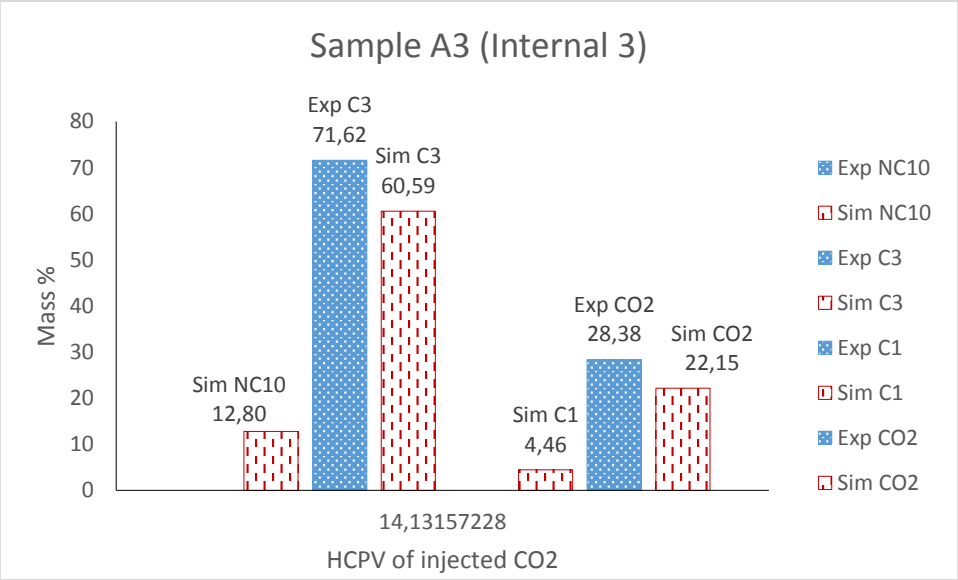

Figure 4.52. Comparison between the composition of the oil and CO_2 analyzed by experiment and numerical simulation for Sample A3 (Internal)

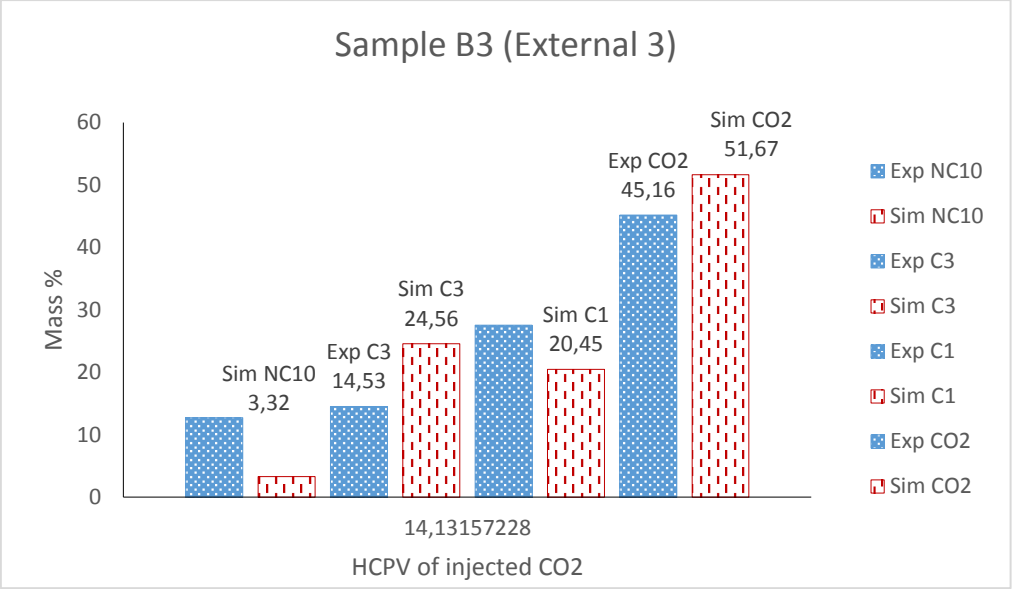

Figure 4.53. Comparison between the composition of the oil and CO_2 analyzed by experiment and numerical simulation for Sample B3 (External)

4.2.10. Live-Oil A at 50°C

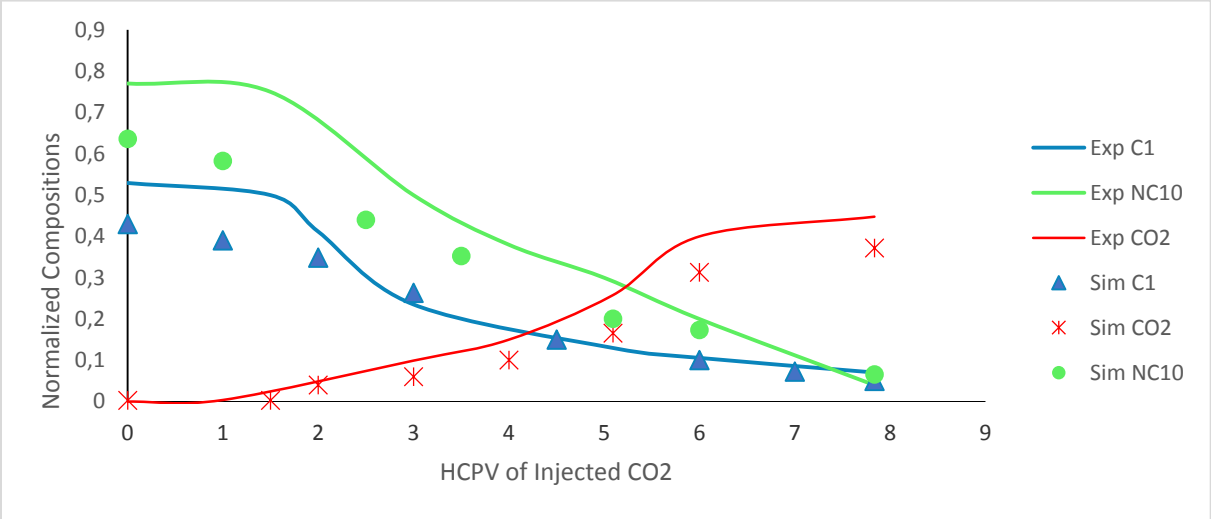

Figure 4.54. Comparison of simulation and experimental normalized molar composition as a function of injected PV of CO_2 for Live-oil A saturated core flooded with CO_2.

Bentheimer core was saturated with Live-oil A and the flooding was conducted at 50°C. The results from experiment and simulations are presented in this section. The trend of the degradation of the n-decane and C_1 is similar to the experiment conducted at 70°C. CO_2 being injected in the core is increasing with the increasing injected PV of CO_2. Sample A1 being collected at the start of the experiment at the PV of 0.1765 is shown in figure 4.48. Core being fully saturated with the oil shows highest percentage of n-decane (58.25 %) but it can be observed that CO_2 has started to produce in the first sample (3.44 %). The sample collected outside the oven at the similar PV (0.1765) also represents the similar trend of the compositions in figure 4.56.

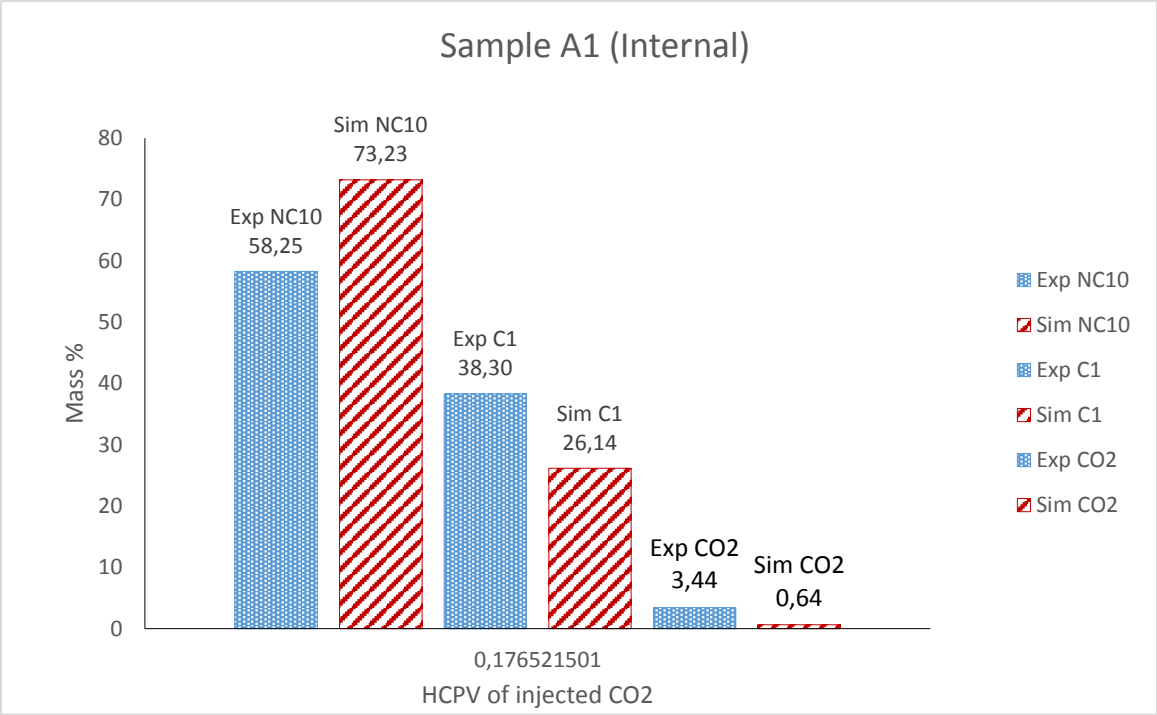

Figure 4.55. Comparison between the composition of the oil and CO_2 analyzed by experiment and numerical simulation for Sample A1 (Internal)

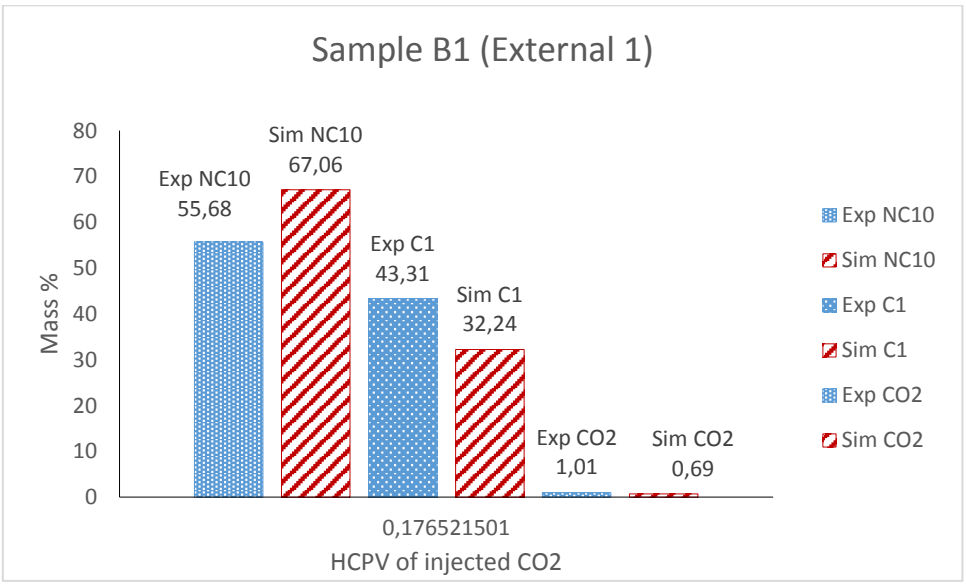

Figure 4.56. Comparison between the composition of the oil and CO_2 analyzed by experiment and numerical simulation for Sample B1 (Internal)

Sample A2 was collected inside the oven close to breakthrough at 5.09 PV. Figure 4.57 shows that equivalent amount of CO_2 has entered in the oil phase and mixed with the oil. The mass percentages of n-decane (32.9 %) is close to CO_2 (48.14 %). The experimental results showed that the amount of CO_2 is higher than n-decane. Whereas, the simulation result showed that

the percentage of n-decane (45.72 %) is higher than CO_2 (34.54 %). However, both the results predicted that CO_2 has become an integrated part of the system at this PV. Figure 4.58 also shows the same trend as sample A2. The mass percentage of CO_2 in the case of experimental results and simulation results were 34.54 % and 40.9 % respectively. C_1 in both the sample remained low (18.96 % in sample A2).

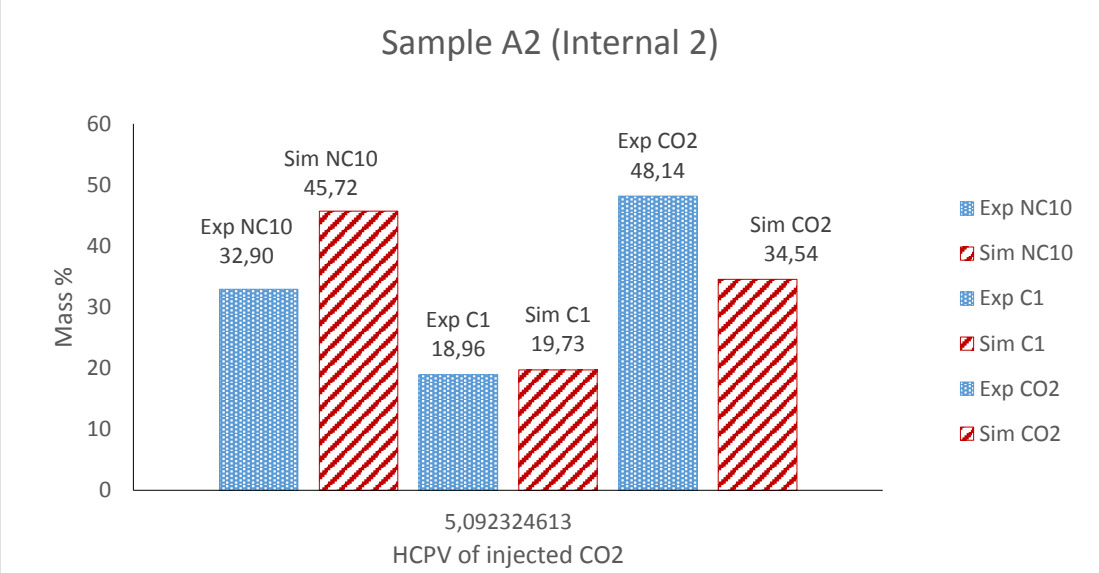

Figure 4.57. Comparison between the composition of the oil and CO_2 analyzed by experiment and numerical simulation for Sample A2 (Internal)

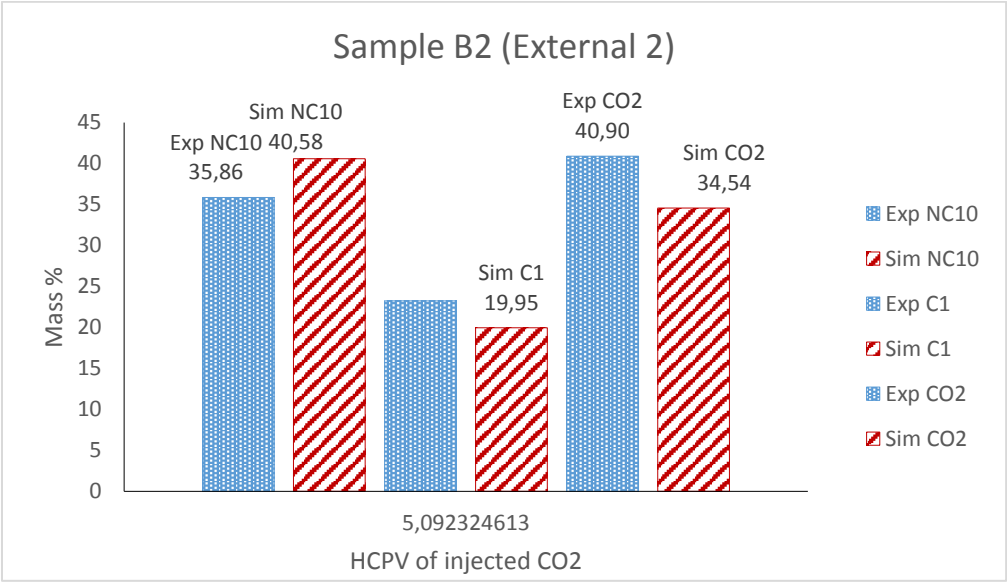

Figure 4.58. Comparison between the composition of the oil and CO_2 analyzed by experiment and numerical simulation for Sample B2 (Internal)

Figure 4.59 represents the composition of the oil and CO_2 in sample A3 taken at 7.835 PV of CO_2 after the breakthrough has achieved. At this stage of the flooding very low percentage of n-decane (12.98 %) and C_1 (10.10 %) remained in the core while rest of the percentage is occupied by CO_2 (76.92 %). The simulation results were also in the agreement with these result. In figure 4.60, the percentage of CO_2 has increased more (91.8 %) due to more injection of CO_2. Only 4.63 % of C_1 is left inside the core.

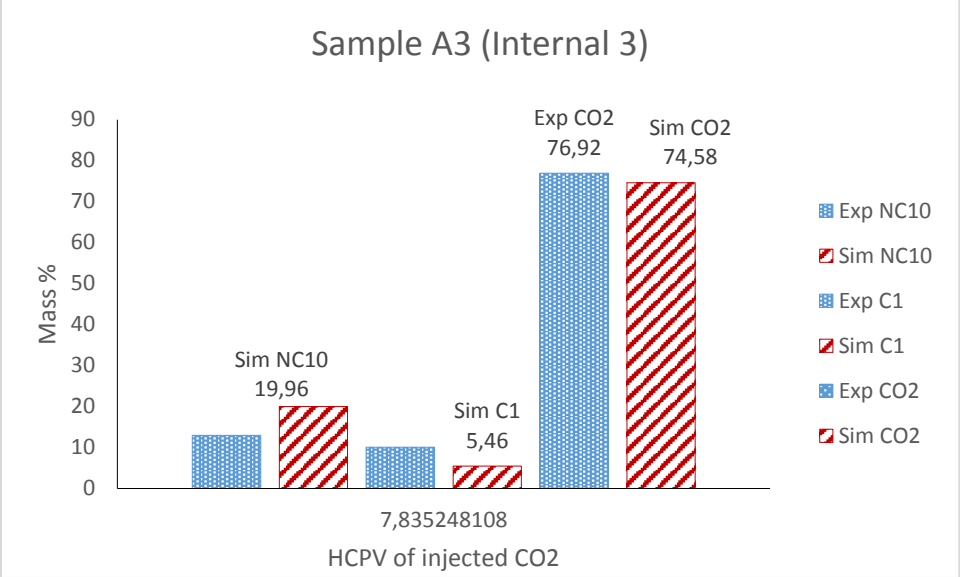

Figure 4.59. Comparison between the composition of the oil and CO_2 analyzed by experiment and numerical simulation for Sample A3 (Internal)

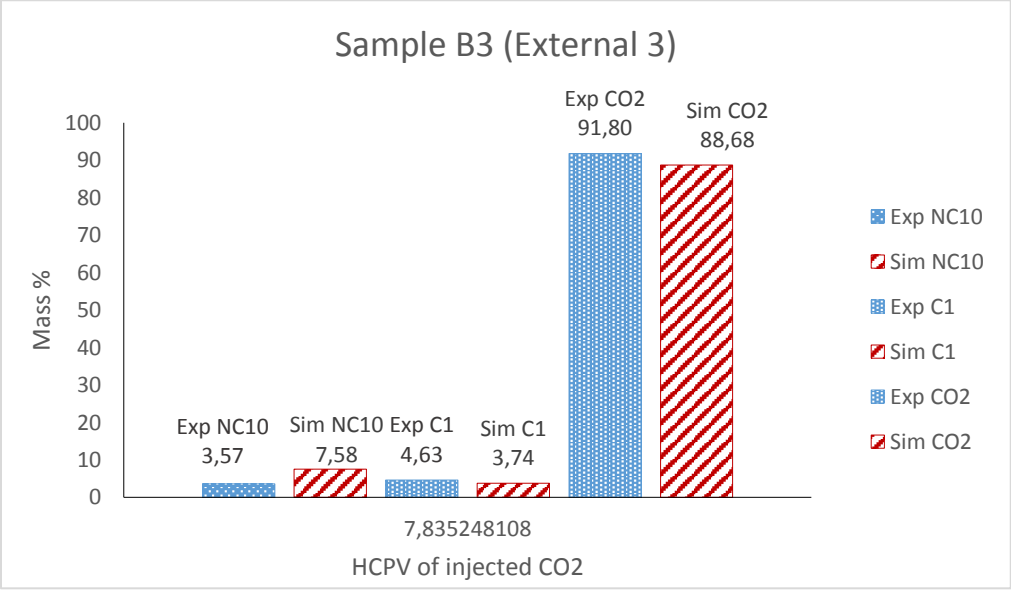

Figure 4.60. Comparison between the composition of the oil and CO_2 analyzed by experiment and numerical simulation for Sample B3 (External)

4.2.11. Live-Oil A 90°C

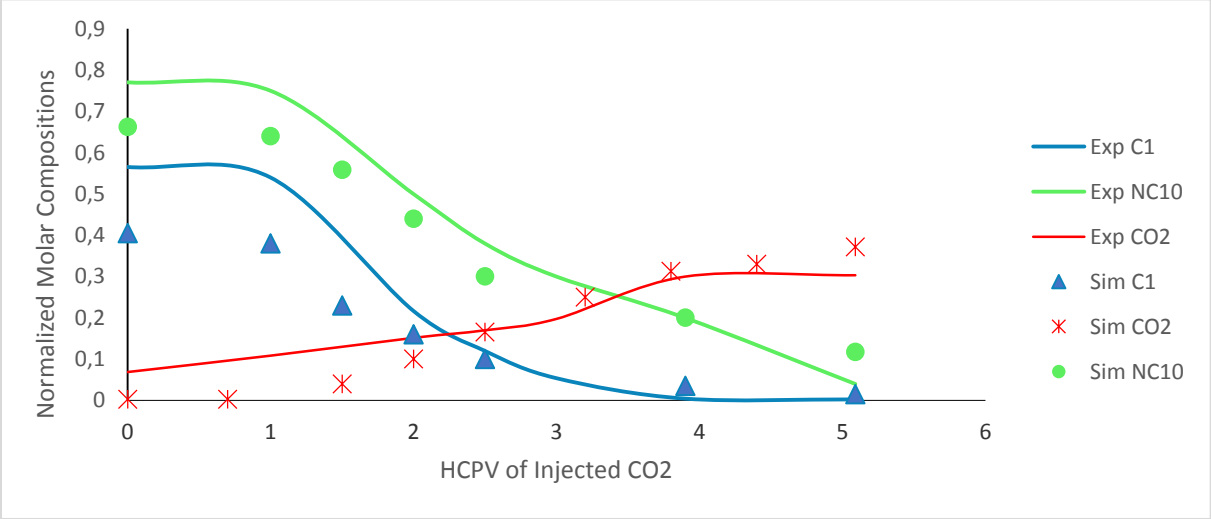

Figure 4.61. Comparison of simulation and experimental normalized molar composition as a function of injected PV of CO_2 for Crude oil saturated core flooded with CO_2.

The last experiment for Live-oil A was conducted at 90°C. The normalized molar compositions for this experiment shows the similar trend as the previous two temperatures (50°C and 70°C). The recovery obtained at this temperature is the highest of all the recoveries achieved from Live-oil A as well as Live-oil B. The consumption of n-decane and methane can be observed in the figure 4.16. Whereas, the increment in the CO_2 is alsonoticeable. Figure 4.62 shows the compositions collected in the first sample A1 inside the oven at 90°C and 200 bars. The highest percentage was occupied by n-decane (74.23 %) and then C_1 (23.27 %).CO_2 (2.50 %) production can also be noticed in the figure. At high temperature, CO_2 maybe more mobile and due to fingering pass through the oil to the production outlet. Figure 4.63 shows the composition collected in sample B outside the oven at the room temperature and pressure. Sample B1 collected at the similar PV (0.173 PV) as sample A1 also shows the similar trends. This is a common trait observed in all the samples collected in the start of the experiment.

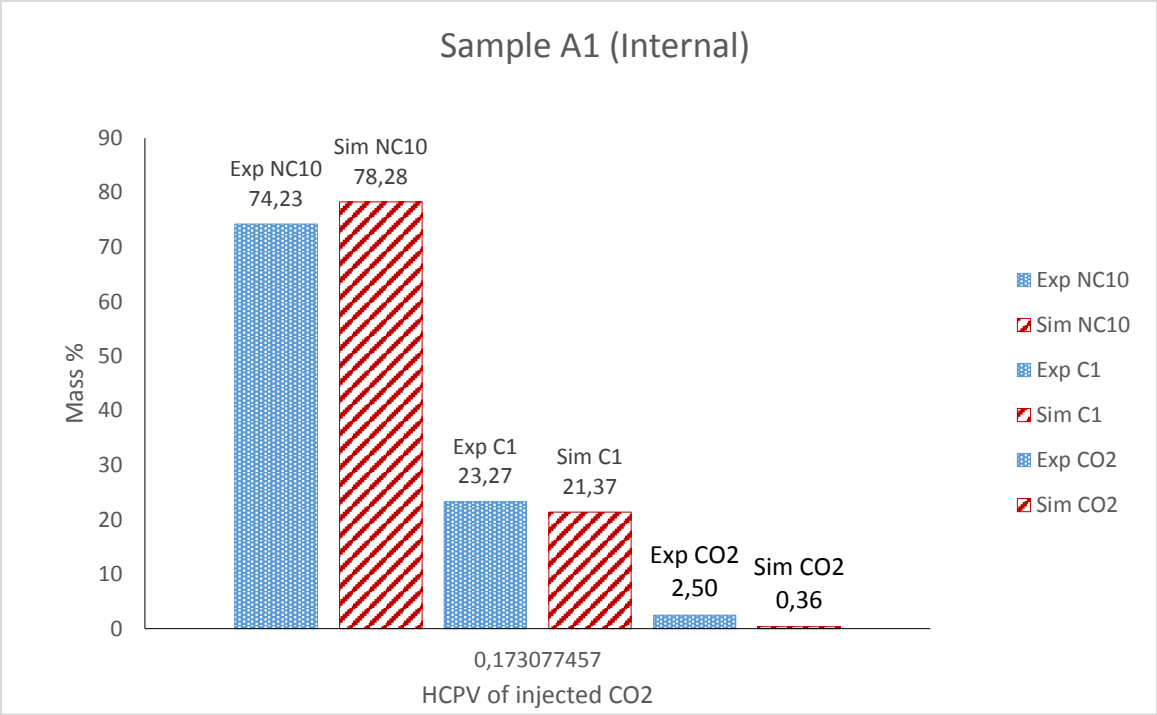

Figure 4.62. Comparison between the composition of the oil and CO_2 analyzed by experiment and numerical simulation for Sample A1 (Internal)

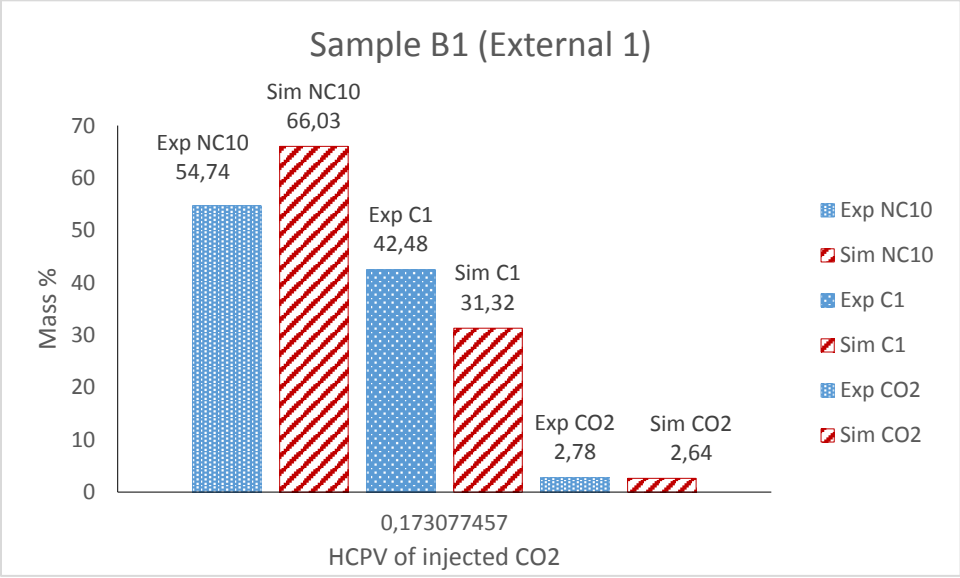

Figure 4.63. Comparison between the composition of the oil and CO_2 analyzed by experiment and numerical simulation for Sample B1 (External)

Figure 4.64 represents the sample A2 taken inside the oven at 2 PV of the injected CO_2. In this sample oil production has reduced (28.20 %) but C_1 has increased to 58.74 %. This may reflect that the vaporized C_1 is being produced after getting extracted by CO_2. The CO_2 production is 13.06 % in the sample. Sample B2 shows a high mass percentage of n-decane.

This maybe because a higher mass of oil was collected in the sample cylinder which affects the overall mass percentage distribution. Sensitivity with respect to oil produced was performed on the simulation results therefore, the simulation results supports the experimental results.

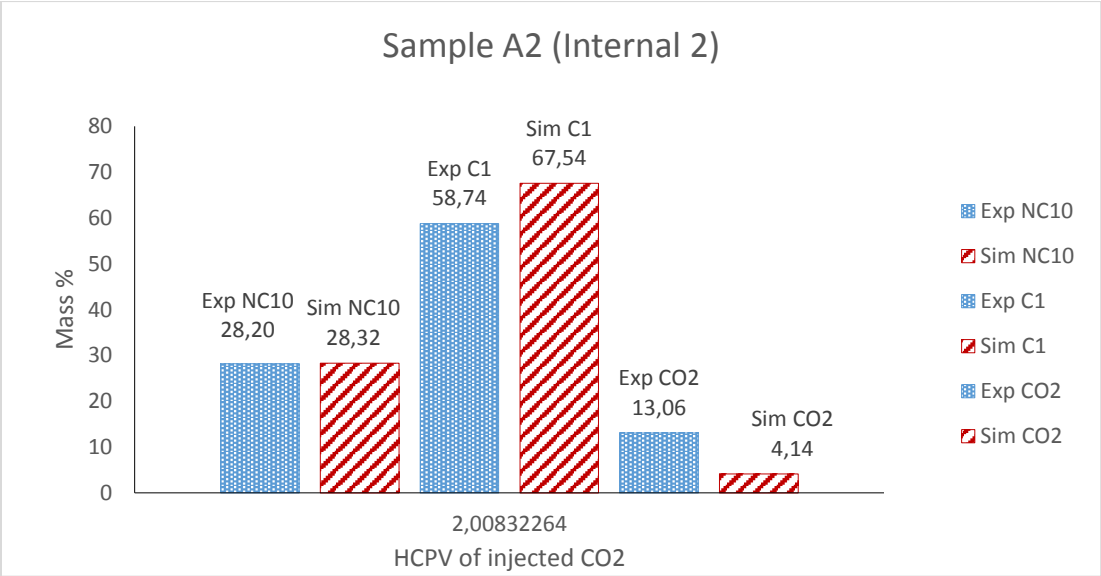

Figure 4.64. Comparison between the composition of the oil and CO_2 analyzed by experiment and numerical simulation for Sample A2 (Internal)

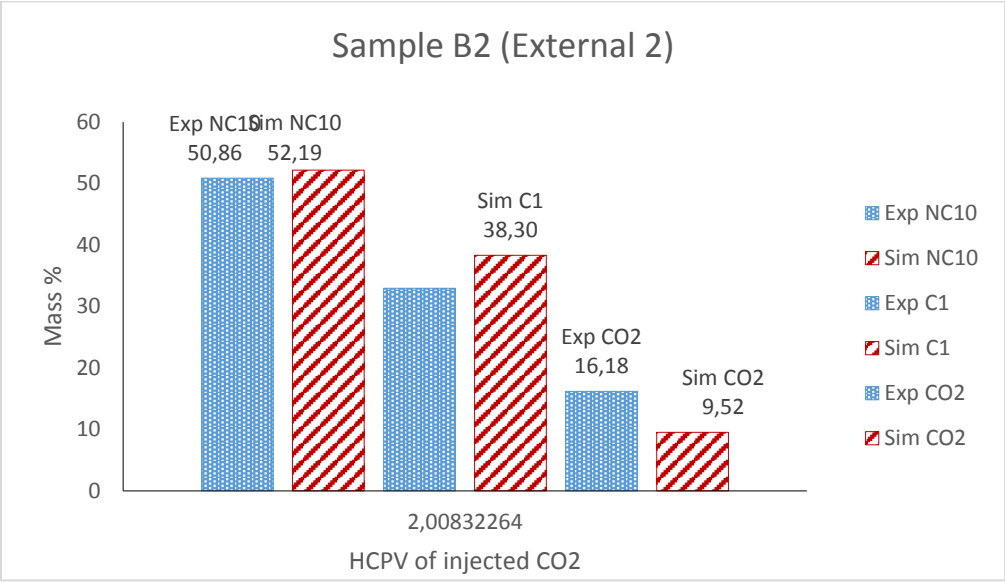

Figure 4.65. Comparison between the composition of the oil and CO_2 analyzed by experiment and numerical simulation for Sample B2 (External)

The final set of samples were collected after the breakthrough was achieved at 3.9 PV of injected CO_2. Because breakthrough was already occurred we can see a high amount of CO_2 (94.27 %) in the figure 4.66. No mass of oil was produced in sample A3, though the simulation result showed 13.87 % of oil because simulation results were expressing the core condition. The mass of C_1 is also very less (5.73 %). The similar trend is shown in figure 4.67

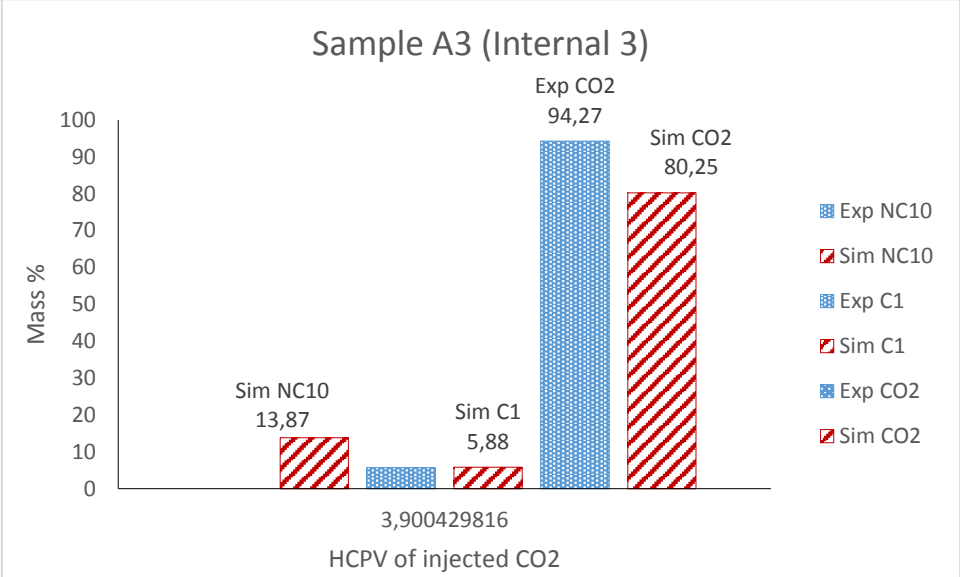

Figure 4.66. Comparison between the composition of the oil and CO_2 analyzed by experiment and numerical simulation for Sample A3 (Internal)

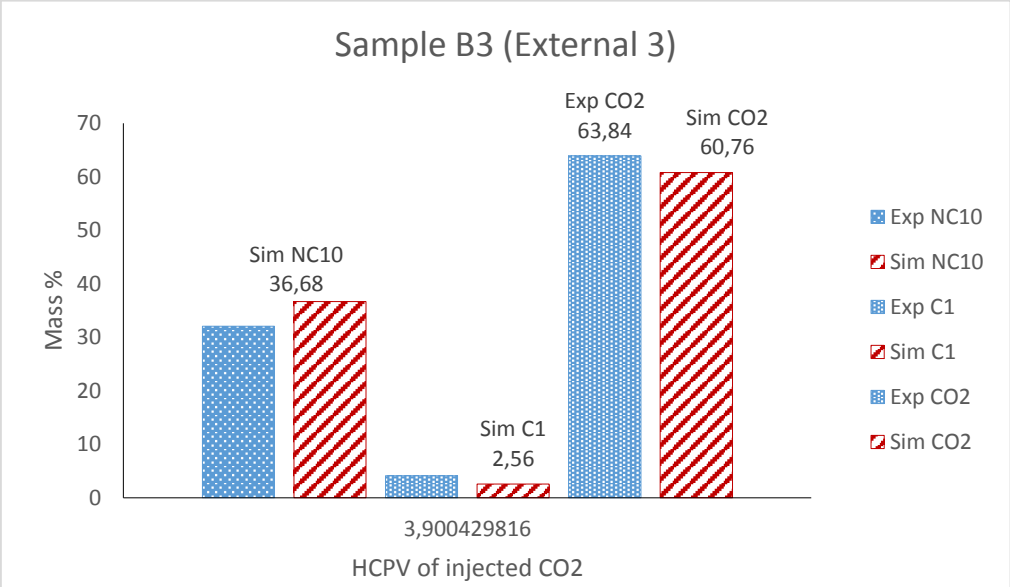

Figure 4.67. Comparison between the composition of the oil and CO_2 analyzed by experiment and numerical simulation for Sample B3 (External)

for sample B3 taken outside the oven at atmospheric temperature and pressure. The only difference it showed that the mass percentage of oil is higher than sample A3 which maybe because for the time the sample was collected a small amount of oil was collected.

The material balance calculation of all the experiments by using experimental analysis and simulation result aids in understanding the mechanism of mass transfer between the oil, light component and CO_2. Performing the same experiment for different composition of oil at three temperatures (50°C, 70°C and 90°C) highlights that with the increase in the temperature the injected PV of CO_2decreases as well as the recovery increases. CO_2 becomes less dense at higher temperature which makes it more mobile and readily soluble in the oil phase making it lighter and easily recoverable. There may be one disadvantage associated with higher temperature, fingering phenomenon of CO_2 can also occur which can cause higher residual of oil in the core. It is also observed that with the increase in temperature, CO_2 production in the sample increased. At 70°C and 90°C, the mass percentage of CO_2 was noticeable in the first set of samples (A1 and B1). The mass percentage increased as the experiment proceeded.

It is further observed that composition of oil also affect the recovery. C_1 was observed to be consumed before C_3.

4.2.12. Viscosity Profiles

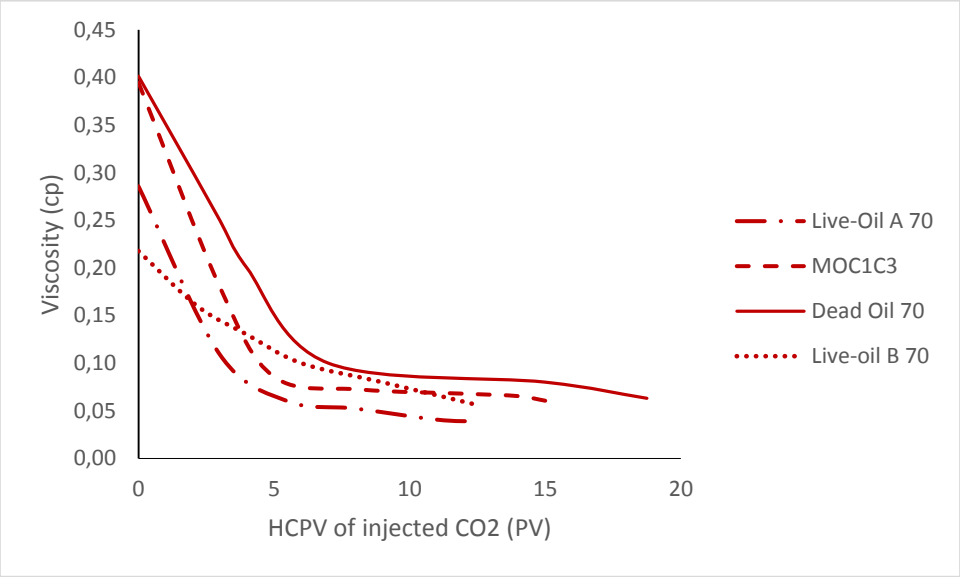

Figure 4.68. Comparison of viscosities of different experiments at 70°C

The material balance performed in this section and the results obtained could be supported by figure 4.68 which compares the viscosity profiles of Live-oil A, Live-oil B, Model oil (Dead oil displaced with CO_2, C_1 and C_3) and Dead oil displaced with CO_2 only. The profile shows that the viscosity of Live-oil A is lesser than live-oil B which satisfies the higher recovery in Live-oil A (80.01 %) than Live-oil B (77.67 %). Whereas, the dead oil flooded with CO_2 only was denser than Model oil (dead oil) flooded with CO_2 mixture (C_1 and C_3) which further satisfied the material balance performed and recoveries calculated for these experiments. The recovery obtained from Model oil displaced with CO_2 mixture (C_1 and C_3) was higher (84.51 %) than dead oil displaced with only CO_2 (82.14 %). Initial oil viscosity of Live-oil A was 0.2858 cp, Live-oil B was 0.2177 cp, Model oil was 0.3948 cp and dead oil was 0.4014 cp which was reduced during gas injection. Model oil appeared to be more efficient than dead oil may be because the light components in the injected gas phase prevent the vaporization of lighter and/ intermediate components from the oil phase causing the prevention in the reduction of the viscosity (Fai-Yengo&Rahnema, 2014).

4.2.13. Density Profiles

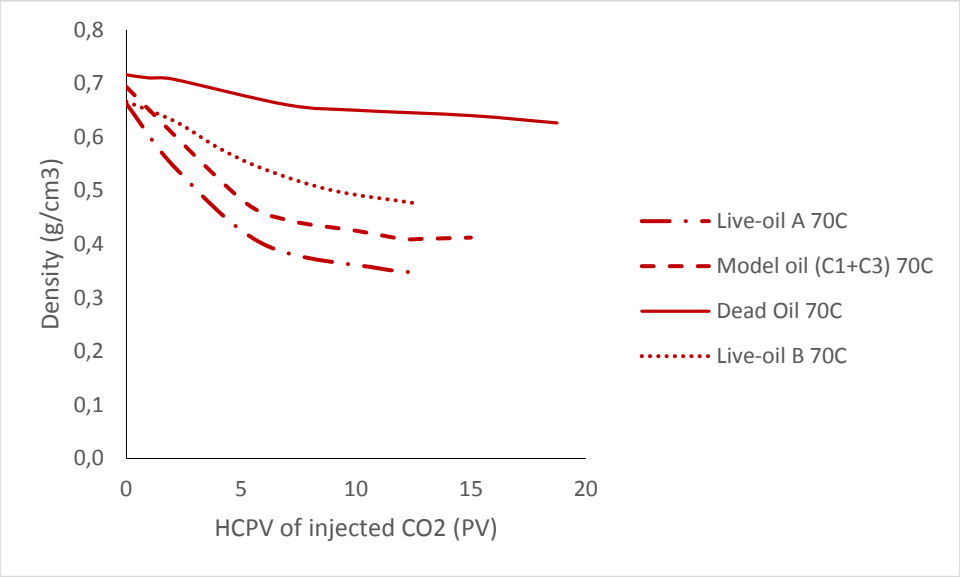

Figure 4.69. Comparison of viscosities of different experiments at 70°C

The density profiles in figure 4.69 also support the results calculated in this section. The original density of live oil A was 0.662 g/cm^3 which was reduced to 0.347 g/cm^3, Live-oil B was originally 0.6662 g/cm^3 and was reduced to 0.4763 g/cm^3, Dead oil was originally 0.7161 g/cm^3 and reduced to 0.64 g/cm^3 and Model oil was initially 0.6939 g/cm^3 which reduced to 0.41 g/cm^3 during the injection of the gas. Live-oil B was denser than Live-oil A due to which higher recovery is obtained from Live-oil A. CO_2 being denser than lighter components when come in contact with the oil, a continuous diffusion into the oil phase takes place causing the oil more dense and more viscous (Fai-Yengo&Rahnema, 2014). But in the case of Model oil (displaced with CO_2 mixture (C_1 and C_3)), initially being denser, when mixed with CO_2 mixture the lighter components replaces the vaporized gas and aid the oil in becoming less dense and less viscous. Thus, we can see that Model oil is less dense than dead oil displaced with CO_2 only.

5. CONCLUSIONS

The conclusions drawn from this study are addressed in this section. It is observed that the recombination of lighter components with the oil adversely affected the recovery by CO_2 flooding. The highest recovery was obtained from Dead oils in all cases of temperature (50°C, 70°C and 90°C) when only CO_2 was flooded in the core. Similarly Live-oil B (C_1 and C_3) reduced the recovery more than Live-A case (recombined oil with C_1 only). The possible reason behind that is the extraction efficiency of CO_2 reduces due to the presence of the light components. Due to this extraction process, the light components are vaporized and CO_2 condenses in the oil phase making it denser and more viscous. In the cases where CO_2 mixture (C_1 and C_3) are used as injected gas, better recovery is obtained which shows that richer gas injection accelerated the oil production. The density and viscosity profiles showed that the oil becomes lighter when the oil interacts with this composition of gas. The temperature also vitally affects the recovery. Highest recovery was achieved at 90°C in all the cases. This may be attributed to the increase in the miscible bank size along with the reduction in IFT resulting in better sweep efficiency.

6. REFERENCES

Alston, R.B., Kokolis, G.P. and James, C.F., 1985. CO2 minimum miscibility pressure: a correlation for impure CO2 streams and live oil systems. *Society of Petroleum Engineers Journal*, *25*(02), pp.268-274.

Alkan,H., Cinar, Y. , Ulker,E. B., 2010. Impact of Capillary Pressure, Salinity and In situ Conditions on CO2 Injection into Saline Aquifers.pp. 1-21.

Anderson, W. G. 1986. Wettability Literature Survey- Part 1: Rock/Oil/Brine Interactions and the Effects of Core Handling on Wettability. *Journal of Petroleum Technology*, 38, pp. 1125-1144.

Anderson, W. G. 1987. Wettability Literature Survey Part 5: The Effects of Wettability on Relative Permeability. *Journal of Petroleum Technology*, 39, pp. 1453-1468.

Al-Sayari, S.S., 2009. The Influence of Wettability and Carbon Dioxide Injection on Hydrocarbon Recovery, Department of Earth Science and Engineering Imperial College, London SW7 2AZ, UK.pp. 1-85.

Brown, R. J. S. & FATT, I. 1956. Measurements of Fractional Wettability of Oil Fields Rocks by the Nuclear Magnetic Relaxation Method.

Baviere, M., 1980. Basic Concepts in Enhanced Oil Recovery Processes, published for SCI. Data from US Department of Energy, Target reservoirs for CO2 miscible flooding. DOE/MC/08341.

Craig, F. F. 1971. The Reservoir Engineering Aspects of Waterflooding. *H. L. Doherty Memorial Fund of AIME.*

Darvish, GH., 2007. Physical Effects Controlling Mass Transfer in Matrix Fracture System During CO2 Injection into Chalk Fractured Reservoirs., Ph.D Thesis, Norwegian University of Science and Technology, Trondheim, Norway

F. F. Li , S. L. Yang, H. Chen , X. Zhang , D. D. Yin, L. P. He & Z. Wang, 2014. An improved method to study CO2–oil relative permeability under miscible conditions .

Gardner, J.W.,Ypma, J.G.J., 1984. An investigation of phase behaviour/macroscopic-bypassing interaction in CO_2 flooding. SPE J. 24, 508-520.

Holm, L.W. &Josendal, V. A., 1982. Effect of Oil Composition on Miscible-Type Displacement by Carbon Dioxide. *Society of Petroleum Engineer Journals*; 22(2), 87-98.

Holm, W. L.1987. Evolution of the carbon dioxide flooding processes. *Journal of petroleum technology* 39.11 pp.1-337.

Johns, R.T., Fayers, J., Orr, F.M., 1994. Effect of Gas Enrichment and Dispersion on Nearly Miscible Displacements in Condensing/Vaporizing Drives. SPE Adv. Tech. Series. 2, 26-34.

Johns, R.T., Sah, P., Subramanian, S., 2000. Effect of Gas Enrichment above the MME on Oil Recovery in Enriched-Gas Floods, SPE J. 3, 331-338.

Johnson, J. P., Pollin, J. S., 1981. Measurement and Correlation of CO2 Miscibility Pressure. SPE/ODE 9790 presented at Enhanced Oil Recovery Symposium Tulsa, Oklahoma, USA, April 5-8.

Klins, M.A., Farouq Ali, S.M., 1981. Oil Production in Shallow Reservoirs by Carbon Dioxide Injection. SPE 10374 presented at SPE Eastern Regional Meeting, Columbus, Ohio, Nov. 4-6.

Klins, M.A. and Bardon, C.P., 1991. Carbon dioxide flooding. *Basic Concepts in Enhanced Oil Recovery*, pp.215-240.

Rojas, G. A., Zhu, T., Dyer, S.B., Thomas, S., Farouq Ali, S.M., 1991. Scaled model studies of CO2 Floods. SPE Res. Eng. May, 169-178.

Mathiassen, O.M., 2003. CO2 as Injection Gas for Enhanced Oil Recovery and Estimation of the Potential on the Norwegian Continental Shelf. 1-95.

Pasala, S.M., 2010. *CO2 displacement mechanisms: Phase equilibria effects and Carbon dioxide sequestration studies* (Doctoral dissertation, The University of Utah). [Online] Available at: http://content.lib.utah.edu/utils/getfile/collection/etd3/id/454/filename/403.pdf, Accessed, 25th June, 2016.

Perkins, T.K., Johnston, O.C., 1963. Review of Diffusion and Dispersion in Porous Media. SPE J. 3, 70-84.

Perkins, T.K., Johnston, O.C., and Hoffman, R.N., 1965. Mechanics of Viscous Fingering in Miscible Systems. SPE J. 5, 301-317.

Peters, E.J., Flock, D.L., 1979. The Onset of Instability during Two-Phase Immiscible Displacement in Porous Media. SPE J. 21, 249-258.

Pizarro, J.O.S., Lake, L.W.: "Understanding Injectivity in Heterogeneous Reservoirs,"paper SPE 39697 presented at the 1998 SPE/DOE Improved Oil Recovery Symposium, Tulsa, April pp.19-22.

Renner, T.A., 1983. Measurement and Correlation of Diffusion Coefficientsfor CO2 and Rich-Gas Applications. J. SPE Res. Eng. 517-523.

Salathiel, R. A. 1973. Oil Recovery by Surface Film Drainage In Mixed-Wettability Rocks. *Journal of Petroleum Technology*, 25, pp. 1216-1224

Shyeh-Yung, J., 1991. Mechanisms of Miscible Oil Recovery: Effects of Pressure on Miscible and Near-Miscible Displacements of Oil by Carbon Dioxide. SPE 22651 presented at SPE Annual Conference and Exhibition, Dallas, Texas. Oct. 6-9.

Trivedi, J., Babadagli, T., 2008. Efficiency of Diffusion Controlled Miscible Displacement in Fractured Porous Media. Transport in Porous Media. 71, 379.

Trivedi, J., Babadagli, T., 2010. Experimental Investigations on the Flow Dynamics and Abandonment Pressure for CO2 Sequestration and Oil Recovery in Artificially Fractured Cores. J. Can. Pet. Tech. 49, 22-27.

Trivedi, J., Babadagli, T., 2009. Experiment and Numerical Modeling of the Mass Transfer between Rock Matrix and Fracture. Chemical Eng. 146, 194- 204.

Verdirer, S., Anderson, I., 2005. Internal Pressure and Solubility Parameter asa Function of Pressure. 2005. Fluid Phase Equilibria. 231, 125-137.

Ydstebø, T., 2013. Enhanced Oil Recovery by CO2 and CO2-Foam in Fractured Carbonates. [Online] Available at:http://bora.uib.no/bitstream/handle/1956/6803/109021444.pdf?sequence=1, Accessed, 25th June, 2016.

Yin, M., 2015. CO 2 miscible flooding application and screening criteria. [Online] Available at:http://scholarsmine.mst.edu/cgi/viewcontent.cgi?article=8422&context=masters_theses, Accessed, 25th June, 2016.

Zick, A., 1986. Combined Condensing Vaporizing Mechanisms in the Displacement of Oil by Enriched Gases. SPE 15493 presented at SPE Annual Technical Conference and Exhibition, New Orleans, Oct. 5-8.